Felipe Augusto André Ishiy

Estudo de Marcadores moleculares no processo de diferenciação osteogênica de células-tronco mesenquimais

São Paulo

2016

Felipe Augusto André Ishiy

Estudo de Marcadores moleculares no processo de diferenciação osteogênica de células-tronco mesenquimais

Evaluation of molecular markers in osteogenic differentiation of mesenchymal stem cells

Tese apresentada ao Instituto de Biociências da Universidade de São Paulo, para a obtenção de Título de Doutor em Ciências, na Área de Biologia/Genética.

Orientadora: Maria Rita dos Santos e Passos-Bueno

Co-oritentador: Roberto Dalto Fanganiello

São Paulo

2016

Ficha Catalográfica

Augusto André Ishiy, Felipe

Estudo de Marcadores moleculares no processo de diferenciação osteogênica de células-tronco mesenquimais

112 páginas

Tese (Doutorado) - Instituto de Biociências da Universidade de São Paulo. Departamento de Genética e Biologia Evolutiva.

1. Potencial osteogênico de células progenitoras 2. Medicina Regenerativa 3. Engenharia de tecidos. Universidade de São Paulo. Instituto de Biociências. Departamento Genética e Biologia Evolutiva.

Comissão Julgadora:

_____	_____
Prof(a). Dr(a).	Prof(a). Dr(a).
_____	_____
Prof(a). Dr(a).	Prof(a). Dr(a).

_____

Profa. Dra. Maria Rita dos Santos e Passos Bueno

Agradecimentos

À Professora Maria Rita, pela oportunidade de trabalhar e aprender aquilo que eu sempre quis, pela orientação, ajuda, suporte, e ensinamentos. Serei eternamente grato por tudo que a senhora fez por mim.

Gerson, agradeço por toda ajuda, pela amizade colaboração e horas "infinitas" na cultura, nas IPS e toda contribuição profissional e amizade.

Roberto meus sinceros agradecimentos pela co-orientação, amizade, pelas conversas, por compartilhar experiências e conhecimento.

Luciano, obrigado pela amizade, pelas conversas, ajuda, caronas, e todo suporte nestes últimos anos.

Aos colegas do laboratório: Erika Yeh, Carol, Lucas, Vanessa, Karina, May, Dani M, Bela, Bruno, Atique, Erika K, Tati, Dani Yumi, Clarice, Ágatha, Camila M, Camila L, Lucas, Gabi, Meire, Naila, Simone e Andressa.

Este trabalho contou com o apoio financeiro do Conselho Nacional de Desenvolvimento Científico e Tecnológico (CNPq) e do Ministério da Ciência, Tecnologia e Inovação do Brasil.

Mãe, Pai, Carlão e Crys obrigado pela força apoio, amor, presença, enfim obrigado por tudo, sem vocês nada faria sentido. Vocês são minha vida.

Dedico esta tese ao meu amigo, meu companheiro de lutas, a pessoa que estava presente nas muitas derrotas e momentos difíceis da minha vida mas que sempre se mostrou um lutador, um médico, um filho, um amigo mais do que especial, um irmão. Carlão você estava, está e sempre estará em todas as conquistas que eu tiver na minha vida, sua luta não foi e nem será em vão. Sempre estaremos juntos. Areguá!

Irma e Luiz Rubião, considero vocês parte da família e agradeço por toda ajuda, vocês fazem parte desta jornada.

Kaju e Marcela, obrigado pela força, presença e acima de tudo pela amizade. Essa conquista também é de vocês. Todos da NDT (Bruno, Rod, Duaik, Pérsis) obrigado pela força e por todo suporte. Vocês tornaram momentos difíceis muito mais leves e fáceis de se lidar.

André, Layla e Família Castiglioni, vocês estiveram presentes durante toda minha vida, Obrigado por tudo.

Tio Balé e Tia Lúcia, vocês abriram a porta da casa de vocês para mim, vocês me deram oportunidade no momento mais difícil da minha vida.

Table of Contents

Abstract

The use of stem cells is a promising therapeutic approach for tissue engineering by their ability to boost tissue regeneration, and to model *in* vitro human genetics disorderssince it provides continuous supplies of cells with differentiation potential. Our study has been focused in the identification of molecules or mechanisms that could contribute to a better osteogenesis in mesenchymal stem cells (MSC). To achieve our goals we have explored the osteopontential differences of stem cells from different sources. In this regard, we have observed that MSCs from human exfoliated deciduous teeth (SHED) presented higher *in vitro* osteogenic differentiation potential (OD) as compared to MSCs derived from human adipose tissue (hASCs). Through microarray analysis and cell sorting, we have shown that IGF2 and CD105 expression levels contribute to these osteopontential cell differences, that is, higher IGF2 expression levels and lower CD105 expression levels were associated with the increased osteogenic potential of SHED as compared to hASCs. The molecular mechanisms associated with the diferent expression levels of IGF2 and CD105 in these cells were also investigated. Despite the advantages of adult MSCs they can exhibit drawbacks such as restricted self-renewal and limited cell amounts. Induced Pluripotent Stem Cells (iPSC) technology has emerged as an alternative cell source, as they provide more homogeneous cellular populations with prolonged self-renewal and higher plasticity. We verified that the OD of MSC-like iPSC differs from MSCs and it depends on the iPSCs originating cellular source. Comparative *in vitro* osteogenesis analysis showed higher osteogenic potential in MSC-like cells derived from iPS-SHED when compared with MSC-like cells from iPS-FIB and SHED. iPSCs can be also used as a tool to model genetic disorders. We have thus proposed to verify if it could be possible to *in vitro*model Treacher-Collins syndrome, a condition with deficient craniofacial bone development. We have compared the effects of pathogenic mutations in *TCOF1* gene in cell proliferation, differentiation potential between MSCs, dermal fibroblasts, neural-crest like and MSC-like cells differentiated from iPSCs.TCS cells showed changes in cell properties anddysregulated expression of chondrogenesis markers during osteogenic and chondrogenic differentiation. In summary, the comparative analysis of stem cells of different sources allow us to identify markers that may facilitate osteogenesis and that it is possible to establish an *in vitro* model to Treacher-Collins syndrome.

Resumo

O uso de células-tronco trata-se de uma abordagem terapêutica promissora para a engenharia de tecidos, devido à sua capacidade na regeneração de tecidos, e para modelamento *in vitro* de distúrbios genéticos humanos, uma vez que fornece um abastecimento contínuo de células com potencial de diferenciação. Nosso estudo se propos a identificar moléculas e mecanismos que contribuem na otimização da osteogênese de células-tronco mesenquimais (MSCs). Para atingir nossos objetivos exploramos as diferenças no potencial osteogênico (PO) de MSCs de diferentes fontes. Observamos que MSCs de polpa de dente decíduo humano (SHED) apresentaram maior PO em comparação com as MSC derivadas de tecido adiposo humano (hASCs). Através de análise de microarray de expressão e *cell sorting,* demonstramos que os níveis de expressão de IGF2 e CD105 contribuem para as diferenças do PO, onde a maior expressão de IGF2 e menor expressão de CD105 estão associadas a maior PO em SHED quando comparado as hASCs. Também investigamos os mecanismos moleculares associados aos diferentes níveis de expressão de IGF2 E CD105 em ambas as fontes celulares. Apesar das vantagens, as MSCs podem apresentar pontos negativos como restrita auto-renovação e menor quantidade de células. Células-tronco pluripotentes induzidas (iPSC) surgem como uma fonte celular alternativa, proporcionando populações celulares homogêneas com auto-renovação prolongada e maior plasticidade. O PO de *MSC-like* iPSC difere de MSCs, e este potencial é dependente da fonte celular em que as iPSCs são obtidas. Análise comparativa de PO *in* vitro demonstrou maior osteogênse em células *MSC-like* derivadas de iPS-SHED quando comparada as células *MSC-like* de iPSCs-fibroblastos e SHED. iPSCs também podem ser utilizadas como ferramenta para investigar doenças genéticas humanas. Propomos a modelagem *in* vitro da síndrome de Treacher-Collins (TSC), doença que acomete as estruturas craniofaciais durante o desenvolvimento ósseo. Comparamos os efeitos de mutações patogênicas no gene TCOF1 na proliferação celular, potencial de diferenciação entre MSCs, fibroblastos dérmicos, *neural-crest like* e células *MSC-like* diferenciadas de iPSCs. Células de pacientes TCS exibiram alterações em propriedades celulares e na expressão de marcadores osteogênicos e condrogênicos. Em resumo, a análise comparativa de células-tronco de diferentes fontes permitiu a identificação de marcadores e mecanismos que podem facilitar a osteogênese e tambem demonstramos que é possível modelar *in vitro* a síndrome de Treacher-Collins.

CHAPTER I

Introduction

1- Introduction

1. Tissue Engineering and Regenerative Medicine

Bone tissue is the supporting structure of our organism responsible for blood cell production and it is an important source of minerals (Freyschmidt, 1993). Due to the importance of this tissue for our organism the development of new therapies in bone tissue engineering and regenerative medicine rises from the necessity to obtain more efficient and satisfactory results in bone reconstruction procedures, particularly in situations that involve large regions to be reconstructed. The current golden standard in bone tissue engineering is the transplantation of autologous bone graft to repair bone loss due to disease, malformation or trauma, but this approach is associated with critical shortcomings, such as pain and morbidity in the graft site, and limited tissue supply (Amini et al., 2012; Bose et al., 2012; Grayson et al., 2015; Healy et al., 2007; Holzwarth & Ma, 2011; Huang et al., 2015).

Tissue engineering can be described as a multidisciplinary area, including knowledge from the fields of engineering, biology and medicine. Langer and Vacanti (1993) proposed that three main pillars conceptually support tissue engineering: progenitor cells, biomaterials/scaffolds and factors/signaling molecules (Casser-Bette et al., 1990; Langer & Vacanti, 1993; Glotzbach et al. 2011). It is essential to understand and characterize each one of these pillars to optimize and enhance bone reconstruction and regenerative processes. Below we describe the importance of

progenitor cells to the establishment of a functional bone with compatibility and integration to the bone tissue environment (Badylak & Nerem, 2010).

1.1 Stem Cells

Stem cells have emerged as a promising tool for regenerative medicine and tissue engineering mainly because of their ability to replicate themselves and originate the same non-specialized cell type over long periods (self-renewal) and due to their differentiation potential capacity (Bianco et al, 2013; He et al, 2009).

Stem cells can be classified depending on their differentiation plasticity (**Figure 1**) that can be divided in two broad types: pluripotent stem cells (human embryonic stem cells - hESCs and induced pluripotent stem cells - iPSCs) that harbor the capacity of differentiation in all three germ layers of the developing embryo and in all adult cell types, and the adult multipotent stem cells (hematopoietic stem cells - HSCs, mesenchymal stem cells - MSCs) that generate specific lineages or tissues and can be found in different adult tissues (Bazley *et al,* 2015; Jung, *et al.* 2012; Phinney and Prockop, 2007; Takahashi and Yamanaka, 2006).

Despite the potential of differentiation in all cell types of the adult body, pluripotent stem cells (hESCs and iPSCs) face considerable obstacles to their use in regenerative medicine and tissue engineering due to the intrinsic capacity of teratoma formation when delivered *in vivo,* and the ethical issues related to the use of human embryos to obtain hESCs (Miura et al, 2009; Okita et al, 2007; Takahashi and Yamanaka, 2006; Takahashi et al, 2007). iPSCs have been shown to develop teratoma more efficiently andmore aggresively *in vivo* when compared to hESCs (Gutierrez-

Aranda et al, 2010). There is still no effective method to circunvent and eliminate the possibility of teratoma formation when using hESCs and iPSCs (Mohseni et al 2014).

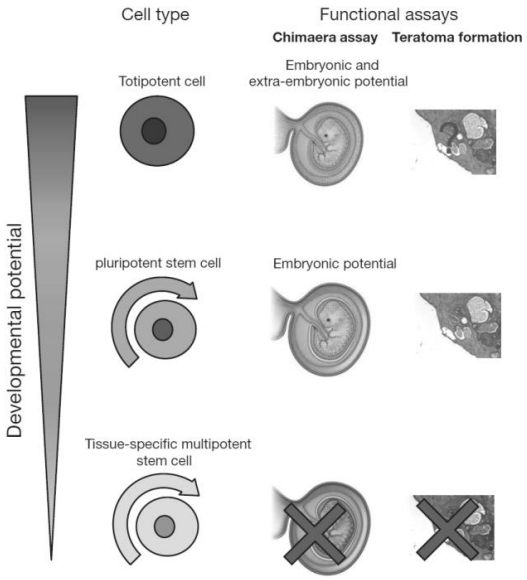

Figure 1. Classification of stem cells depending on their developmental potency (Adapted from Angeles *et al,* Nature, 2015).

Mesenchymal Stem Cells - MSCs (Caplan, 1991) offer several advantages in autologous cell therapy and tissue engineering field due to lower risk of tumorigenicity (when compared with hESCs or iPSCs), immunomodulatory properties and easier access and their easy obtainment when compared with ESCs (Bara et al 2014; Caplan and Dennis, 2006).

MSCs can act in different and essential steps of bone maintenance (Bielby et al, 2007) and during bone regeneration after trauma. During the first moment (hours to days after injury) MSCs contribute to the local immunomodulation process through production of immunosuppressive factors (Grayson et al, 2015; Najar et al, 2016; Nauta, et al, 2007). After days or weeks of injury, MSCs can supply osteo-

chondroprogenitor cells to repair the bone tissue due to their capacity of multipotent differentiation (Bruder et al, 1994; Chamberlain et al, 2007; Guan et al, 2012).

These multipotent, plastic-adherent and colony-forming cell populations can be characterized through an immunophenotype marker panel (positive staining for CD73, CD90 and CD105, and negative for CD11B or CD14, CD19 or CD79α, CD34, CD45 and HLA-DR), whichwas first characterized in bone marrow-derived stem cells-BMSCs (Dominic et al, 2006; Friedenstein et al 1966, 1970; Pittenger et al, 1999).

In the last decades, MSCs have been isolated from several human adult tissues such as peripheral blood (Zvaifler *et al*., 2000), umbilical cord blood (Erices *et al.*, 2000), fetal tissues (Campagnoli *et al.*, 2001), adipose tissue (Zuk *et al.,* 2001; Zuk *et al.*, 2002), amniotic liquid (In'tanker *et al*., 2003), umbilical *cord* (Sarugaser *et al.,* 2005), dental pulp (Gronthos *et al.,* 2000; Miura et al., 2003), from *orbicularis oris* muscle (Bueno et al., 2009), among others.

Despite the discovery of new sources, markers and use of stem cells, Bone Marrow Mesenchymal Stem Cells (BMSCs) remained the most studied adult stem cells (Friedenstein et al., 1966; Kadiyala et al., 1997; Nakagawa et al, 2016; Rada et al, 2011; Seong et al., 2010). BMSCs and other stem cell sources have been used in clinical trials specifically to skeletal regeneration and bone tissue engineering as exemplified in **Figure 2,** demonstrating the importance and potential use of these cell sources for regenerative medicine. In stem cell research field there are multiple avenues now open including: stem cells as tools for modeling human diseases mechanisms, identification of bioactive factors and regenerative medicine (Bianco et al, 2013).

After bone injury the organism initiates a cascade of key regenerative steps including action of proinflammatory cytokines, homing of osteogenic progenitor cells

and immune cells. Thus, the introduction of progenitor cells/stem cells during these events could be essential to achieve optimal osteogenesis (Dimitriou et al, 2005; Grayson et al, 2015).

Clinical trials in which stromal cells were used for skeletal regeneration

Indication	Cell source	Cell processing and delivery	Clinical trial
MSC			
Non-union of bone	Autologous	Direct injection	NCT00512434, NCT01788059
		Implantation with carrier	NCT00250302, NCT01626625, NCT01958502
ONFH	Autologous	Direct injection	NCT02065167
		Implantation with carrier	NCT01605383
Other (spine fusion, osteoarthritis)	Autologous	Direct injection	NCT01210950
		Implantation with carrier	NCT01552707
	Allogeneic	Direct injection	NCT01603836
		Implantation with carrier	NCT00001391
ASC			
Non-union of bone	Autologous	Implantation with carrier	NCT01532076
	Allogeneic	Direct injection	NCT02140528
ONFH	Autologous	Direct injection	NCT01643655
Other (spine fusion, osteoarthritis)	Autologous	Direct injection	NCT01501461, NCT01885819, NCT02142842
		Implantation with carrier	NCT01633892

Figure 2. Examples of Clinical trials in bone tissue engineering using BMSCs and hASCs as an alternative source of mesenchymal stem cells for skeletal regeneration (Abbreviations: ASC, adipose-tissue derived stromal cell, MSC, bone marrow-derived stromal cell; ONFH: osteonecrosis of the femoral head, NCT- clinical trial number) (Adapted from Grayson *et al,* Nature, 2015).

1.2 Alternative MSC sources

Recently efforts to search alternative sources of adult MSCs for bone tissue engineering and regenerative medicine arise due to some limitations presented by BMSCs such as pain, morbidity, possibility of infection during the invasive extraction

process, and low quantity of mesenchymal stem cells obtained (Caplan, 2009; Derubeis and Cancedda, 2004).

Two promissing MSC types are stem cells from human dental pulp cells (Grontos et al., 2001; Miura et al, 2003) and human adipose tissue-derived stem cells-hASCs (Zuk et al., 2002). These two cell sources have shown important characteristics for regenerative medicine/bone tissue engineering such as: accessible source without morbidiy and pain (**Figure 3**), multipotential differentiation and higher proliferation capacity when compared with BMSCs (Gronthos et al., 2000; Kerkis et al., 2006; Laino et al., 2006; Mizuno et al, 2010; Nakamura et al, 2009). Regarding human dental pulp cells, we will focus on those obtained from exfoliated teeh (SHED, Miura et al., 2003) instead of from adult human teeth (DPSC- Gronthos et al., 2001), as this represents one the cell sources here studied.

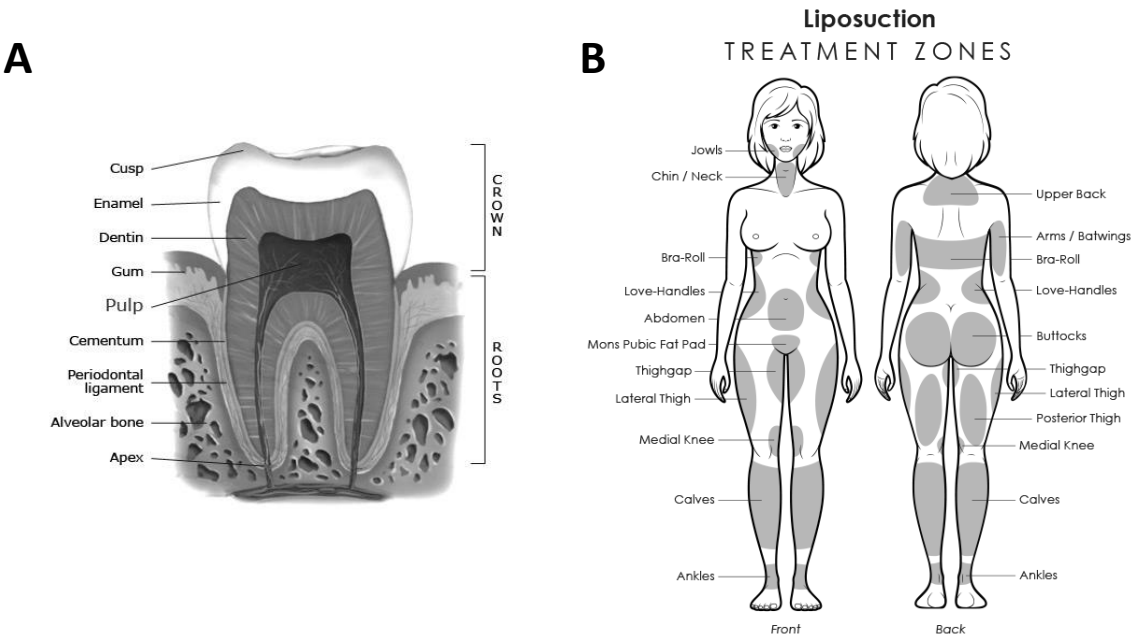

Figure 3.A- Scheme demonstrating the pulp localization in the teeth structure (Adapted from http://www.studiodentaire.com/en/glossary/pulp.php); **B**- Localization of adipose tissue in which liposuction can be performed to obtain ASCs (Adapted from http://drmathewplant.com/liposuction-toronto/). As the cells are obtained from the discarded tissue, this procedure does not cause any additional morbidity or pain to the donor individuals.

SHED exhibits important characteristics to achieve promising results in bone regeneration such as maintenance of cellular plasticity and immunophenotype after freeze-thaw cycles (d'Aquino et al. 2009; Laino et al., 2005; Laino et al., 2006; Huang et al., 2009), *in vivo* bone formation in animal models (Alongi et al, 2010, de Mendonca Costa et al, 2008), and this cell type was used in human clinical applications (D´Aquino et al, 2009; Giuliani et al, 2013).

The international Fat Applied Technology Society adopted the term adipose-derived stem cell (ASCs) to identify the alternative source of MSCs that were firstly described by Zuk et al (2002) (Baer et al, 2012). The material extracted from human subjects under local anesthesia (Mizuno et al, 2012) in which these cells can be obtained is routinely discarded after aesthetics liposuction procedures, and it was demonstrate that obesity incidence has increased substantially in the past years, thus facilitating the obtainment of the necessary material to isolate ASCs (Bourin et al, 2013; Gimble et al., 2007; Witkowska-Zimny & Walenko, 2011).

The autologous use of ASCs facilitates the use of this source in clinical trials and treatments of different kind of diseases as: peripheral vascular/cardiovacular diseases (number clinical trial-NCT01211028), soft tissue augmentation of craniofacial structure (Yoshimura et al, 2008), articular cartilage lesion (NCT01399749) and craniofacial bone reconstruction (Lendeckel et al, 2004; Mesimaki et al, 2009), but despite the easiness obtainemnt ASCs present lower osteogenic potential when compared with SHED (Fanganiello et al., 2015).

Although SHED and hASCs show promising characteristics for regenerative medicine, which is the best cellular source to bone tissue engineering remains to be established. Stem cells from different sources cells might possess differences in their *in*

vitro differentiation potential towards osteoblastic cells (Al-Nbaheen et al 2013). These differences are not completely understood, and they could be partly related to their tissue of origin (Baksh et al., 2007; Huang et al., 2009; Kern et al., 2006). The selection of the best cellular source, or the best subpopulation could be performed through the dissection of possible markers or mechanisms related to enhanced osteogenesis.

The efficacy of treatments using MSCs are still unsatisfactory due to cellular heterogeneity presented by the MSC populations leading to experimental variability, compromising the proliferation and differentiation capacity. It is not possible to morphologically distinguish MSCs from fibroblasts, the *ex-vivo* MSC cultures contain phenotypically distinct cellular types in different commitment stages, and there is no unanimity of intrinsic and specific surface molecules to distinguish MSCs and to differentiate these cells from other cell types (Lv *et al.,* 2014; Mizuno *et al*., 2012).

1.3 Different approaches to understand the osteogenic potential of MSCs

In order to find the best cellular source for bone tissue engineering and regenerative medicine, different approaches are being used such as: Cell reprogramming technology (Takahashi and Yamanaka, 2006), mesenchymal stem cells differentiated from pluripotent stem cells (Barberi et al, 2005) and the study of specific molecular markers and transcriptional pathways, and methodologies to obtain a more homogeneous cellular population to understand the osteogenic potential differences between MSCs (Chung et al, 2013; Levi et al, 2010).

The main methodology employed to this purpose is the use of surface markers to isolate, characterize and compare different subpopulations of MSCs. Using different

surface markers, CD49 and STRO-1, Rada and collaborators (2011) isolated subpopulations of rat adipose derived stem cells and observed differences in osteogenic potential and mesenchymal stem cells markers. Other groups have isolated from dental pulp stem cells a subpopulation called SBP-DPSC (Stromal bone producing-dental pulp stem cell) positive for c-Kit, CD34 and negative for CD45, and this cell population exhibited *in vitro* and *in vivo* osteogenesis and were highly clonogenic (Laino et al, 2005; Papaccio et al 2006).

MSCs are expanded in monolayer plastic flasks and during this expansion process a certain population of cells are selected leading to changes in their phenotype (Bara et al, 2014). A significant immunophenotypic change in hASCs has been shown during serial cellular passage with temporal alteration of mesenchymal stem cell markers as: CD29 (Cluster of differentiation- Adhesion marker), CD34 (Hematopoietic), CD73, 90 and 105 (Mesenchymal) (Mitchell et al. 2006, McIntosh et al. 2006).

CD90 (THY-1) is a mesenchymal stem cell marker associated with osteoblastogenic lineages (Hosoya et al, 2012). Sorted subpopulations of hASCs with higher expression of CD90 exhibited higher *in vitro* and *in vivo* osteogenic differentiation when compared with subpopulations with lower CD90 expression and the heterogeneous (unsorted) populations (Chung et al, 2013).

Another interesting surface marker that has been used to isolate subpopulations of MSCs is the mesenchymal stem cell surface marker: endoglin (CD105), a transmembrane co-receptor of TGFB1 that regulates the proliferation, differentiation potential, immune response and angiogenesis as described in **Figure 4** (Nassiri *et al.,* 2011*;* Whitman, and Raftery 2005; Sanz-Rodriguez *et al.*, 2004; Warrington *et al*, 2005).

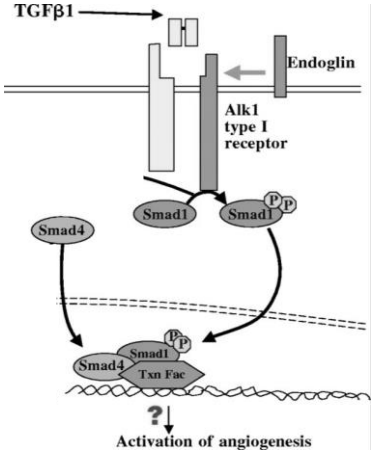

Figure 4. Role of Endoglin acting as a co-receptor of TGFB1 in the regulation of angiogenesis (Adapted from Whitman, and Raftery 2005)

Inhibition of TGFB1 by the receptor kinase inhibitor SB431542 (**Figure 5**) leads to an acceleration of BMP signaling and consequently the maturation of osteoblastic mesenchymal cells, with higher alkaline phosphatase activity and extracellular matrix mineralization (Maeda et al., 2004). In a complementary assay, recombinant TGFB1 treatment repressed cellular proliferation and *in vitro* osteogenic differentiation in adipose derived stem cells from humans and mice (Levi et al, 2010).

Subpopulations negative for the mesenchymal surface marker CD105 (Endoglin) of murine bone marrow stem cells showed higher *in vitro* osteogenesis, adipogenesis and capacity of immunomodulation when compared with positive CD105 subpopulation and heterogeneous (unsorted) population (Anderson *et al,* 2013).

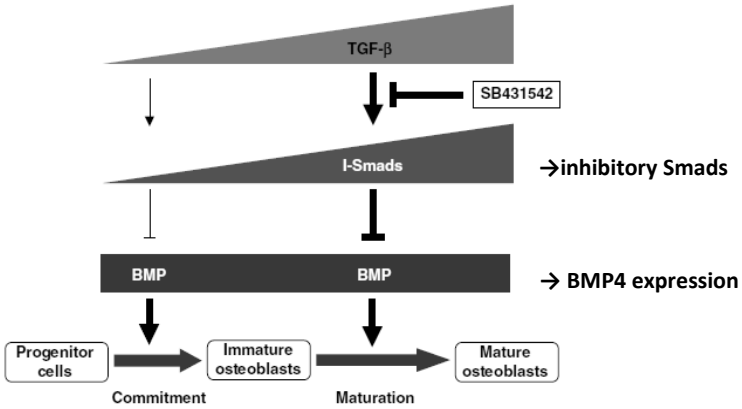

Figure 5. Scheme showing the BMP, SMADs and TGFB1 cross talk during osteogenesis. BMP induces the osteogenic differentiation acting in the early and late maturation of osteoblasts. Due to TGFB signaling, inhibitory SMADs suppress BMP and osteogenic differentiation. The presence of the TGFB1 receptor kinase inhibitor **SB431542,** suppress the expression of TGFB1 leading to an acceleration of BMP signaling and enhancement of osteogenesis (Adapted from Maeda *et al*, 2004).

Single-cell transcriptional analysis of hASCs, has demonstrated that different expression levels of CD105 were correlated with osteogenic markers expression and osteogenesis. Subpopulation of hASCs sorted for lower CD105 expression showed higher *in vitro* and *in vivo* osteogenic potential when compared with higher CD105 expression subpopulation and with the heterogeneous-unsorted population (Levi et al., 2011). Despite the important correlation between CD105 and osteogenesis, this study did not explore which molecules are involved in the regulation of CD105 expression. It is still unexplored if this correlation can be observed in MSCs obtained from other tissue sources.

Beyond the heterogeneity issue, MSCs differentiation potential can diverge among tissue of origin (Robey, 2011), present cellular replicative senescence (after long *in vitro* expansion somatic cells presents a restricted ability of self-renewal)

(Campis and Fagnagna, 2007; Ksiasek, 2009), and lower quantity of colony forming units-fibroblastic (CFU-f) per tissue during aging as observed at **Figure 6** (Caplan, 2007).

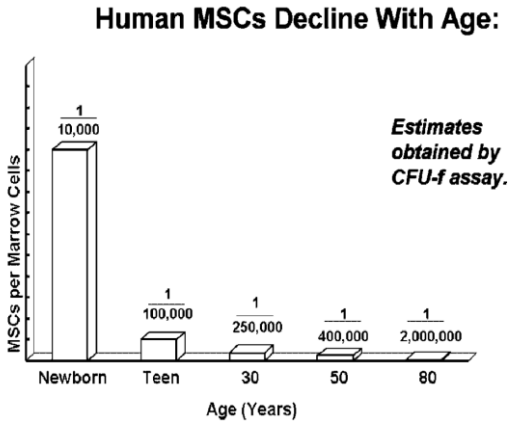

Figure 6. The number of colony forming units-fibroblastic (CFU-f) decline with aging, and the quantity of MSCs in bone marrow is reduced in adult and elderly subjects when compared to teens or newborn. (Adapted from Caplan, 2007).

1.4 iPSCs: an innovative technology

Cell reprogramming technology is an interesting way to bypass the lower expansion capacity of MSCs that limit their use in regenerative medicine (Katsara et al, 2011; Yoshida and Yamanaka, 2010). For example, iPSCs allow the derivation of countless cells with self-renewal capacity and pluripotential (Yu et al, 2007; Chin et al, 2009). In 2006 Takahashi and Yamanaka demonstrate that mature somatic cells could be reprogrammed through a retrovirus-mediated transduction method using four defined transcription factors (*OCT4, SOX2, KLF4*, and *C-MYC*). After transduction cells acquire a "pluripotency state" with properties similar to ESCs, such as capacity of differentiation into any cell type, gene expression profile of ESCs, high proliferation rate and self-renewal (Aasen et al, 2008; Puri and Nagy, 2012).

The main advantage using iPSCs approach is the simplicity and reproducibility of the technique that establish new avenues in regenerative medicine, basic research and disease modeling (Haraguchi et al, 2012; Tabar and Studer, 2014; Yamanaka, 2012). IPSCs can be directly derived from somatic tissues of adult subjects, avoiding the considerable concerns of ESCs use, such as ethical issues related to destruction of human embryos (ESCs are derived from the inner cell mass of mammalian blastocysts) and the probability of immunological rejections due to allograft ESCs use, and since the demonstration of iPSCs technology the number of publications in this area has considerably increased as illustrated in **Figure 7** (Cahan and Daley, 2013; Stadtfeld and Hochedlinger, 2010; Yamanaka, 2009). IPSCs can be obtained in a wide range of age, from newborns up to 74 years old, (Hossini et al, 2015), differently from MSCs that demonstrated limitation related to patient-age obtainment (Caplan, 2007).

The first strategy for cellular reprogramming was the use of retroviral and lentiviral transduction of "Yamanaka factors" (*OCT4, SOX2, KLF4*, and *C-MYC*), but these transgene insertions could disrupt the sequence of native genes leading to genetic modifications (Yoshida and Yamanaka, 2010).

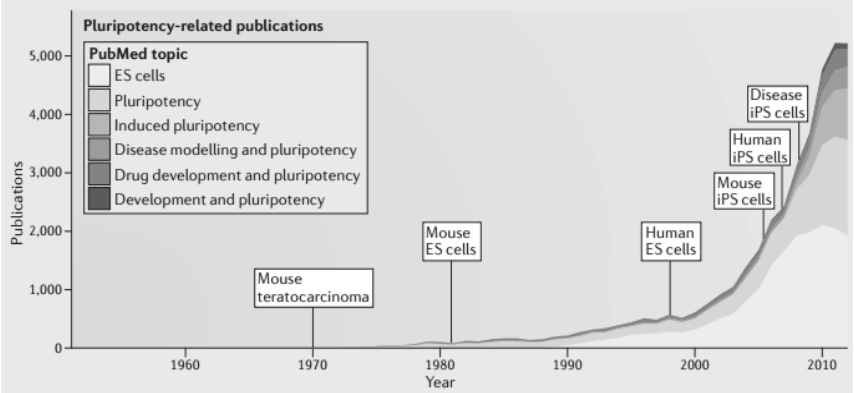

Figure 7. Somatic cells reprogramming to iPSCs in mouse 2006 (Takahashi and Yamanaka, 2006) and human dermal fibroblasts in 2007 (Yamanaka et al, 2007) increased and expanded the use of pluripotent stem cells for

regenerative medicine, drug screening, and disease modeling (Park et al, 2008). The publications in iPSCs area increased and the ESCs studies diminished (Adapted from Cahan and Daley, 2013).

Thus, laborious efforts and new methodologies have been developed to increase the reprogramming efficiency and reduce the needs of genetic modifications such as adenovirus, plasmid vector, removable transposon and episomal vector systems (Kaji et al, 2009; Okita et al, 2008 Okita et al, 2011; Stadtfeld et al, 2008; Woltjen et al, 2009; Yusa et al, 2009). Different human cell types derived from several somatic tissues can be used to obtain iPSCs. Human dermal fibroblasts were the first cell type used to obtain iPSCs (Takahashi et al., 2007) and thereafter several other somatic cell types as keratinocytes (Aasen et al, 2008), primary fetal tissues and adult MSCs (Park et al, 2008), fresh peripheral blood (Loh et al, 2009 and 2010), SHED (Yan et al, 2010), BMSCs (Megges et al, 2015) and hASCs (Zapata-Linares et al, 2016) have been successfully used. Mesenchymal stem cells derived from iPSC, called MSC-like cells, have been investigated as a good alternative cell source for bone regeneration. It is possible that these cells can better recapitulate bone development and being an intermediate cell-type between iPSCs and a fully specialized and differentiated lineage limit the drawbacks related to teratoma formation and open the possibilities to clinical use (Barberi et al, 2005; Jung et al, 2012; Guzzo et al, 2012).

There are diverse methods to obtain mesenchymal-like cells from pluripotent stem cells such as: isolating cells that migrate from embryoid bodies (EBs) formed via suspension culture (Hwang et al, 2008), monolayer differentiation through epithelial-mesenchymal transition that derives mesenchymal progenitor cells (Boyd et al, 2009), single-cell plating of iPSCs in gelatin-coated plates with mesenchymal induction media

(Nakagawa et al, 2009), culturing iPSCs on thin fibrillar type-I collagen coating (Liu et al, 2012) and the use of a small molecule inhibitor - transforming growth factor pathway inhibitor SB431542 (Chen et al, 2012).

MSC-like cells show the same characteristics of MSCs extracted from adult tissues without displaying *in vivo* tumor formation (Hematti et al, 2011; Gruenloh et al, 2011; Villa-diaz et al, 2012). MSCs differentiated from iPSCs exhibited greater regenerative potential, higher survival rate, telomerase activity and less senescence when compared with BMSCs (Diederichs and Tuan, 2014), and showed *in vitro* immunomodulatory properties (Giuliani et al 2011).

MSC-like cells also showed important properties in animal models such as: survival and commitment when differentiated to the chondrogenic lineage (Hwang et al 2008), potential utility in periodontal regeneration due to a considerable increment of mineralized tissue and bone regeneration in a periodontal defect animal model (Hynes et al 2013), enhancement of the vascular and muscle regeneration ameliorating severe limb ischemia (Lian et al 2010) and new bone formation process in calvarial defects in immunocompromised mice (Villa-diaz et al, 2012). However, it is still unclear if the osteopotential properties vary depending on the cell source used for cell reprogrammation by the pluripotency factors.

1.5 iPSCs as tool for *in vitro* disease modeling

Most of the knowledge on the mechanisms of human genetic diseases has been based on mouse models. This biological system approach have been considered the golden standard for modeling *in vivo* human disease, but the species-specific

differences between mice and humans related to physiological, biochemical, molecular and anatomical aspects have prompt the search for new methods to model human diseases (Tiscornia et al. 2011).

iPSCs have recently arisen as a new promising option to model human diseases *in vitro* and there are currently several successful examples such as studies of mechanisms related to Alzheimer´s disease (Israel et al, 2012; Yagi et al, 2011), Cardiotoxicity (Cohen et al, 2011), Down syndrome (Shi et al, 2012), Fragile X syndrome (Sheridan et al, 2011), Parkinson´s disease (Byers et al, 2011; Devine et al, 2011; Sanchez-Danes et al, 2012), Diabetes, Types 1 and 2 (Maehr et al, 2009; Ohmine et al, 2012), Multiple sclerosis (Song et al, 2012), Rett syndrome (Ananiev et al, 2011), autism spectrum disorders (Griesi-Oliveira et al., 2013; Machado et al., 2016) and many others. It would be also invaluable to model craniofacial disorders, as cranial human development is quite peculiar and might involve species-specific signaling.

One main advantage of cell reprogramming is that it enables the study and analysis of a specific disease (**Figure 8**), including rare disorders and syndromes in which the involvement of the individual's genome containing disease-specific alterations is mandatory (Trounson et al, 2012). Further, iPSCs can be differentiated towards cell types affected by the disease, under optimal conditions to observe relevant phenotypes. For example Miller and collaborators (2013) developed a strategy to induce aging features in iPSCs to model *in vitro* Parkinson's disease. Thus, the advent of iPSCs from patients paved the way to obtain different cell types from the same subject, which was previously not possible, revealing disease-relevant cellular pathology and enlightening human disease at the molecular and cellular level (Grskovic et al 2011).

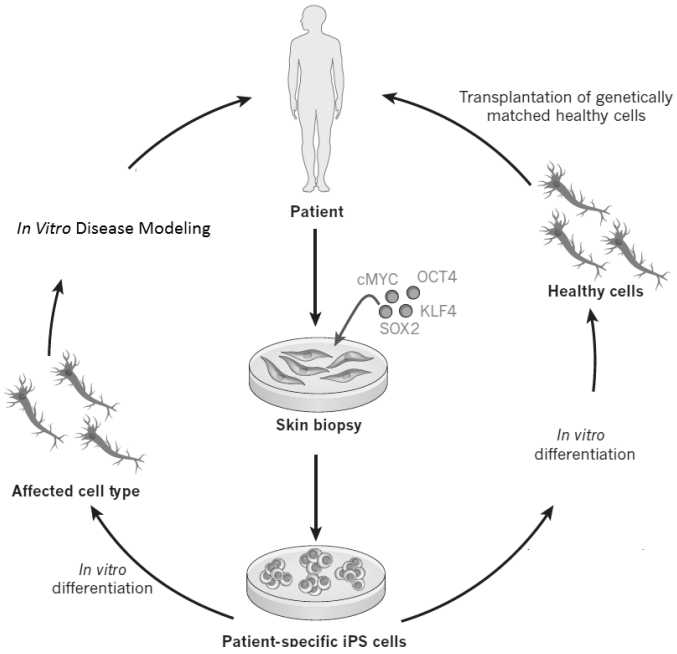

Figure 8. Applications of iPSCs. Cellular reprogramming technology allows the use of patient-specific cells from skin biopsy for example, and through the generation of iPSCs they can be used in the treatment of diseases (tissue engineering/Regenerative medicine) or to model and study some specific disease (Adapted from Robinton and Daley, Nature, 2012).

Here we describe the use of iPSC technology to model human developmental disease in which the pathogenic mutation is associated with craniofacial bone malformation. We selected the Treacher-Collins syndrome, an autosomal dominant rare mandibulofacial dysostosis that affects the craniofacial structures during human development. The main objective of this approach is to contribute to the comprehension and elucidation of new pathways and important mechanisms to bone neoformation and differentiation, more specifically the craniofacial bone formation. Despite the great advance in the field of stem cells in bone regeneration, as listed in **Figure 2**, the number of clinical trials in this area is still limited. Therefore, we expect that the *in vitro* recapitulation of craniofacial bone development can fill some missing lacuna in this field. This knowledge will possibly contribute to new molecules and

pathways associated to this process, which in turn allow the development of better protocols in human bone reconstruction and therapies.

1.6 Treacher-Collins Syndrome

Treacher-Collins syndrome (TCS) is a rare autosomal dominant mandibulofacialdysostosis present in 1:50,000 live births (Online Mendelian inheritance in Man (OMIM) TCS1, OMIM #154500; TCS2, OMIM#613717; TCS3, OMIM #248390) affecting facial morphogenesis (Phelps et al, 1981; Jones et al, 2008). The classic findings of this syndrome present variable expressivity such as antimongoloid slanting of the palpebral fissures, colobomas of the lower eyelids, hypoplasia of the facial bones, alteration of the external and middle ear ossicles resulting in some cases in conductive hearing loss, and cleft palate (Edwards et al, 1997; Mittmadn and Rodman, 1992; Trainor et al., 2009). Most patients require distraction osteogenesis during their rehabilitation in order to correct facial bone hypoplasia, but such interventions often do not provide good, long-lasting results (Kobus & Wójcicki, 2006; McCarthy & Hopper, 2002; Plomp et al 2016). Therefore, both craniofacial development and regeneration are compromised in these patients. Understanding the role of TCOF1 in these process possibly will shed new light on bone reconstruction.

TCS results from genetic alterations in TCOF1, POLR1C and POLR1D, that lead to nonsense-mediated mRNA decay or truncations, and the vast majority of TCS cases are caused by loss-of-function mutations in TCOF1 (Splendore et al., 2000). The gene TCOF1 encodes the TREACLE protein, a 144 kDa nucleolar phosphoprotein associated with ribosome biogenesis, (Gonzales et al., 2005), being essential for proper cell

growth and proliferation (Sakai et al, 2016). On the other hand, mutations in POLR1C and POLR1D are associated with deterioration of RNA polymerase I/III also leading to deficiency in ribosome biogenesis (Dauwerse et al., 2011; Trainor and Merrill, 2014).

This deficiency in ribosome biogenesis leads to lower cell proliferation, higher neuroepithelial apoptosis and insufficient formation of migrating cranial neural crest cells, that prompt the hypoplasia of craniofacial elements such as bone, cartilage and connective tissue, therefore the most affected cellular type in TCS is the neural crest cells, and the severe TCS cases needs major reconstructive surgeries that are rarely fully corrective (Jones et al 2008).

Understanding embryonic development is important to unravel the mechanisms that lead to the phenotype. NCCs emerge from the neuroepithelium and migrate into the pharyngeal arches, and then in the next step they proliferate and differentiate in important craniofacial structures such as cartilage, facial bones and connective tissue (Bhatt et al., 2013; Gong et al., 2014; Twigg & Wilkie, 2015).

In animal models for TCS, TCOF1 knockout leads to impairment of ribosome biogenesis resulting in higher apoptosis rate and deficit in the NCCs proliferation, culminating in cartilage and facial bone hypoplasia (Dixon et al., 1997; Jones et al., 1999; Dixon et al., 2006; Jones et al., 2008; Weiner et al., 2012). The use of animal models does not always reveal all mechanisms and cellular types affected in human TCS subjects, thus the use of iPSC technology with the capacity of differentiation in a wide range of cell types is essential to study human pathogenic mutations in *TCOF1*.

The possibility to recapitulate human embryogenesis through the use of iPSC technology is a promising strategy to study human craniofacial diseases, including TCS. Since NCCs are the most affected cellular type in TCS animal models, the

differentiation of iPSCs in iPSC-derived NCCs (iNCCs) is essential to observe if cells derived from TCS subjects present alterations related to important cellular properties like cell proliferation, apoptosis and differentiation potential (Menendez et al., 2013; Sakai et al., 2016).

Therefore the generation of iNCCs from iPSCs from TCS and control subjects will be essential to compare and observe alteration of cellular properties, and complement data acquired from animal models. The *in vitro* modeling and derivation of human iPSCs, iNCCs and MSC-like cells could further elucidate the underlying pathogenetic mechanism of TCS, especially in regards to the osteodifferentiation of craniofacial bones affected by the syndrome. This knowledge may provide foundation for the improvement of bone therapeutic strategies in the future.

Objectives

The main objectives of this work are:

• To compare the osteogenic potential of mesenchymal stem cells derived from exfoliated deciduous teeth and human adipose tissue and dissect the factors that lead to the differences related to*in vitro* osteogenesis in these mesenchymal stem cells;

• To verify if the osteogenic differentiation potential of mesenchymal cells derived from induced pluripotent stem cells depends on the somatic cell source.

• To verify if iPSCs can be used to model Treacher-Collins Syndrome.

CHAPTER II

Increased *In Vitro* Osteopotential in SHED Associated with Higher *IGF2* expression When Compared with hASCS

Stem Cell Rev and Rep (2015) 11:635–644
DOI 10.1007/s12015-015-9592-x

Increased In Vitro Osteopotential in SHED Associated with Higher *IGF2* Expression When Compared with hASCs

Roberto Dalto Fanganiello[1] · Felipe Augusto Andre Ishiy[1] · Gerson Shigeru Kobayashi[1] · Lucas Alvizi[1] · Daniele Yumi Sunaga[1] · Maria Rita Passos-Bueno[1]

Published online: 1 May 2015
© Springer Science+Business Media New York 2015

Abstract Mesenchymal stem cell (MSC) osteogenic differentiation potential varies according to factors such as tissue source and cell population heterogeneity. Pre-selection of cell subpopulations harboring higher osteopotential is a promising strategy to achieve a thorough translation of MSC-based therapies to the clinic. Here, we searched for novel molecular markers predictive of osteopotential by comparing MSC populations from two sources harboring different osteogenic potentials. We show that MSCs from human deciduous teeth (SHED) have an intrinsically higher osteogenic potential when compared with MSCs from human adipose tissue (hASCs) under the same in vitro controlled induction system. Transcriptome profiling revealed *IGF2* to be one of the top upregulated transcripts before and during early in vitro osteogenic differentiation. Further, exogenous IGF2 supplementation enhanced alkaline phosphatase activity and matrix mineralization, and inhibition of IGF2 lessened these parameters in SHED and hASCs, validating *IGF2* as an osteogenic factor in these MSCs. Further, we found *IGF2* to be biallelically expressed in SHED, but not in hASCs. We observed a 4 % methylation increase in the imprinting control region within the *IGF2-H19* locus in SHED, and this is mainly due to 2 specific CpG sites. Thus, we suggest that *IGF2* upregulation in SHED is due to loss of imprinting. This study unravels osteogenic properties in SHED, implying *IGF2* as a potential biomarker of MSCs with higher osteopotential, and unveils *IGF2* loss-of-imprinting in SHED.

Keywords SHED · hASCs · In vitro osteopotential · *IGF2* · Imprinting · Biallelic expression

Introduction

Studies on the use of mesenchymal stem cells (MSCs) for cellular therapies with the ultimate goal of bone regeneration are mainly based on their capacity of self-renewal, direct differentiation toward the osteogenic lineage and the ability to secrete trophic factors that may contribute to bone repair [1, 2]. These characteristics have been firstly explored in bone marrow mesenchymal stem cells (BMSCs) both in the lab and in different clinical scenarios [3–5]. However, BMSCs are scarce, and bone marrow harvesting remains painful and laborious. Therefore, there is an increasing interest in studying osteogenic cells from more convenient tissue sources, such as dental pulp and adipose tissue.

Stem cells from human exfoliated deciduous teeth (SHED), a specific type of dental pulp stem cell (DPSC), are potentially useful due to their differentiation plasticity, noninvasive isolation process, and similarity to osteoprogenitor cells [6–9]. SHED have been used to repair cranial defects in immunocompromised mice [10], to reconstruct trabecular bone in systemic lupus erythematosus-like MRL/lpr mice [8], and to aid critical-size calvarial defect regeneration in Wistar rats [11]. Human adipose tissue-derived stem cells (hASCs) represent another promising MSC type since they can be harvested from the stromal-vascular fraction of adipose tissue in abundant quantities by a simple surgical procedure. Their osteogenic potential has been demonstrated by the use of different culture

Electronic supplementary material The online version of this article (doi:10.1007/s12015-015-9592-x) contains supplementary material, which is available to authorized users.

✉ Roberto Dalto Fanganiello
robertofanganiello@gmail.com

[1] Departamento de Genética e Biologia Evolutiva, Instituto de Biociências, Universidade de São Paulo, Rua do Matao, 277, sala 200, Sao Paulo, SP, Brazil 05508-090

conditions containing osteoinductive factors [12–15] and hASCs were used in clinical trials, however, with a limited number of cases [16, 17].

In spite of these reports, evidence for sound clinical efficacy of the use of MSCs for bone regeneration has been challenging to confirm, and the therapeutic mechanisms supposedly leading to bone formation are incompletely understood and increasingly speculative. In addition, no therapy based on MSCs has yet had FDA approval [18]. Despite many studies examining SHED- and hASC-mediated osteogenesis and bone formation [6, 8–10, 19–23], the molecular rules that govern their osteopotential are still under debate. Variable differentiation potential is seen both in MSCs from different tissue sources and in cellular populations from the same tissue source, the latter being attributed to cell heterogeneity [24], and success of MSC-based bone regenerative medicine could be improved with pre-selection of cells harboring higher osteogenic potential [23, 25–27]. Therefore, this study has three main aims: 1) to compare the in vitro osteopotential of SHED and hASCs under the same induction system; 2) to identify molecular mechanisms governing osteogenic properties in these MSCs; 3) to identify predictive markers of osteogenic potential in these MSCs.

Material and Methods

Ethics and Financial Interest Statement

This study was approved by the Institute of Biosciences'Human Research Ethics Committee (permit number 104.120.09). We certify that no financial support or benefits have been received by any co-author or from any commercial source directly or indirectly related to the work reported in this article.

Isolation of Dental Pulp and Adipose-Tissue Derived Stem Cells

SHED populations were isolated from donated deciduous teeth obtained upon signed informed consent by the subjects'legal guardians. Dental pulps were extracted from normal deciduous teeth of six subjects (aged from 6 to 10 years). Donors were previously evaluated for systemic diseases and oral infections and subjects with these conditions were excluded. Dental pulp fragments were retrieved with a barbed nerve broach instrument and cells were isolated according to the protocol described in Miura et al., 2003 [6].

hASCs were isolated from sub-abdominal adipose tissue obtained after liposuction procedures upon informed consent. Adipose tissue was obtained from six subjects (aged from 24 to 68 years) undergoing elective liposuction procedure. The unprocessed lipoaspirate was washed with equivalent volume of PBS supplemented with 1 % Pen Strep (Life Technologies, CA., USA) and enzymatically dissociated with 0.075 % collagenase type I (Sigma-Aldrich, St. Louis, USA). Enzyme activity was neutralized with DMEM/F12 (Life Technologies, CA., USA) containing 10 % fetal bovine serum (FBS; Life Technologies, CA., USA). Infranatant was centrifuged at 1, 200xg for 5 minutes to pellet cells. Cells were seeded in 6-well culture plates (Corning, N.Y., USA) containing MSC growth medium (DMEM/F12 supplemented with 15 % FBS, 1 % Pen Strep and 1 % MEM non-essential aminoacids (Life Technologies, CA., USA).

After 14 days, SHED and hASCs cultures were washed with 1x PBS, dissociated with TrypLE (Life Technologies, CA, USA) and seeded at a 10 [4] cells/cm [2] concentration onto 25 cm [2] culture flasks (Corning, N.Y., USA). Cells were kept in MSC growth medium at 37 °C in a 5 % CO2 humidified incubator and maintained in semi-confluence to prevent differentiation. Passages were done every 4–5 days and medium was refreshed every 3 days. All experiments were performed between the third and fifth subculture, with n=6 for the SHED and the hASCs groups and samples were not pooled.

Immunophenotyping

Immunophenotype characterization of cultured SHED and hASC populations was done by flow cytometry analysis. Cellular populations were harvested with TrypLe (Invitrogen, CA, USA), washed with 1x PBS and incubated with BSA for 1 hour at 4 °C with the following anti-human antibodies: CD29-PECy5, CD34PerCP, CD31-PE, CD45-FITC, CD90-R-PE, CD73-PE, CD105-PE (Becton, Dickinson and Company, NJ, USA). Matched control samples were incubated with PBS free of antibodies. Cell suspensions were washed with PBS, and 10,000 labeled cells were analyzed using a Guava easyCyte flow cytometer running the Guava ExpressPlus software (Merck Millipore, Darmstadt, Germany). Experiments were done in technical triplicates for each cell sample and for each antibody.

In vitro Osteogenic Differentiation Experiments

Subconfluent cell populations of SHED and hASCs were treated with osteogenic induction medium containing DMEM-Low Glucose (Life Technologies, CA., USA) supplemented with 10 % FBS (Invitrogen, CA., USA), 50μM ascorbate-2-phosphate, 10 mM β-glycerophosphate, 0.1μM dexamethasone (Sigma-Aldrich, St. Louis, USA), 100 U/ml penicillin, 100 g/ml streptomycin (Invitrogen, CA., USA) with media changes every three days. Alkaline phosphatase activity was assessed through a biochemical assay on the 9th day of in vitro osteogenic differentiation (SHED: n=6; hASCs: n=6). Briefly, cells were provided with phosphatase substrate (Sigma-Aldrich, St. Louis, USA) and the resulting p-

nitrophenol was quantified colorimetrically using a Multiskan EX ELISA plate reader (Thermo Scientific, MA., USA) at 405 nm. Calcium matrix production was analyzed after 21 days of in vitro osteogenesis by Alizarin Red-S staining (SHED: n=6; hASCs: n=6). Cells were washed three times with 1xPBS, fixed with a 70 % ethanol solution for 30 minutes at room temperature, followed by three distilled water washes and finally stained with a 0.2 % Alizarin Red-S solution (Sigma-Aldrich, St. Louis, USA) for 30 min at room temperature. Staining was removed with a solution of 20 % methanol / 10 % acetic acid and measured colorimetrically using a Multiskan EX ELISA plate reader at 450 nm. As a negative control for both assays we used the same cells cultivated in regular proliferation medium. Experiments were done in technical triplicates for each time point and for each cell line.

RNA Extraction, Microarray and qRT-PCR Experiments

SHED and hASCs at 80 % confluence seeded in 25 cm [2] cell culture flasks were used for in vitro osteoinduction followed by RNA extraction and microarray / RT-qPCR assays. Total RNA was isolated from osteogenic medium-treated cells and untreated cells using a Nucleospin RNA II kit (Macherey-Nagel, Duren, Germany), following manufacturer's instructions. RNA quality and concentration were measured by 2 % agarose gel electrophoresis and Nanodrop ND-1000 (Thermo Scientific, MA., USA), respectively.

Gene expression microarray assays were performed at three time points of early in vitro osteogenesis: immediately before induction (day 0) and at days 4 and 6 of osteoinduction. cDNA was prepared with Affymetrix GeneChip WT cDNA Synthesis and Amplification Kit (Affymetrix, CA., USA), following manufacturer's instructions. cDNA fragmentation and labeling was performed with Affymetrix GeneChip WT Terminal Labeling Kit (Affymetrix, CA., USA) and 5.5 µg of labeled cDNA target was used to hybridize Affymetrix GeneChip Human Gene 1.0 ST array chips (Affymetrix, CA., USA) for 16 h at 45 °C, following manufacturer's instructions. Chips were washed and stained using an Affymetrix GeneChip Fluidics Station 450 and scanned using an Affymetrix GCS 3000 scan (Affymetrix, CA., USA). Raw microarray data were normalized through Robust Multichip Average preprocessing method [28] and the ComBat method was applied for the batch effect corrections [29]. Only genes showing high expression variance among arrays were retained through the use of interquartile range (IQR=1). Multi-class Significance Analysis of Microarrays (SAM, $p \leq 0.05$ [30],) adjusted by False Discovery Rate [31] was used to detect the differentially expressed genes (DEGs) for each time-point (immediately before induction and at days 4 and 6 of osteoinduction) in each stem cell group (BMSCs, SHED and hASCs). Ingenuity Pathway Analysis (IPA®, QIAGEN Redwood City, www.qiagen.com/ingenuity) software was used for gene interaction analysis and functional classification of differentially expressed genes. Hierarchical clustering was performed with EXPANDER (EXpression Analyzer and DisplayER - http://acgt.cs.tau.ac.il/expander/), under standard parameters.

Gene expression of osteogenic markers (*DLX5*, *RUNX2*, *BGLAP* and *ALP*) and *IGF2* was quantified before (T0) and after one, two and three days (T1, T2 and T3) of in vitro osteogenic induction by qRT-PCR (SHED: n=3; hASCs: n=3). Briefly, one microgram of total RNA extracted from SHED and from hASCs populations (SHED: n=3; hASCs: n=3) was converted into cDNA using Superscript II, according to manufacturer's recommendations. cDNAs from each cell type were pooled and used as a calibrator. qRT-PCR reactions were performed in triplicates with final volume of 25 µL, using 20 ng cDNA, 2X SYBR Green PCR Master Mix, and 50 nM – 200 nM of each primer. Fluorescence was detected using ABI Prism 7500 Sequence Detection System, under standard temperature protocol. Primers were designed with Primer-BLAST (http://www.ncbi.nlm.nih.gov/tools/primer-blast/; see Table S1 for primer sequences). Primers' amplification efficiencies (E) were determined by serial cDNA dilutions expressed in $\log_{10}$ in which $E=10^{-1/slope}$. Expression of target genes was assessed relative to a calibrator cDNA pool (ΔCt). GeNorm v3.4 [32] was used to calculate normalization factors for each sample, considering *GAPDH*, *HPRT1* and *SDHA* endogenous expression. The final expression values were determined based on a previous method [33] dividing $E^{-\Delta Ct}$ by the corresponding normalization factor. Primers and reagents were supplied by Life Technologies.

Western Blotting

SHED and hASCs were plated at a density of 4000 cells/cm [2] in 75 cm [2] flasks and cultured until 80 % confluence in MSC growth medium and serum-starved in DMEM/F12 without FBS for 48 h. Total protein lysates were obtained using RIPA Buffer (1 % NP-40, 0.5 % SDS, 0.5 % Sodium Deoxycholate, 50 mM Tris–HCl, 150 mM NaCl and 1 mM EDTA) containing protease and phosphatase inhibitor cocktails (Sigma-Aldrich, St. Louis, USA). Protein concentration was determined using a bicinchoninic acid assay kit according to manufacturer's instructions (Thermo Fisher Scientific, IL., USA). Total cell lysates (20 µg) were separated by SDS-PAGE and dry-transferred to nitrocellulose membranes with the iBlot system (Life Technologies, CA., USA) according to manufacturer's recommendations. Membranes were blocked in buffer TBS-T (1 M Tris–HCl pH 7.5, 5 M NaCl, 0.1 % Tween-20) 5 % BSA under constant stirring for 1 h at room temperature, washed 4x with TBS-T, and incubated with anti-IGF2 (1:1000 dilution in TBS-T/BSA; SAB1408589 – Sigma-Aldrich, St. Louis, USA) primary antibody overnight at 4 °C. Detection was performed using anti-rabbit IgG, HRP-

linked Antibody (1:2000 dilution in TBS-T/BSA; Cell Signaling) under constant stirring for 1 h at room temperature, ECL Prime substrate (GE Healthcare), and Image Quant LAS 4000 Mini (General Electrics). β-actin was used as a loading control (HRP-linked anti-β-actin, Abcam). The intensity of the bands was determined by densitometry using NIH ImageJ software (http://rsbweb.nih.gov/ij/). IGF2 protein levels were quantified and normalized to the corresponding β-actin levels.

IGF2 and Chromeceptin Treatments

To test the effects of IGF2 supplementation and chromeceptin treatment (C0868 – Sigma-Aldrich, St. Louis, USA) on SHED and hASCs osteogenic potential, we added IGF2 (ProsPec, CYT-265) and chromeceptin (Sigma-Aldrich, St. Louis, USA) to the osteogenic medium at a concentration of 2x10 [2] nM and 0.3 μM respectively, in independent experiments. Alkaline phosphatase activity was assessed after 9 days of in vitro osteogenesis and alizarin red-S staining was performed after 21 days of osteoinduction for both treatments. These experiments were performed in 3 SHED and 3 hASC independent populations.

IGF2 Genotyping

Genotypes of 10 SHED and 10 hASCs populations for potential IGF2 polymorphisms were determined by PCR and Sanger sequencing of genomic DNA and cDNA. Optimal annealing temperatures for each primer pair was determined by PCR on a gradient thermal cycler (Table 1).

Bisulfite Sequencing

Bisulfite treatment was used to convert unmethylated cytosines to uracil. Two micrograms of genomic DNA were bisulfite treated using the Epitect Bisulfite Kit (QIAGen), following manufacturer's recommendations. From 20 μl of eluted converted DNA, 1 μl was used for subsequent PCR. Primers sequences *TGAGATTTTTTTTGTAGGGTTTATG* and *AAAA CACCTCATTATTCCCCTAATAT* were used to amplify the *IGF2* converted region, with the following cycling conditions: 95 °C for 5 min followed by 40 cycles of 94 °C for 30 sec, 54 °C for 3 min, 72 °C for 1 min and one cycle of 72 °C for 5 min. PCR products were cloned using the TOPO TA Cloning kit (Life Technologies, CA., USA) and 10 clones per sample were submitted to sequencing reaction using the BigDye® Terminator v3.1 Cycle Sequencing Kit (Life Technologies, CA., USA) and sequenced in the ABI 3730 DNA Analyzer. Finally, CpG methylation levels in each clone were calculated using the BISMA (Bisulfite Sequencing DNA Methylation Analysis) online tool.

Statistical Analysis

Continuous variables were expressed by mean and standard deviation, and groups were compared by Student's *t*-test. A p-value<0.05 was considered statistically significant. Tests were done using the GraphPad InStat software (GraphPad) [34].

Results

After isolation, both SHED and hASCs displayed spindle-shaped fibroblastoid morphology. They showed a similar and homogeneous immunophenotype regarding the panel of cell surface markers: SHED and hASCs expressed similarly high levels of mesenchymal markers (>95 % for CDs 29, 73, 90, 105) and low levels of endothelial (<2 % for CD31) and hematopoietic (<2 % of CDs 34 and 45) markers. Thus, these results attest their mesenchymal origin (figure S1).

Both cell groups showed increased expression of osteogenic markers after three days of in vitro osteogenesis (*RUNX2*, *ALP* and *BGLAP* in SHED and *RUNX2*, *ALP* and *DLX5* in hASCs). Alkaline phosphatase (ALP) activity was higher and mineralized matrix was produced, respectively, after 9 and 21 days of osteoinduction in SHED and hASCs (Fig. 1a-d). Even though SHED and hASCs responded positively to osteoinduction, gene expression of osteogenic markers was generally higher in SHED when compared with hASC populations (Fig. 1a). Additionally, ALP activity after 9 days of osteoinduction and extracellular matrix mineralization after 21 days of in vitro osteogenesis were increased 1.61-fold ($p<0.05$) and 2.24-fold ($p<0.0001$), respectively, in SHED when compared with hASCs (Fig. 1b-d). These results

Table 1 Primers used for real-time quantitative PCR experiments

Gene	NCBI reference sequence code	Forward sequence	Reverse sequence
RUNX2	NM_001024630.3	AGTGGACGAGGCAAGAGTTTC	GTTCCCGAGGTCCATCTACTG
ALP	NM_000478.4	GATACAAGCACTCCCACTTCATCTG	CTGTTCAGCTCGTACTGCATGTC
GAPDH	NM_001256799.1	TGCACCACCAACTGCTTAGC	GGCATGGACTGTGGTCATGA
HPRT1	NM_000194.2	TGACACTGGCAAAACAATGC	GGTCCTTTTCACCAGCAAGCT
SDHA	NM_004168.2	TGGGAACAAGAGGGCATCTG	CCACCACTGCATCAAATTCA

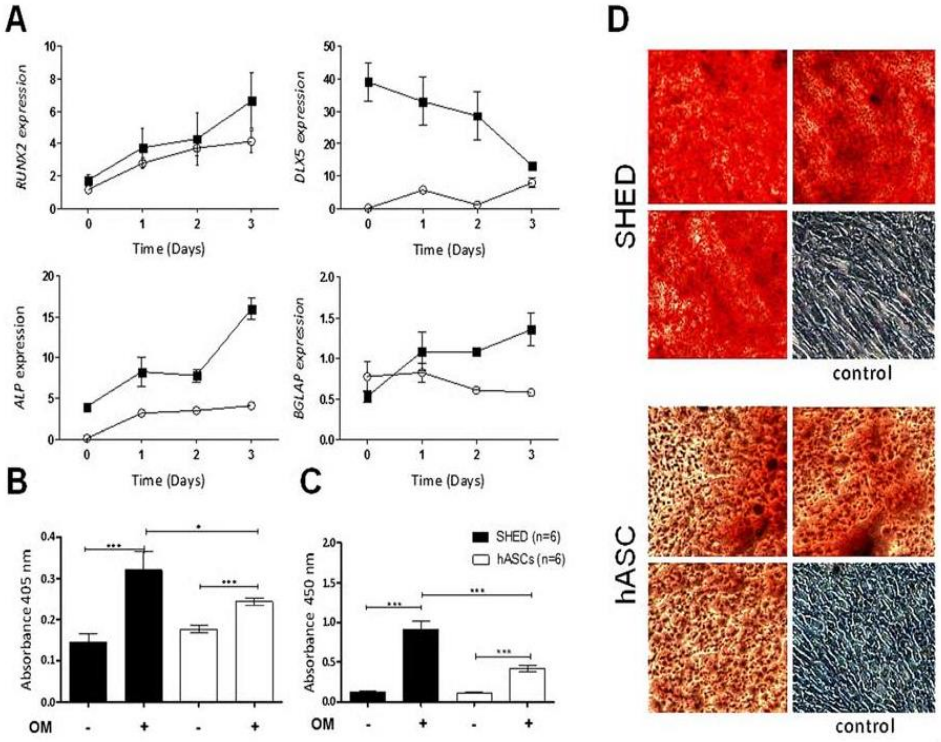

Fig. 1 Analysis of early osteogenesis in SHED and hASCs (n=6 per cell type). **a**) qRT-PCR results for *DLX5*, *RUNX2*, *ALP* and *BGLAP* during the first 3 days of osteoinduction. Quantification of alkaline phosphatase activity (**b**) and alizarin red-S staining (**c**), respectively at the 9th and 21st day of in vitro osteogenic differentiation. **d**) Representative micrographs of the alizarin red-S staining after 21 days of in vitro osteoinduction

suggest that SHED present increased in vitro osteogenic potential as compared to hASCs.

In order to investigate the molecular mechanisms behind the osteogenic differences between SHED and hASCs, we performed global gene expression profiling during three time points of early in vitro osteogenesis: immediately before induction (day 0) and at days 4 and 6 of osteoinduction in SHED and hASCs, using human BMSCs (hBMSCs) as a positive control. By comparing the expression profiles in these three time points for each cell group, we identified 34 differentially expressed genes (DEGs) in SHED, 87 in hASCs and 198 in hBMSCs. We first tested if DEGs exclusively shared by SHED and hBMSCs groups during early osteogenesis contribute to enrichment in pathways associated with osteogenesis. Eleven differentially expressed transcripts were common between hBMSCs and SHED, but they were not identified as DEGs in hASCs; further, through the use of the Ingenuity Pathway Analysis software, we observed that Interleukin 17A (p<6.13 e-4) and RXR/RAR pathways (p<1.85 e-4), both previously associated with osteogenesis, were the most enriched in SHED and hBMSC groups. On the other hand, 43 DEGs were shared exclusively by hBMSCs and hASCs, and using IPA we observed that Serine biosynthesis (p<4.75 e-5) and Superfamily of Serine and Glycine Biosynthesis (p<9.94e-5), none of them involved in osteogenesis, were identified as the most enriched pathways in this group. These data, together with the osteogenic differentiation comparison, show an overall increase in SHED osteopotential when compared with hASCs.

In a second analysis aiming to identify molecular markers predictive of osteodifferentiation capacity, we performed a hierarchical clustering of each cell population grouped per time point. *IGF2* and *ITGA8* were revealed as the top upregulated transcripts in SHED and hBMSCs in comparison with hASCs at day 0 (before osteoinduction), and *IGF2* remained upregulated in these MSCs until day 6 of early osteogenesis (Fig. 2a). Considering the important role played by *IGF2* during bone formation, remodeling and homeostasis [35, 36], and the upregulated pattern of *IGF2* in early osteogenesis in SHED and hBMSCs, we selected *IGF2* for validation of mRNA and protein expression in SHED cultures in comparison with hASCs cultures. Both *IGF2* mRNA upregulation and higher IGF2 protein production were observed in SHED as compared to hASCs before osteoinduction (day 0, average of 32.2-fold upregulation in *IGF2* mRNA, $p \leq 0.01$, n=10 per cell group, and p<0.05, n=11 per cell group for IGF2 protein expression) (Fig. 2b-c). We also validated *IGF2* mRNA upregulation during the first 8 days of in vitro osteogenesis (Fig. 2c).

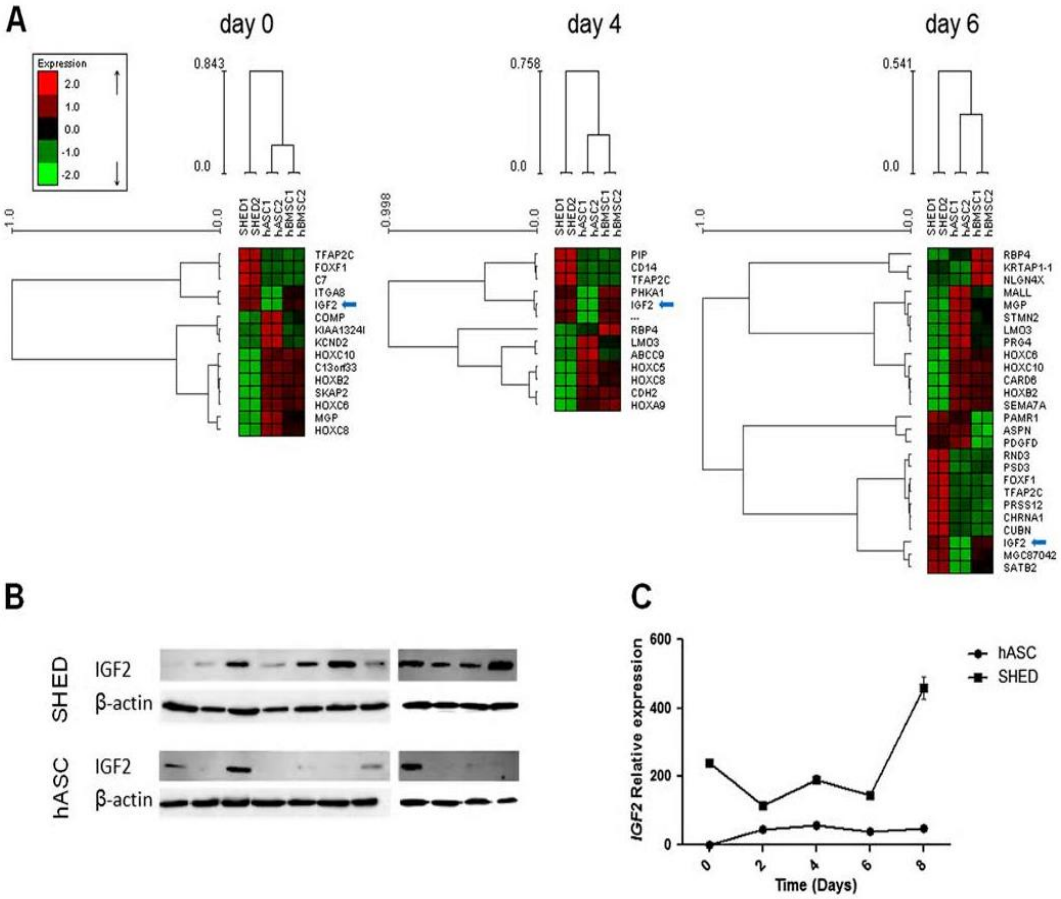

Fig. 2 **a**) Hierarchical clustering analysis showing expression patterns of differentially expressed transcripts during early in vitro osteogenesis in SHED, hASCs and hBMSCs (n=2 per cell type, days 0, 4 and 6). *IGF2* upregulation in SHED and hBMSC is indicated by the *blue arrows*. **b**) Western blotting for IGF2 detection in SHED and hASCs (n=11 for each sample, day 0), anti β-actin antibody was used as loading control. **c**) qRT-PCR of *IGF2* during the first 8 days of in vitro osteoinduction in SHED and hASCs (n=3 per cell type)

To characterize the effect of IGF2 signaling during osteogenesis in SHED and hASCs we added exogenous IGF2 to the osteogenic medium used for in vitro osteoinduction. This treatment intensified osteogenesis both in SHED and in hASC cultures, shown by enhanced ALP activity after 9 days of osteoinduction (1.19 times in SHED, $p<0.01$; 1.30 times in hASCs, $p<0.001$, n=3 per cell group, Fig. 3a) and mineralized matrix production after 21 days of in vitro osteogenesis (3.04 times in SHED, $p<0.05$; 4.41 times in hASCs, $p<0.001$, n=3 per cellular group, Fig. 3a). Next, we administered chromeceptin, an IGF2 inhibitor at both the transcriptional and signaling levels, during in vitro osteoinduction. Chromeceptin treatment led to a significantly lower ALP activity (2.43 times in SHED, $p<0.001$; 2.482 times in hASCs, $p<0.001$, n=3 per cell group, Fig. 3b) and matrix mineralization (1.351 times in SHED, $p<0.01$; 1.572 times in hASCs, $p<0.05$, n=3 per cell group, Fig. 3b) both in SHED and hASCs. These results show a direct correlation between IGF2 pathway activation and in vitro osteogenesis in these MSCs.

We hypothesized that *IGF2* upregulation in SHED may be due to an increase in methylation of the CpG-rich imprinting controlling center within the *IGF2-H19* intergenic region [37, 38] or deviations from the monoallelic expression accounted for this locus. First, we determined the methylation status of 17 CpG sites in the *IGF2-H19* intergenic region (n=10 per cellular population and n=10 clones per sample) by bisulfite sequencing. SHED samples had 50.9 % of methylated CpGs in comparison with 46.9 % in hASCs ($p\leq0.0001$). Since this difference could be due to site-specific increased methylation, we next compared the differences in methylation per site and verified that sites 3 and 16 have significantly higher methylation on SHED samples when compared with hASCs (20.1 % increase, p=0.014 and 18.3 % increase, p=0.023, respectively).

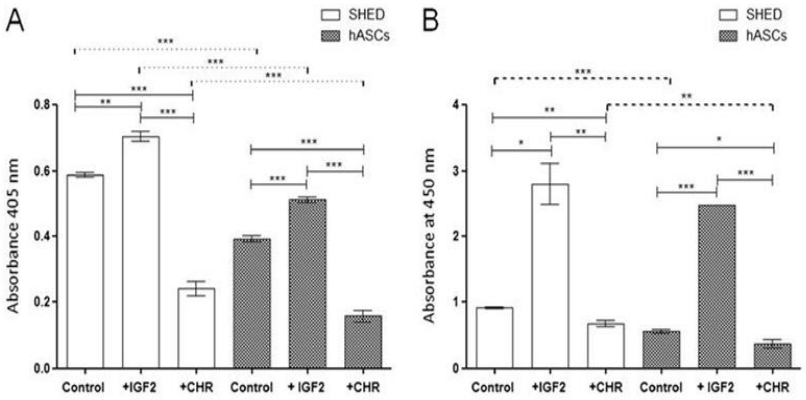

Fig. 3 **a**) Alkaline phosphatase activity and (**b**) alizarin red-S quantification of SHED and hASC in vitro osteogenesis, respectively after 9 and 21 days of osteoinduction with addition of exogenous IGF2 (+IGF2) or chromeceptin (+CHR), an IGF2 inhibitor at the transcriptional and signaling levels (n=3 per cell type)

Additionally, to investigate whether allelic transcriptional imbalances could be leading to the higher *IGF2* expression observed in SHED, we genotyped the *IGF2* polymorphism rs3168310 in SHED and hASCs (n=10 per cell population) by sequencing their genomic DNA as well as cDNA. Four SHED and one hASC population were informative (heterozygous at one or more polymorphisms at the genomic level – Fig. 4). In this group, the hASC population was homozygous at the cDNA level, thus displaying *IGF2* monoallelic expression, as expected. Conversely, the informative SHED populations were heterozygous at the cDNA level, which indicates *IGF2* biallelic expression in these cells. Sequencing of an additional polymorphism (rs2230948) confirmed these results (data not shown).

Discussion

Even though it is well established that SHED and hASCs are capable of undergoing osteogenesis in vitro, we show in this study that SHED have higher osteogenic potential when compared with hASCs under the same in vitro controlled conditions: SHED populations display higher gene expression of four hallmark osteogenesis markers (*RUNX2*, *DLX5*, *ALP* and *BGLAP*) during the first three days of in vitro

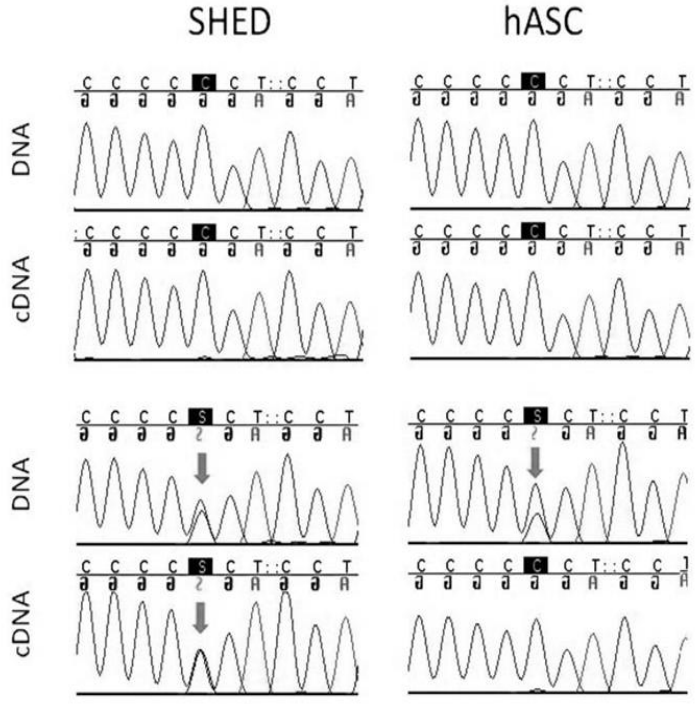

Fig. 4 Electropherograms of DNA and cDNA sequencing of rs3168310 (C/G) *IGF2* polymorphism in SHED and hASC samples (n=10 per cell type). *Blue arrows* indicate heterozygosis

osteodifferentiation, higher alkaline phosphatase (ALP) activity after 9 days of osteoinduction and produce more mineralized matrix after 21 days of in vitro osteogenesis, when compared with hASCs.

To better understand the molecular underpinnings of these variations in osteogenic differentiation efficiency, we performed microarray-based genome-wide expression profiling in three time points spanning early SHED and hASC in vitro osteogenesis. Interleukin-17A (IL-17A) and Retinoid X Receptor / Retinoic Acid Receptor (RXR/RAR) pathways, the most enriched pathways in SHED and hBMSCs during early osteogenesis, are recognized as important mediators of bone metabolism and homeostasis [39–41]. However, no enrichment of osteogenesis pathway was observed in hASCs. These results endorse that enrichment of these pathways during early in vitro osteogenesis of SHED and hBMSCs are in line with the higher in vitro osteogenic potential displayed by them as compared with hASCs.

The comparative transcriptome analysis grouping each cellular population per time point (0, 4 and 6 days of in vitro osteoinduction) led to the identification of *IGF2* as a differentially expressed transcript before and during early osteoinduction in SHED and hBMSCs. We demonstrated that both IGF2 mRNA and protein are upregulated in SHED when compared with hASCs, suggesting that IGF2 plays an important role in the increased in vitro osteogenesis observed in SHED when compared with hASCs.

We validated IGF2 as an osteogenic factor in SHED by verifying that supplementation with exogenous IGF2 enhanced alkaline phosphatase and matrix mineralization both in SHED and hASCs while treatment with chromeceptin efficiently inhibited osteogenesis in both cell types. Moreover, hASCs supplementation with IGF2 during in vitro osteogenesis rescues their osteogenic potential, which becomes very similar to SHED osteopotential. In fact, IGF2 is known to be highly expressed in bone tissue and is recognized to promote bone formation and remodeling [35, 42–44]. It has also been shown that upregulation of IGF2 is implicated in priming MSC differentiation into osteoprogenitor cells, in in vivo osteogenesis and in adult bone remodeling in mice [45].

The finding of endogenous upregulation of *IGF2* before osteoinduction in a MSC population with intrinsically higher osteopotential suggests that this molecule can be a candidate predictive biomarker of bone formation. In this regard, with the purpose of identifying differentiation-stage specific markers defining ex vivo osteoblastic phenotype, Twine et al. 2014 studied the gene expression profile of immortalized hMSC-TERT cells during different time-points of in vitro osteogenesis and identified *IGF2* as a late-stage osteogenic differentiation gene, with peak expression at 9 days of osteoinduction [46]. Even though *IGF2* upregulation was not reported in time points earlier than 9 days of in vitro differentiation, we do not believe this is in discordance with our results since the authors used only one type of MSCs to investigate temporal variations in gene expression during in vitro osteogenesis.

It is possible that the upregulation of *IGF2* in SHED is related to a different pre-differentiation state, to an enrichment of osteolineage progenitor cells or to an altered regulation pattern, which could be linked to the cell source niche. In this manuscript we report a global increase of 4 % in methylation of the *IGF2-H19* intergenic imprinting controlling region (ICR) in SHED, in comparison with hASCs, and these differences were mainly due to significantly higher methylation in two CpG sites in SHED populations, where methylation was increased at least more than 18 % for each site, compared with hASCs. We speculate that this mechanism could be associated with the biallelic *IGF2* expression found in SHED populations but not in hASCs. Although the differences in methylation are not more than two fold, it is well known that the stoichiometry of *IGF2* loss of imprinting leading to a doubling of *IGF2* mRNA abundance does not always occur [47]. Even though *IGF2* is maternally imprinted in most human tissues and transcribed exclusively from the paternally inherited chromosome [48], loss of imprinting has been observed in several situations. For example, *IGF2* overexpression due to dysregulation of *IGF2* imprinting is a hallmark of many human malignant tumors, including osteosarcoma, lung neoplasms, ovarian cancers and Wilms tumor, and it also occurs in Beckwith-Wiedemann Syndrome, a human genetic disease characterized by fetal overgrowth, organomegaly and tumor predisposition [49]. Loss of imprinting of *IGF2* has also been reported in normal human tissues, such as fetal and adult liver [50, 51], brain [52], newborn cord blood [53] and cervical tissue [54].

We suggest that *IGF2* upregulation in SHED is thus related to loss of imprinting. We cannot rule out that the *IGF2* expression differences between SHED and hASCs are due to the age difference of the primary donor tissues; however, in that case we would have observed the opposite, that is, older cells would be more likely to lose *IGF2* imprinting. In line with our findings, there is an increasing body of literature implicating epigenetic regulation as an important modulator of MSC osteogenesis [55–59].

As demonstrated in several studies, mesenchymal stem cells isolated from the dental pulp tissue of adult teeth (DPSCs) harbor a robust osteogenic potential [23, 25–27] and their use in clinical scenarios has commenced [60, 61]. In light of that, the findings outlined in this report help to provide a more solid ground to the use of SHED in stem-cell based tissue engineering and regenerative medicine.

Conclusion

In summary, this study contributes to the elucidation of intrinsic osteogenic properties associated with SHED and hASCs,

indicates *IGF2* as a potential biomarker to pre-select cells with increased osteogenic potential and reveals loss of *IGF2* imprinting in SHED. We expect that our findings will be helpful for a more thorough translation of the stem cell-based bone regeneration technology to the clinic. We also believe that our findings will contribute to the challenging issue of attaining better reproducibility and clinical efficacy in MSC-mediated bone formation.

Acknowledgments We would like to thank Constancia Gotto Urbani for secretarial assistance, Andressa Gois Morales and Simone Gomes Ferreira for technical support. We also thank Erika Yeh, PhD (University of California, San Francisco) and Luciane Portas Capelo, PhD (Federal University of Sao Paulo, Sao Jose dos Campos) for stimulating discussions. This work was supported by grants from the Brazillian Ministry of Health, Fundação de Amparo à Pesquisa do Estado de São Paulo (CEPID/FAPESP), Coordenação de Aperfeiçoamento de Pessoal de Nível Superior (CAPES), and Conselho Nacional de Desenvolvimento Científico e Tecnológico (CNPq).

Disclosure of Potential Conflict of Interest No potential conflict of interest was disclosed.

Author Contributions Roberto Dalto Fanganiello: conception and design, collection and assembly of data, data analysis and interpretation, manuscript writing

Felipe Augusto Andre Ishiy: collection and assembly of data, data analysis and interpretation, manuscript writing

Gerson Shigeru Kobayashi: data analysis and interpretation, manuscript writing

Lucas Alvizi: conception and design, collection and assembly of data, data analysis and interpretation, manuscript writing

Daniele Yumi Sunaga: conception and design, collection and assembly of data, data analysis and interpretation, manuscript writing

Maria Rita Passos-Bueno: conception and design, data analysis and interpretation, manuscript writing, financial support, administrative support

References

1. Caplan, A. I., & Correa, D. (2011). The MSC: an injury drugstore. *Cell Stem Cell, 9*, 11–5.
2. Kean, T. J., Lin, P., Caplan, A. I., & Dennis, J. E. (2013). MSCs: delivery routes and engraftment, cell-targeting strategies, and immune modulation. *Stem Cells International, 2013*, 732742.
3. Krebsbach, P. H., Mankani, M. H., Satomura, K., Kuznetsov, S. A., & Robey, P. G. (1998). Repair of craniotomy defects using bone marrow stromal cells. *Transplantation, 66*, 1272–8.
4. Shayesteh, Y. S., Khojasteh, A., Soleimani, M., Alikhasi, M., Khoshzaban, A., & Ahmadbeigi, N. (2008). Sinus augmentation using human mesenchymal stem cells loaded into a beta-tricalcium phosphate/hydroxyapatite scaffold. *Oral Surgery, Oral Medicine, Oral Pathology, Oral Radiology, and Endodontics, 106*, 203–9.
5. Nolff, M. C., Gellrich, N. C., Hauschild, G., et al. (2009). Comparison of two beta-tricalcium phosphate composite grafts used for reconstruction of mandibular critical size bone defects. *Veterinary and Comparative Orthopaedics and Traumatology, 22*, 96–102.
6. Miura, M., Gronthos, S., Zhao, M., et al. (2003). SHED: stem cells from human exfoliated deciduous teeth. *Proceedings of the National Academy of Sciences of the United States of America, 100*, 5807–12.
7. Graziano, A., d'Aquino, R., Laino, G., et al. (2008). Human CD34+ stem cells produce bone nodules in vivo. *Cell Proliferation, 41*, 1–11.
8. Yamaza, T., Kentaro, A., Chen, C., et al. (2010). Immunomodulatory properties of stem cells from human exfoliated deciduous teeth. *Stem Cell Research & Therapy, 1*, 5.
9. Wang X, Sha XJ, Li GH, et al. Comparative characterization of stem cells from human exfoliated deciduous teeth and dental pulp stem cells. Archives of oral biology 2012.
10. Seo, B. M., Sonoyama, W., Yamaza, T., et al. (2008). SHED repair critical-size calvarial defects in mice. *Oral Diseases, 14*, 428–34.
11. de Mendonca, C. A., Bueno, D. F., Martins, M. T., et al. (2008). Reconstruction of large cranial defects in nonimmunosuppressed experimental design with human dental pulp stem cells. *The Journal of Craniofacial Surgery, 19*, 204–10.
12. Levi, B., & Longaker, M. T. (2011). Concise review: adipose-derived stromal cells for skeletal regenerative medicine. *Stem cells (Dayton, Ohio), 29*, 576–82.
13. Goh, B. C., Thirumala, S., Kilroy, G., Devireddy, R. V., & Gimble, J. M. (2007). Cryopreservation characteristics of adipose-derived stem cells: maintenance of differentiation potential and viability. *Journal of Tissue Engineering and Regenerative Medicine, 1*, 322–4.
14. Dragoo, J. L., Choi, J. Y., Lieberman, J. R., et al. (2003). Bone induction by BMP-2 transduced stem cells derived from human fat. *Journal of Orthopaedic Research, 21*, 622–9.
15. Hattori, H., Sato, M., Masuoka, K., et al. (2004). Osteogenic potential of human adipose tissue-derived stromal cells as an alternative stem cell source. *Cells, Tissues, Organs, 178*, 2–12.
16. Lendeckel, S., Jodicke, A., Christophis, P., et al. (2004). Autologous stem cells (adipose) and fibrin glue used to treat widespread traumatic calvarial defects: case report. *Journal of Cranio-Maxillo-Facial Surgery, 32*, 370–3.
17. Mesimaki, K., Lindroos, B., Tornwall, J., et al. (2009). Novel maxillary reconstruction with ectopic bone formation by GMP adipose stem cells. *International Journal of Oral and Maxillofacial Surgery, 38*, 201–9.
18. Daley, G. Q. (2012). The promise and perils of stem cell therapeutics. *Cell Stem Cell, 10*, 740–9.
19. Levi, B., Peault, B., & James, A. W. (2014). Bone tissue engineering and regeneration. *BioMed research international, 2014*, 137529.
20. Halvorsen, Y. D., Franklin, D., Bond, A. L., et al. (2001). Extracellular matrix mineralization and osteoblast gene expression by human adipose tissue-derived stromal cells. *Tissue Engineering, 7*, 729–41.
21. Zuk, P. A., Zhu, M., Mizuno, H., et al. (2001). Multilineage cells from human adipose tissue: implications for cell-based therapies. *Tissue Engineering, 7*, 211–28.
22. Hattori, H., Masuoka, K., Sato, M., et al. (2006). Bone formation using human adipose tissue-derived stromal cells and a biodegradable scaffold. *Journal of Biomedical Materials Research, Part B: Applied Biomaterials, 76*, 230–9.
23. Laino, G., Graziano, A., d'Aquino, R., et al. (2006). An approachable human adult stem cell source for hard-tissue engineering. *Journal of Cellular Physiology, 206*, 693–701.
24. Anderson, P., Carrillo-Galvez, A. B., Garcia-Perez, A., Cobo, M., & Martin, F. (2013). CD105 (endoglin)-negative murine mesenchymal stromal cells define a new multipotent subpopulation with distinct differentiation and immunomodulatory capacities. *PLoS One, 8*, e76979.
25. Laino, G., d'Aquino, R., Graziano, A., et al. (2005). A new population of human adult dental pulp stem cells: a useful source of living autologous fibrous bone tissue (LAB). *Journal of Bone and Mineral Research, 20*, 1394–402.

26. Papaccio, G., Graziano, A., d'Aquino, R., et al. (2006). Long-term cryopreservation of dental pulp stem cells (SBP-DPSCs) and their differentiated osteoblasts: a cell source for tissue repair. *Journal of Cellular Physiology, 208*, 319–25.
27. d'Aquino, R., Graziano, A., Sampaolesi, M., et al. (2007). Human postnatal dental pulp cells co-differentiate into osteoblasts and endotheliocytes: a pivotal synergy leading to adult bone tissue formation. *Cell Death and Differentiation, 14*, 1162–71.
28. Irizarry, R. A., Hobbs, B., Collin, F., et al. (2003). Exploration, normalization, and summaries of high density oligonucleotide array probe level data. *Biostatistics, 4*, 249–64.
29. Johnson, W. E., Li, C., & Rabinovic, A. (2007). Adjusting batch effects in microarray expression data using empirical Bayes methods. *Biostatistics, 8*, 118–27.
30. Tusher, V. G., Tibshirani, R., & Chu, G. (2001). Significance analysis of microarrays applied to the ionizing radiation response. *Proceedings of the National Academy of Sciences of the United States of America, 98*, 5116–21.
31. Benjamini, Y., Drai, D., Elmer, G., Kafkafi, N., & Golani, I. (2001). Controlling the false discovery rate in behavior genetics research. *Behavioural Brain Research, 125*, 279–84.
32. Vandesompele J, De Preter K, Pattyn F, et al. Accurate normalization of real-time quantitative RT-PCR data by geometric averaging of multiple internal control genes. Genome Biol 2002;3: RESEARCH0034.
33. Pfaffl, M. W. (2001). A new mathematical model for relative quantification in real-time RT-PCR. *Nucleic Acids Research, 29*, e45.
34. Rohde, C., Zhang, Y., Reinhardt, R., & Jeltsch, A. (2010). BISMA–fast and accurate bisulfite sequencing data analysis of individual clones from unique and repetitive sequences. *BMC Bioinformatics, 11*, 230.
35. Langdahl, B. L., Kassem, M., Moller, M. K., & Eriksen, E. F. (1998). The effects of IGF-I and IGF-II on proliferation and differentiation of human osteoblasts and interactions with growth hormone. *European Journal of Clinical Investigation, 28*, 176–83.
36. Boonen, S., Mohan, S., Dequeker, J., et al. (1999). Down-regulation of the serum stimulatory components of the insulin-like growth factor (IGF) system (IGF-I, IGF-II, IGF binding protein [BP]-3, and IGFBP-5) in age-related (type II) femoral neck osteoporosis. *Journal of Bone and Mineral Research, 14*, 2150–8.
37. Ulaner, G. A., Vu, T. H., Li, T., et al. (2003). Loss of imprinting of IGF2 and H19 in osteosarcoma is accompanied by reciprocal methylation changes of a CTCF-binding site. *Human Molecular Genetics, 12*, 535–49.
38. Zhang, H., Niu, B., Hu, J. F., et al. (2011). Interruption of intrachromosomal looping by CCCTC binding factor decoy proteins abrogates genomic imprinting of human insulin-like growth factor II. *The Journal of Cell Biology, 193*, 475–87.
39. van Bezooijen, R. L., Van der Bent, C., Papapoulos, S. E., & Lowik, C. W. (1999). Oestrogenic compounds modulate cytokine-induced nitric oxide production in mouse osteoblast-like cells. *The Journal of Pharmacy and Pharmacology, 51*, 1409–14.
40. Goswami, J., Hernandez-Santos, N., Zuniga, L. A., & Gaffen, S. L. (2009). A bone-protective role for IL-17 receptor signaling in ovariectomy-induced bone loss. *European Journal of Immunology, 39*, 2831–9.
41. Osta, B., Lavocat, F., Eljaafari, A., & Miossec, P. (2014). Effects of interleukin-17A on osteogenic differentiation of isolated human mesenchymal stem cells. *Frontiers in Immunology, 5*, 425.
42. CA, C. (1996). The role of insulin-like growth factors and binding proteins in bone cell biology. In J. B. Bilezikian LGR & G. A. Rodan (Eds.), *Principles of bone biology* (pp. 607–18). San Diego: Academic.
43. Canalis, E. (1993). Insulin like growth factors and the local regulation of bone formation. *Bone, 14*, 273–6.
44. Subburaman Mohan DJB. IGF System Components and Their Role in Bone Metabolism. In: Rosenfeld RG, Roberts, Charles, ed. The IGF System. Contemporary Endocrinology: Humana Press; 1999: 457–96.
45. Hardouin, S. N., Guo, R., Romeo, P. H., Nagy, A., & Aubin, J. E. (2011). Impaired mesenchymal stem cell differentiation and osteoclastogenesis in mice deficient for Igf2-P2 transcripts. *Development, 138*, 203–13.
46. Twine, N. A., Chen, L., Pang, C. N., Wilkins, M. R., & Kassem, M. (2014). Identification of differentiation-stage specific markers that define the ex vivo osteoblastic phenotype. *Bone, 67*, 23–32.
47. Vu, T. H., Nguyen, A. H., & Hoffman, A. R. (2010). Loss of IGF2 imprinting is associated with abrogation of long-range intrachromosomal interactions in human cancer cells. *Human Molecular Genetics, 19*, 901–19.
48. Ohlsson, R., Nystrom, A., Pfeifer-Ohlsson, S., et al. (1993). IGF2 is parentally imprinted during human embryogenesis and in the Beckwith-Wiedemann syndrome. *Nature Genetics, 4*, 94–7.
49. Ping, A. J., Reeve, A. E., Law, D. J., Young, M. R., Boehnke, M., & Feinberg, A. P. (1989). Genetic linkage of Beckwith-Wiedemann syndrome to 11p15. *American Journal of Human Genetics, 44*, 720–3.
50. Davies, S. M. (1994). Developmental regulation of genomic imprinting of the IGF2 gene in human liver. *Cancer Research, 54*, 2560–2.
51. Kalscheuer, V. M., Mariman, E. C., Schepens, M. T., Rehder, H., & Ropers, H. H. (1993). The insulin-like growth factor type-2 receptor gene is imprinted in the mouse but not in humans. *Nature Genetics, 5*, 74–8.
52. Pham, N. V., Nguyen, M. T., Hu, J. F., Vu, T. H., & Hoffman, A. R. (1998). Dissociation of IGF2 and H19 imprinting in human brain. *Brain Research, 810*, 1–8.
53. Dai, Y. M., Hu, Y. L., Wang, Z. Q., & Li, J. (2007). [Loss of imprinting of IGF2 in cord blood of newborns of Chinese Han population]. Zhonghua yi xue yi chuan xue za zhi=Zhonghua yixue yichuanxue zazhi =. *Chinese Journal of Medical Genetics, 24*, 10–4.
54. Douc-Rasy, S., Barrois, M., Fogel, S., et al. (1996). High incidence of loss of heterozygosity and abnormal imprinting of H19 and IGF2 genes in invasive cervical carcinomas. Uncoupling of H19 and IGF2 expression and biallelic hypomethylation of H19. *Oncogene, 12*, 423–30.
55. Eslaminejad, M. B., Fani, N., & Shahhoseini, M. (2013). Epigenetic regulation of osteogenic and chondrogenic differentiation of mesenchymal stem cells in culture. *Cell Journal, 15*, 1–10.
56. Teven, C. M., Liu, X., Hu, N., et al. (2011). Epigenetic regulation of mesenchymal stem cells: a focus on osteogenic and adipogenic differentiation. *Stem Cells International, 2011*, 201371.
57. Im, G. I., & Shin, K. J. (2015). Epigenetic approaches to regeneration of bone and cartilage from stem cells. *Expert Opinion on Biological Therapy, 15*, 181–93.
58. Hemming, S., Cakouros, D., & Isenmann, S. (2014). EZH2 and KDM6A act as an epigenetic switch to regulate mesenchymal stem cell lineage specification. *Stem Cells (Dayton, Ohio), 32*, 802–15.
59. Paino, F., La Noce, M., & Tirino, V. (2014). Histone deacetylase inhibition with valproic acid downregulates osteocalcin gene expression in human dental pulp stem cells and osteoblasts: evidence for HDAC2 involvement. *Stem Cells (Dayton, Ohio), 32*, 279–89.
60. d'Aquino, R., De Rosa, A., Lanza, V., et al. (2009). Human mandible bone defect repair by the grafting of dental pulp stem/progenitor cells and collagen sponge biocomplexes. *European Cells & Materials, 18*, 75–83.
61. Giuliani, A., Manescu, A., Langer, M., et al. (2013). Three years after transplants in human mandibles, histological and in-line holotomography revealed that stem cells regenerated a compact rather than a spongy bone: biological and clinical implications. *Stem Cells Translational Medicine, 2*, 316–24.

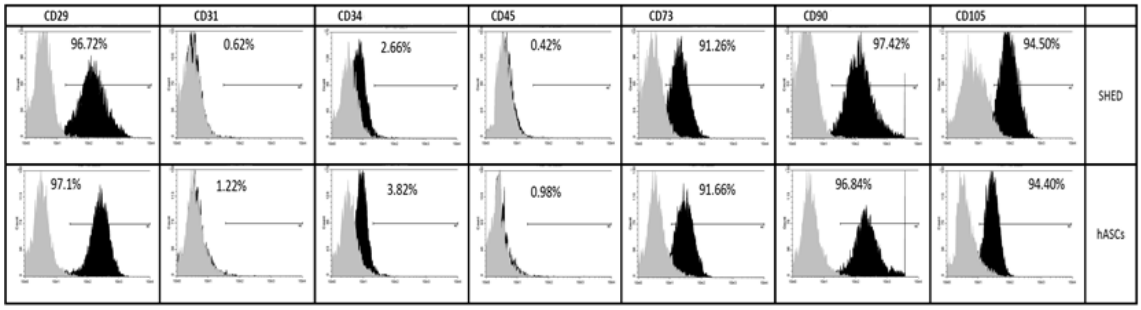

Supplementary Figure 1 Representative surface antigen profiling of SHED and hASCs labeled with antibodies against mesenchymal, endothelial and hematopoietic antigens. Grey histograms represent isotype controls and black histograms represent the conjugated antibody for each antigen. Mean expression rates are indicated above each graph and displayed as mean +/− SD.

CHAPTER III

CD105 low expression levels promotes increased osteogenesis in SHED and depends on microRNA regulation

CD105 low expression levels promotes increased osteogenesis in SHED and depends on microRNA regulation.

Authors:

Felipe Augusto André Ishiy[1] MSc; Roberto Dalto Fanganiello[1] PhD; Gerson Shigeru Kobayashi[1] MSc; Patrícia Semedo Kuriki[1] PhD; Maria Rita Passos-Bueno[1] PhD.

1 – Departamento de Genética e Evolução, Instituto de Biociências, Universidade de São Paulo, São Paulo, Brasil.

Emails:

Felipe Augusto Andre Ishiy - felipe.ishiy@gmail.com

Roberto DaltoFanganiello - robertofanganiello@gmail.com

Gerson Shigeru Kobayashi - gshigeruk@gmail.com

Patrícia Semedo Kuriki - patricia.semedo@gmail.com

Maria Rita Passos-Bueno - passos@ib.usp.br

Introduction

Transplantation of autologous bone grafts is considered the golden standard procedure in osteogenic bone replacement (Amini *et al.,* 2012; Healy *et al.,* 2007). Although this strategy has been important to regenerate bony structures lost or damaged due to trauma, diseases, or congenital malformations, difficulties such as morbidity and lack of tissue supply have placed tissue engineering based on adult mesenchymal stem cells (MSCs) as a promising approach for bone reconstruction (Bose *et al.,* 2012; Holzwarth & Ma, 2011).

Thorough translation of MSC-based therapy to clinical practice faces significant challenges such as poor understanding of the molecular mechanisms governing differences in osteogenic plasticity of MSCs from different tissues of origin (Bakshet al., 2007; Huang et al., 2009; Kern et al., 2006). A better understanding of these mechanisms can guide the selection of an optimal source or sub-population of MSCs to be used in cell-based bone repair, as well as to help disentangle the molecular pathways responsible for these differences. This knowledge may also lead to the discovery of novel molecular markers to be used to select cells for bone biology research and/or therapy.

Stem cells from **h**uman **e**xfoliated **d**eciduous teeth (**SHED**) are an invaluable MSC type to investigate osteogenic potential and a promising cell source for cellular and/or translational studies, as they exhibit stable immunophenotype during long-term cultivation, maintain *in vitro* and *in vivo* plasticity after several passages and freeze-thaw cycles, and display fast population doubling and high *in vitro* and *in vivo* differentiation potential (d'Aquino et al. 2009; Lainoet al., 2005; Laino et al., 2006; Huang et al., 2009). Moreover, we have shown that SHED exhibit higher osteopotential when compared with human adipose-tissue derived stem cells (hASCs) under the same in vitro conditions, which is at least in part correlated with increased IGF2 levels (Fanganiello et al., 2015).

Expression of CD105 (endoglin), a transmembrane TGFB1 co-receptor, was shown to be inversely correlated with osteogenic potential in hASCs. Even though diminished *TGFB1/SMAD2* signaling in hASCs with low CD105 expression ($CD105^{low}$) was suggested to be associated with osteogenic potential, the molecular mechanisms involved in regulation of CD105 expression and

osteogenesis are currently unknown (Levi et al 2011). Chung et al (2012) suggested that higher expression of CD90 presented a positive correlation with osteogenic differentiation in hASCs (Chung *et al.*, 2012).

In the present manuscript, we have tested if CD105 is also a predictive marker of osteogenic potential in SHED. To achieve this goal, we conducted several experiments comparing CD105 expression levels and osteogenic differentiation in populations and subpopulations of SHED and hASCs. The results suggested a strong correlation of CD105 low levels and increased osteogenic potential also in SHED. We next investigated the involvement of IGF2 and microRNAs in the regulation of CD105 expression in SHED cells.

Material andMethods

Ethics statement

This study was approved by the Institute of Biosciences Human Research Ethics Committee (permit number 104.120.09) of the University of Sao Paulo. SHED populations were isolated from donated deciduous teeth obtained upon signed informed consent by the subjects' legal guardians. hASCs were isolated from sub-abdominal adipose tissue, obtained from liposuction procedures. Signed informed consent was also obtained from the subjects.

Harvesting of SHED and adipose tissue-derived stem cells

Human sub-abdominal adipose tissue was obtained from 9 subjects (aged from 24 to 68 yearsold) undergoing elective liposuction procedure. Unprocessed lipoaspirates were washed with equivalent volumes of PBS supplemented with 100 U/ml of penicillin and 100 µg/ml of streptomycin (Life Technologies) and enzymatically dissociated with 0.075% collagenase type I (Sigma-Aldrich). Enzyme activity was neutralized with Dulbecco's Modified Eagle's Medium/Ham's F12 (DMEM/F12; Invitrogen, CA., USA) containing 10% Fetal Bovine Serum (FBS; Life Technologies). Infranatant was centrifuged at 1,200xg for 5 minutes to pellet cells. Cells were seeded in 75 cm^2 culture flasks (Corning) containing DMEM/F12 supplemented with 15% FBS, 100 U/ml penicillin, 100 µg/ml streptomycin, 2 mM L-glutamine, and 2 mM nonessential amino acids (Life Technologies)

Dental pulps were extracted from normal deciduous teeth from nine subjects (between 6 and 10 years of age). Donors had been previously evaluated for systemic diseases and oral infections, and subjects with these conditions were excluded. SHED were obtained by enzymatic digestion as described in Miura *et al*, 2003. SHED were maintained in 6-well culture plates containing DMEM/F12 supplemented with 15% FBS, 100 U/ml penicillin, 100 µg/ml streptomycin, 2 mML-glutamine, and 2 mM nonessential amino acids.

After 14 days, cells were washed with PBS, dissociated with TrypLE (Life Technologies) and 10^4 cells were seeded in 25 cm^2 culture flasks (Corning). Cells were kept at 37°C in a 5% CO_2 incubator and maintained in semi-confluence in

order to prevent differentiation. Passages were done every 4-5 days and medium was refreshed every 3 days. All experiments were performed between the third and the fifth subculture.

Immunophenotyping

Immunophenotype characterization of hASCs and SHED populations was done by flow cytometry analysis. Cells were harvested with TrypLE (Life Technologies, and resuspended to 10^5 cells in 100uL of PBS containing 1% BSA. Cells were separately labeled with FITC, PE, PE-Cy5, PERCP-Cy5.5 or APC-H7 conjugated rat anti-human antibodies CD29, CD31 (Biolegend), CD34, CD45, CD73, CD90 and CD105 (Becton Dickinson) on ice and protected from light for 40 min. An isotype-matched mAb was used as a control (Becton Dickinson). Cell suspensions were washed with PBS, and 10,000 labeled cells were analyzed using a Guava EasyCyte flow cytometer running the Guava Express Plus software (EMD Millipore). The immunophenotyping experiments were done in technical triplicates for each cell sample and for each antibody.

Fluorescence Activated Cell Sorting (FACS)

Staining with anti-CD105-PE (Becton Dickinson) was performed on 10^7 cells, followed by acquisition in a FACSAria II cytometer (Becton Dickinson), according to manufacturer's recommendations. Briefly, after exclusion of debris and doublets, cells positively stained for CD105 were separated into subpopulations, based on fluorescence: cells with the lowest CD105 expression, below the 20^{th} percentile ($CD105^{low}$), and cells with the highest CD105 expression, above the 80^{th} percentile ($CD105^{high}$). We sorted four cell cultures of each type according to these parameters (hASC-$CD105^{low}$ and hASC-$CD105^{high}$; SHED-$CD105^{low}$ and SHED-$CD105^{high}$). After expansion, cells were seeded in 12-well plates (Corning) and assessed for *in vitro*osteogenic differentiation through alkaline phosphatase activity and Alizarin Red staining assays.

Analysis of *in vitro* osteogenic differentiation

Subconfluent ASC and SHED populations were treated with StemPro® Osteogenesis Differentiation Kit (Life Technologies), 100 U/ml penicillin, 100

µg/ml streptomycin with media changes every three days through 21 days of osteogenic differentiation.

Alkaline phosphatase activity was quantified on the 9th day of *in vitro* osteogenic differentiation. Cells were treated with phosphatase substrate (Sigma-Aldrich) and the resulting p-nitrophenol was quantified colorimetrically using a Multiskan EX ELISA plate reader (Thermo Scientific) at 405 nm.

Mineralized matrix production was assessed after 21 days of *in vitro* osteogenesis with Alizarin Red staining. Briefly, cells were washed three times with PBS, fixed with a 70% ethanol solution for 30 minutes at room temperature, followed by three distilled water washes and finally stained with a 0.2% Alizarin Red solution (Sigma-Aldrich) for 30 minutes at room temperature. Staining was removed with a solution of 20% methanol / 10% acetic acid and measured colorimetrically using a Multiskan EX ELISA plate reader (Thermo Scientific) at 450nm.

As a negative control for both colorimetric assays, cells maintained in regular culture medium were used. Experiments were done in technical triplicates for each time point and for each cell line.

MicroRNA target prediction analysis

Identification of microRNAs potentially regulating CD105 expression was carried out with two software: Ingenuity Pathway Analysis (IPA®, QIAGEN Redwood City, www.qiagen.com/ingenuity). Putative microRNAs identified with IPA were confirmed with TargetScan Human v6.2 (http://www.targetscan.org). All analyses were performed using standard parameters.

RNA and microRNA extraction

Total RNA isolation was performed with NucleoSpin RNA II kit (Macherey-Nagel), following manufacturer's recommendations. RNA quality and concentration were assessed using Nanodrop 1000 and agarose gel electrophoresis. Only RNA samples with absorbance ratio 260/280>1.8, preserved rRNA ratio (28S/18S) and no signs of degradation were used. MicroRNA fractions

were extracted using the mirVanamiRNA Isolation Kit (Life Technologies), following manufacturer's recommendations.

Real-Time Quantitative PCR (RT-qPCR)

One microgram of total RNA was converted into cDNA using Superscript II, according to the manufacturer's recommendations. cDNAs from each cell type were pooled. RT-qPCR reactions were performed in triplicates with final volume of 20 µL, using 20 ngcDNA, 2X Fast SYBR Green PCR Master Mix, and 50 nM – 200 nM of each primer. Primers were designed with Primer-BLAST (http://www.ncbi.nlm.nih.gov/tools/primer-blast/; see **Table S1** for primer information). Primer amplification efficiencies (E) were determined by serial cDNA dilutions expressed in $\log_{10}$ in which $E = 10^{-1/slope}$.

Reverse transcription and quantification of microRNAs were performed, respectively, with Taqman microRNA Reverse Transcription Kit and qPCR Master Mix (Life Technologies), following manufacturer's recommendations.

Fluorescence was detected using the Applied Biosystems 7500 Fast Real-Time PCR System (Life Technologies), under standard temperature protocol. Expression of target genes and microRNAs was assessed relative to a calibrator cDNA (ΔCt). Finally, GeNorm v3.4 was used to calculate normalization factors for each sample (Vandesompele et al, 2002), considering endogenous expression of *GAPDH*, *HPRT1* and *SDHA* for mRNA assays, and RNU58A, RNU66 and RNU6B for microRNA assays. Final expression values were determined by dividing $E^{-\Delta Ct}$ by the corresponding normalization factor (Pfaffl, 2001). Primers and reagents were supplied by Life Technologies.

***IGF2* treatment**

As previously described by Fanganiello et al. (2015) we supplemented basal medium of SHED and hASCs with IGF2 (ProsPec, CYT-265) at a concentration of $2x10^2$nM, in independent experiments. After 24 hours RNA were extracted using a Nucleospin RNA II kit (Macherey-Nagel, Duren, Germany), following manufacturer's instructions, RNA quality and concentration were measured by 2% agarose gel electrophoresis and Nanodrop ND-1000 (Thermo Scientific, MA., USA),

respectively. Gene expression assays of RT-qPCR were performed as previously described.

MicroRNA mimic and inhibitor assays

SHED were nucleofected with the Human MSC Nucleofector Kit (Lonza) in an AmaxaNucleofector II device (Lonza), applying program U-23, and following manufacturer´s recommendations. Synthetic hsa-mir-1287 mirVANA mimic and inhibitor oligonucleotides (Life Technologies) were nucleofected in parallel with a pmaxGFP positive control plasmid (Lonza) to evaluate transfection efficiency, following manufacturer's recommendations. Forty-eight hours after transfection, cells were submitted to total RNA and microRNA extraction to assess hsa-mir-1287 and CD105 expression.

Statistical analysis

Continuous variables were expressed by mean and standard deviation, and the groups were compared by Student's t-test. A p-value < 0.05 was considered statistically significant. Tests were done using the GraphPad software (GraphPad).

RESULTS

Characterization of SHED and hASC populations

Both hASCs and SHED populations showed typical MSC immunophenotype (≥ 95% staining for CD29, CD73, CD90, CD105 and ≤ 5% staining for CD31, CD34, CD45, n=9 per cell group) at the 3rd passage.

In general, all assessed osteogenesis-associated transcripts were upregulated in SHED in comparison with hASCs during the first 6 days of osteoinduction (**Supplementary figure 1A, B, C and D**). Further, after 9 days of differentiation, alkalyne phosphatase (ALP) activity was 2.29 times higher in SHED ($p<0.001$) and, after 21 days of differentiation, alizarin red staining showed a 2.37-fold increase in calcium deposition in SHED, when compared with hASCs ($p<0.001$; **Supplementary Figure 1E, F and G**). These results confirm that the SHED show increased *in vitro* osteopotential in comparison with hASCs (Fanganiello *et al.,* 2015).

CD105 expression is inversely correlated with SHED`s and with hASCs` osteogenic potential

Quantification of *CD105* gene expression by real-time quantitative PCR (RT-qPCR) and of CD105 protein expression by flow cytometry revealed that undifferentiated SHED showed lower CD105 mRNA (6.3 fold, $p<0.05$) and protein (7.56 fold, $p<0.001$) expression compared with hASCs (**Figure 1A and B**). SHED and hAScs did not present protein and mRNA expression differences for CD90 (**Figure 1C and D**). Also, undifferentiated SHED displayed higher expression of osteogenic markers (*ALP*, *RUNX2*, *DLX5* and *IGF2*) compared with hASCs ($p<0.001$) (**Figure 1E**). After 4 days of osteoinduction, CD105 was downregulated in hASC in comparison with day 0 ($p<0.01$) while CD105 was upregulated in SHED ($p<0.05$). After 6 days of *in vitro* osteogenesis, CD105 was consistently upregulated in hASC in comparison with SHED (**Figure 1F**).

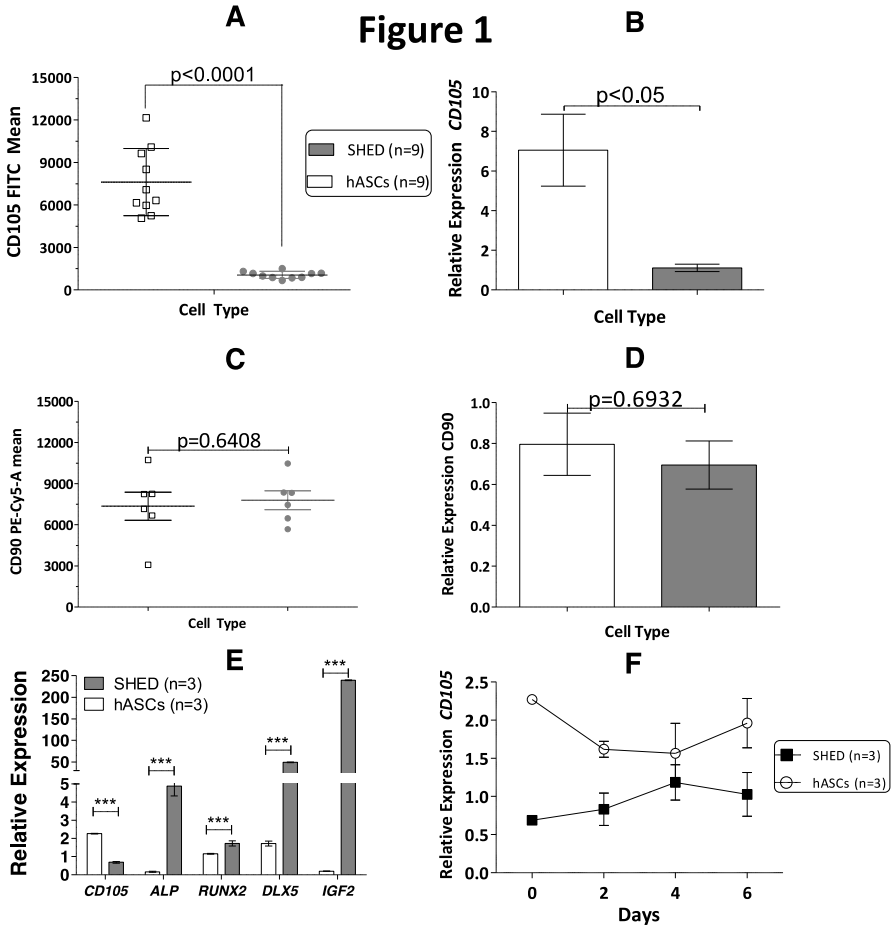

Figure 1- A. CD105 immunophenotype in SHED and hASCs (n=9 per lineage); **B.** Relative expression of CD105 in hASCs and SHED in undifferentiated cells; **C.** CD90 immunophenotype in SHED and hASCs (n=6 per lineage); **D.** Relative expression of CD90 in hASCs and SHED in undifferentiated cells; **E.** Relative expression of *CD105, ALP, RUNX2, DLX5* and *IGF2* at basal state in SHED and hASCs (n=3 for each cell type). **F.** Relative expression of *CD105*during *in vitro* osteoblastogenic differentiation at 0, 2, 4 and 6 days (hASC n=3 and SHED n=3). The comparison between different times in hASCs were T0-T2 (**), T0-T4 (*) and T0-T6 (*), and in SHED T0-T4 (*) T0-T6 (**). ACTb, TBP and HMBS were used as endogenous control. Tests with $p<0.05$ were considered to be statistically significant.

The results thus far prompted us to investigate if lower CD105 expression is correlated with the higher osteogenic potential exhibited by SHED. We sorted subpopulations of SHED and hASCs with high and low CD105 expression ($CD105^{high}$ and $CD105^{low}$, respectively). Sorted subpopulations from both cell types kept their low and high enrichment expression of CD105 even after one week in culture (**Supplementary Figure 2**).

Next, we subjected both sorted and unsorted cell populations to *in vitro* osteogenic differentiation. For both SHED and hASCs, $CD105^{low}$ cells showed higher ALP activity ($p<0.01$) compared with $CD105^{high}$ cells. (**Figure 2A**). Alizarin

red staining (**Figure 2B**) showed more matrix mineralization in SHED-CD105^{low} compared with SHED-CD105^{high} ($p<0.01$) and the same pattern was observed in hASCs subpopulations: hASCs-CD105^{low} displayed higher calcium deposition compared with hASCs-CD105^{high} ($p<0.001$). Finally, SHED-CD105^{low} showed higher alkaline phosphatase activity ($p<0.01$) and matrix mineralization ($p<0.01$) compared with hASCs-CD105^{low} (**Figures 2A and B**). These results show that CD105 expression is inversely correlated with osteopotential in SHED, and that the hASCs and SHED share this inverse correlation of CD105 expression and osteogenesis.

Figure 2

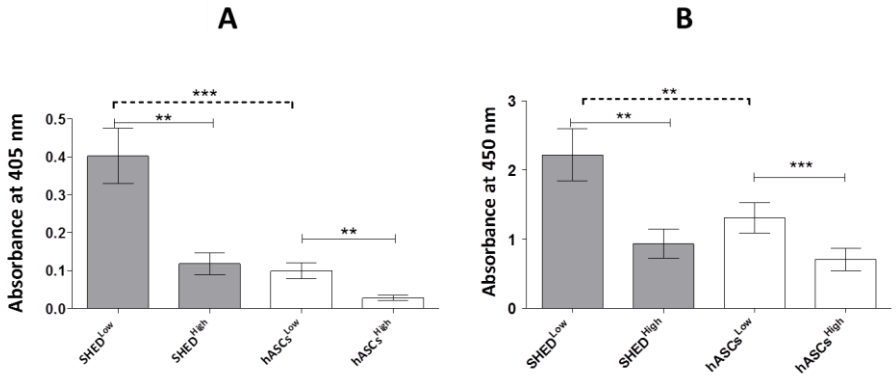

Figure 2- Quantification of (**A**) alkaline phosphatase activity (absorbance of 405 nm) at 9 days and (**B**) Alizarin Red Staining (absorbance at 450 nm) at 21 days of osteogenic differentiation of CD105 low and high expression populations of SHED (n=4) and hASCs (n=4). Tests with $p<0.05$ were considered to be statistically significant (**$p<0.01$, ***$p<0.001$).

To acessed if the differential expression of CD105 between hASCs and SHED could modify the downstream protein expression of SMADs we quantify through western blotting the expression and phosphorylation of SMADs 1/5 and 2. Since CD105 may act as a co-receptor in the TGF-β pathway, we sought to determine the basal activation status of the BMP pathway in undifferentiated SHED and hASCs. Albeit we did not observe any obvious correlation between phospho-SMAD1/5 and CD105 expression, total SMAD1 and SMAD5 associated with the activation of BMPs (Horbelt et al, 2012; Xiao et al., 2007) were increased in SHED as compared to hASCs (**Supplementary Fig. 3**)

hsa-mir-1287 regulates CD105 expression in SHED and in hASCs

Transcriptional regulation of key osteogenic genes by miRNAs is considered to be an important mechanism controlling osteogenic differentiation in MSCs (Wang et al., 2013 Eskildsen et al., 2011 Li et al., 2008 Deng et al., 2013). We used Ingenuity Pathway Analysis and Target Scan softwares to search for microRNAs possibly involved in downregulation of CD105 and potentially associated with osteogenic potential regulation (**Figure 3A**). After using both softwares, four microRNAS were predicted to suppress CD105 expression: hsa-mir-1287, miR-1207-5p, miR-4751-5p and miR-4649-5p (**Figure 3B**). miR-1207-5p and miR-4649-5p were neither expressed in SHED nor in hASCs, and miR-4751-5p expression was not significantly different between hASCs and SHED. hsa-mir-1287 was found to be significantly upregulated in SHED (**Figure 4A and B**).

To confirm the involvement of hsa-mir-1287 in CD105 regulation, we performed loss-of-function and gain-of-function assays by transfecting SHED with a synthetic hsa-mir-1287 mimic and inhibitor. Synthetic inhibitor lea to decreased expression of hsa-mir-1287 ($p<0.01$), which resulted in a 1.90-fold increase in CD105 mRNA ($p<0.001$) (**Figure 4C**). Conversely, addition of the synthetic miR-1287 mimic led to increment of total miR-1287 ($p<0.001$), resulting in a 1.86-fold decrease in CD105 mRNA expression ($p<0.001$) (**Figure 4D**).

We next tested if has-mir-1287 expression was correlated with its host gene, *PYROXD2* (Intragenic microRNA database- miRIAD). *PYROXD2`s* mRNA expression was not significantly different between SHED and hASCs (p=0.1723, **Figure 4F**).

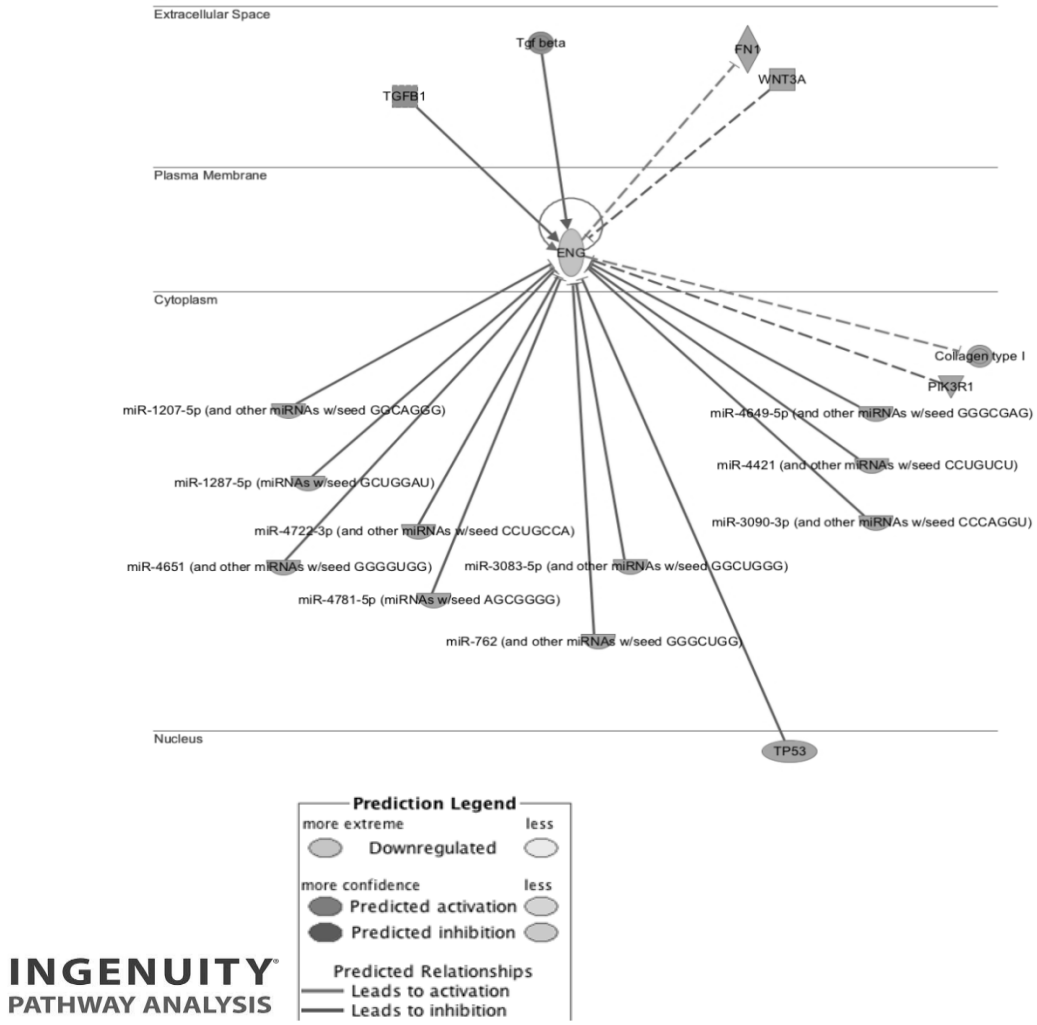

Figure 3 A: Scheme showing molecules predicted to negatively regulate CD105 (ENG) through in Silico analysis of CD105 (ENG) pathway using Ingenuity Pathway Analysis Software.

Search for predicted microRNA targets in mammals

MicroRNA	CD105 (*ENG*)
miR-1207-5p	Predict to regulate
miR-1287	Predict to regulate
miR-3083-5p	Non-predict to regulate
miR-3090-3p	Non-predict to regulate
miR-326-5p	Non-predict to regulate
miR-4421	Non-predict to regulate
miR-4649-5p	Predict to regulate
miR-4651	Non-predict to regulate
miR-4781-5p	Predict to regulate
miR-762	Non-predict to regulate

Figure 3 B: List of ten microRNAs predicted to regulate CD105 (ENG) selected in Ingenuity Pathway Analysis that were reanalyzed using a second *in silico* prediction software specific for microRNA (Target Scan Human software). Blue color microRNAs indicate positive regulatory pairing for CD105 at the 3´UTR region and Red color microRNAs indicate negative regulatory pairing for CD105.

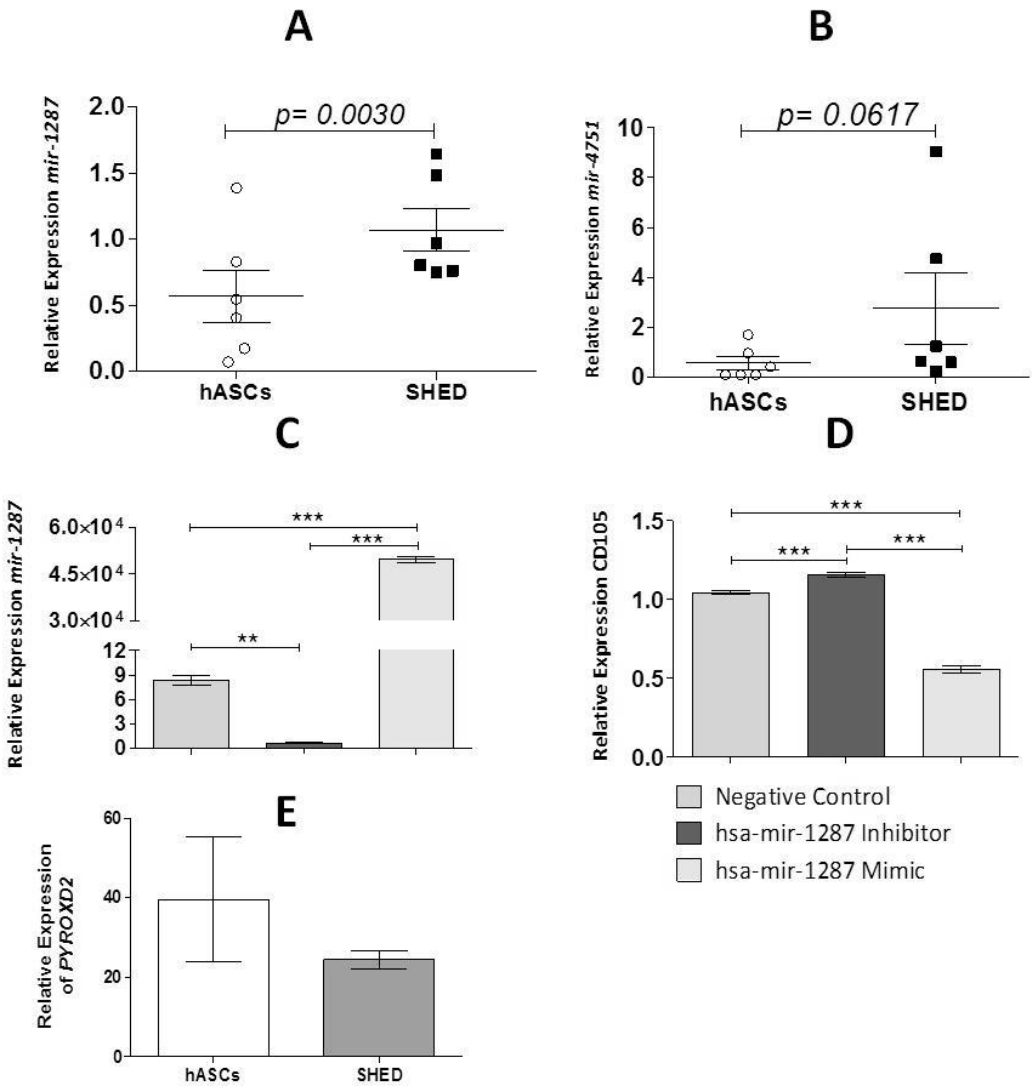

Figure 4- Quantification through qRT-PCR of **A-**hsa-mir-1287 and **B-**Mir-4651 predicted to bind CD105 in SHED and hASCs (n=6 per cell population); Quantification of **C**-Mir-1287 and **D**-CD105 through qRT-PCR after 48 hours after transfection of SHED with Mimic and Inhibitor of microRNA hsa-mir-1287. A scrambled sequence of microRNA was used as negative control. RNU58A, RNA U66 and U6 were used as endogenous controls for hsa-mir-1287 and ACTb, TBP and HMBS for CD105. **E-** Correlation analysis of *IGF2* and *CD105* relative expression (p=0.3021 and R value=0.1311) **F-** RelativeExpression of *PYROXD2 host*-gene of has-mir-1287 in SHED and hASCs (n=6 per cell population). Tests with $p<0.05$ were considered to be statistically significant (**$p<0.01$, ***$p<0.001$)

IGF2 exogenous treatment does not downregulate CD105 in SHED and hASCs.

In Fanganiello et al, 2015 we show that the SHED higher osteogenic potential is associated with higher *IGF2* expression. Through qRT-PCR we verified that SHED (**Figure 5A**) and hASCs (**Figure 5B**) presented an inverse correlation between *IGF2* and CD105 expression before *in vitro* osteoinduction. In order to test if the activation of IGF2 pathway could downregulate CD105 expression, we treated SHED and hASCs with exogenous *IGF2*. After treatment SHED and hASCs showed higher expression of *IGF2, ALP* and *RUNX2,* but CD105 was not consistently downregulated (**Figure 5C**).

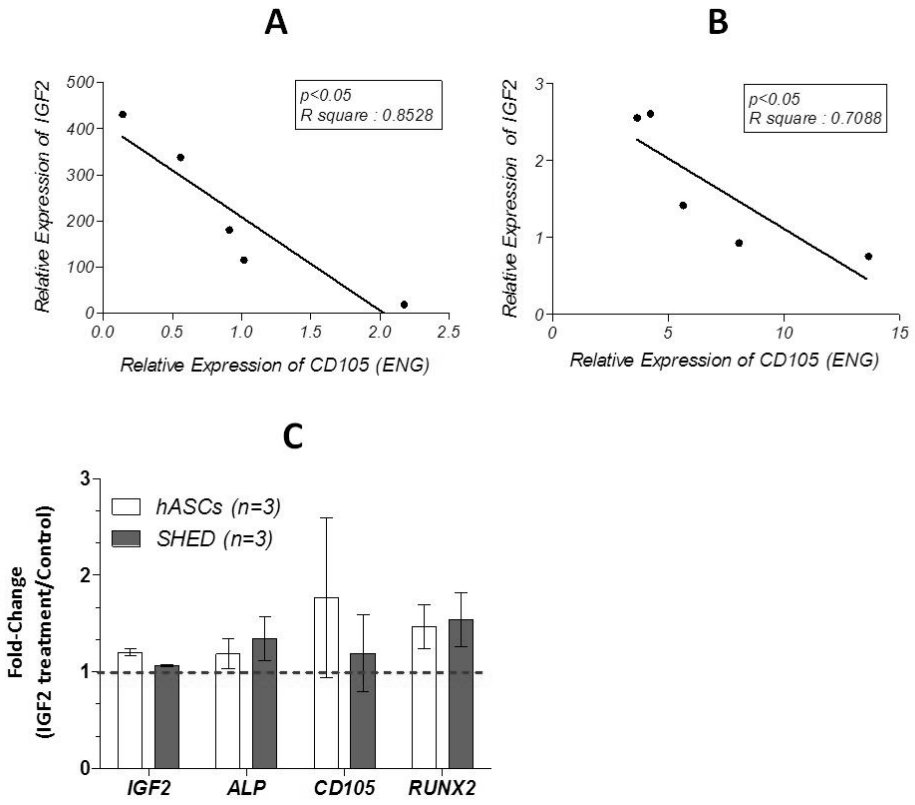

Figure 5- Correlation analysis of IGF2 and CD105 expression in **A–** SHED (n=5) and **B-**hASCs (n=5) at basal state. ACTb, TBP and HMBS were used as endogenous controls. Two-tailed Pearson's correlation test was used to observe the correlation between IGF2 and CD105. **C-** Fold-change between IGF2 treated and non-treated cells (SHED and hASCs). Tests with $p<0.05$ were considered to be statistically significant (**$p<0.01$, ***$p<0.001$)

Discussion

It is already established that MSCs from different sources, such as bone marrow (Cheng *et al.*, 1994; Egusa et al., 2007), adipose tissue (Zuk *et al.*, 2001; Levi *et al.*, 2010) dental pulp (Miura *et al.,* 2003; De Mendonça *et al.,* 2008) and many other tissues are capable of *in vitro* and *in vivo* osteogenic differentiation, but the understanding of the molecular mechanisms governing osteodifferentiation potential in MSCs is still not fully characterized (Augello and De Bari 2010; Satija et al. 2007; Siddappa et al. 2007).

After confirming SHED higher *in vitro* osteogenic potential, previously reported in Fanganiello et al, (2015) and CD105 expression`s inverse correlation with hASCs osteopotential, first reported in Levi et al (2011), analysis of CD105 expression levels in SHED showed that these cells present lower expression of mRNA and protein levels of CD105 when compared with hASC. In addition, SHED-$CD105^{low}$ subpopulations exhibited the highest *in vitro* osteodifferentiation potential, when compared to all other groups, including hASCs. These results support the hypothesis that the inverse correlation between CD105 expression and increased osteopotential is not restricted to hASCs. In line with this finding, down-regulation of CD105 was also associated with multipotential MSCs derived from umbilical cord blood (Jim *et al.*, 2009). On the other hand, this association may be restricted to MSCs, since we did not observe correlation between low-CD105 expression levels and MSC-like cells increased osteogenic potential (Ishiy et al., 2015) Despite the differential expression of CD105 we did not observed statistical differences between hASCs and SHED of protein and phosphorylation of SMADs.

We have shown previously that the intrinsically higher osteogenic potential in SHED when compared with hASCs was positively associated with augmented *IGF2* expression, which in turn seem to involve epigenetic regulation (Fanganiello et al., 2015). However, the lower expression of CD105 exhibited by SHED was not found to be correlated with the differential *IGF2* expression. To reinforce this hypothesis we observed an inverse expression correlation between *IGF2* and CD105 in SHED and hASCs, but *IGF2* treatment did not homogeneously alter the expression of CD105, thus the differential expression of CD105 in SHED and hASCs could not be associated with the expression of *IGF2.* Therefore, CD105 expression

levels in SHED and hASC might be regulated by other pathways and thus suggest that osteogenic potential in adult MSCs may be a multifactorial process, as already previously suggested by others (Chung et al. 2012; Dragoo et al. 2003; Gohet al. 2007).

In silico analysis suggest that more than 30% of human genes are regulated by microRNAs (Lewis *et al.,* 2005) and in mammals miRNAs are predicted to control the activity of 50-60% of all protein coding genes (Friedman et al., 2009; Krolet al., 2010). Moreover, the relationship between microRNAs and osteogenic potential has been demonstrated in several studies: miR-346 acts as a positive regulator of osteogenic differentiation in hBMSCs by targeting the Wnt/β-catenin pathway (Wang *et al.,* 2013) and miR-138 inhibits osteogenesis in hBMSCs (Eskildsen *et al.,* 2011). Moreover, miR-31 improved the osteogenic potential of rat ASCs both *in vitro* and *in vivo* (Deng *et al.*, 2013) and miR-22 was identified as an important regulator of the balance between osteogenic and adipogenic differentiation of hASCs (Huang *et al.,* 2012).

Among the microRNAs predicted *in silico* to regulate CD105 expression, miR-1287 was significantly higher expressed in SHED when compared with hASC. In addition, we observed that higher expression of hsa-mir-1287 leads to CD105 downregulation, and inhibition of hsa-mir-1287 promoted upregulation of CD105. These findings suggest for the first time that hsa-mir1287 is associated with CD105 regulation and osteogenic differentiation in MSCs. The role of has-mir-1287 were not yet explored in humans and apparently expression of this microRNA was found in human carcinoma tissues, but its role in this process is still not understood (Nygaard et al., 2009; Wang *et al.*, 2013).

hsa-mir-1287 is located in the exonic region (exon 8) of *PYROXD2* (pyridine nucleotide-disulphideoxidoreductase domain 2, chromosome 10), which is associated with oxidoreductase activity [provided by RefSeq, Sep 2009]. We found no correlation between hsa-mir-1287 and PYROXD2 expression in SHED and hASCs, in agreement with data available in the microRNA dabatase (MIRIAD). These observations suggest that the regulation of hsa-mir-1287 is not dependent on *PYROXD2* expression and might have an independent promoter which regulates its expression autonomously from its host gene *PYROXD2*.

Tissue of origin has been proposed as a critical factor that could influence the differentiation potential in MSCs (Kolf *et al.,* 2007) and the differential expression of mir-1287 between SHED and hASCs could be explained by the fact that these two cell sources are obtained from different tissues. Adipose tissue is derived from mesoderm and it is composed of different cell types such as endothelial cells, fibroblastoid cells, and adult stem cells (Luzi *et al.,* 2008; Tholpady *et al.,* 2006). On the other hand, SHED are obtained from specialized tissues formed mainly by neural-crest cells, harboring high plasticity and showed to be associated with higher expression of osteogenic markers (Graziano *et al.*, 2008; Huang *et al.,* 2009; Mayo *et al.,* 2014; Trubiani *et al.,* 2006, Fanganiello et al., 2015).

CD105 has been used as a mesenchymal marker in the MSCs characterization panel (Dominic et al, 2005), and were recently described as an important osteogenic marker in hASCs. In this study we demonstrated that differences in the *in vitro* osteogenesis between hASCs and SHED are related to the differential expression of CD105, and due to the easiness use of CD105 to the isolation of populations with different expression reinforce the importance of CD105 to the osteogenic potential of MSCs. hASCs and SHED shared similar expression of CD90, a protein membrane with positive correlation with the osteogenic potential of MSCs (Chung et al., 2012), which allows us to speculate that the osteogenic differences between these two cell sources is not correlated with CD90 expression.

Modulation of BMP pathway by TGF-β is involved in proper specification of osteoblast fate, and lower expression of CD105 should lead to increased phosphorylation of SMAD2 (Whitman, and Raftery 2005; Maeda et al., 2004; Levi et al, 2010), and consequently to induction of osteogenesis by TGFB/BMP. BMP pathway activation is not influenced by CD105 expression in undifferentiated cells. However, the increment in SMAD1 and SMAD5 expression in SHED suggests that lower CD105 expression may be associated with increased osteogenic potential upon differentiation, which may take place due to greater availability of BMP pathway SMADS, facilitating osteodifferentiation. Although, in a preliminary experiment we did not observe obvious correlation between CD105 levels and SMADs phosphorylation, we observed higher expression of SMAD5 in

undifferentiated SHED. However, this should be tested during the differentiation stage.

In summary, we showed here that CD105 could be used to select SHED cells with increased osteogenic potential and the CD105 expression in these cells might be regulated by microRNA hsa-mir-1287. Cell sorting based methodologies could enhance cell quality/quantity for a specific phenotype, and this knowledge allows the improvement of cell selection for MSC-based skeletal defect treatments. Our findings also point towards the possibility to control osteogenic potential in MSCs, particularly in SHED, by manipulation of hsa-mir-1287 levels to regulate CD105/TGF-β pathway, a strategy that not necessarily require cell sorting. However, further studies are necessary considering the observation of has-mir-1287 expression in cancer cells.

Acknowledgements:

We thank Meire Aguena, Simone Gomes Ferreira and Andressa Gois Morales for technical assistance and Constancia Gotto Urbani for secretarial assistance. This work was supported by grants from the Brazilian Ministry of Health, the Foundation for Research Support of the State of Sao Paulo (FAPESP) and the National Council for Scientific and Technological Development (CNPq).

References

Amini, A., Laurencin, C. &Nukavarapu, S. Bone Tissue Engineering: Recent Advances and Challenges. *Critical Reviews™ in Biomedical Engineering* 40, 363408 (2012).

An, F., Wang, X., Liu, W., Gao, Y., Ma, J., Xu, X., Chen, S., et al.. [Expressions of clinical significances of p-extracellular regulated kinase 1/2 and matrix metalloproteinase-9 in cervical squamous cell carcinoma].*Zhongguoyixuekexueyuanxuebao. ActaAcademiaeMedicinaeSinicae* 34, 590–4 (2012).

Anderson, P., Carrillo-GÃlvez, A., García-Pérez, A., Cobo, M. &Martín , F. CD105 (Endoglin)-Negative Murine Mesenchymal Stromal Cells Define a New Multipotent Subpopulation with Distinct Differentiation and Immunomodulatory Capacities. PLoS ONE 8, e76979 (2013).

Augello, Andrea, and Cosimo De Bari. 2010. "The regulation of differentiation in mesenchymal stem cells." Human gene therapy 21(10): 1226–38.

Baksh, Dolores, Raphael Yao, and Rocky S Tuan. 2007. "Comparison of proliferative and multilineage differentiation potential of human mesenchymal stem cells derived from umbilical cord and bone marrow." Stem cells (Dayton, Ohio) 25: 1384–92. Available at: http://www.ncbi.nlm.nih.gov/pubmed/17332507.

Bernabeu, Carmelo, Barbara a Conley, and Calvin P H Vary. 2007. "Novel biochemical pathways of endoglin in vascular cell physiology." Journal of cellular biochemistry 102(6): 1375–88. Available at: http://www.pubmedcentral.nih.gov/articlerender.fcgi?artid=2199238&tool=pmcentrez&rendertype=abstract [Accessed November 19, 2013].

Bose, S., Roy, M. &Bandyopadhyay, A. Recent advances in bone tissue engineering scaffolds. *Trends in biotechnology*30, 546–54 (2012)

Cheng S L, J W Yang, L Rifas, S F Zhang, and L V Avioli. Differentiation of human bone marrow osteogenic stromal cells in vitro: induction of the osteoblast phenotype by dexamethasone. Endocrinology. Volume 134 Issue 1 - Jan 1, 1994

Chung, *et al*. CD90 (Thy-1)-Positive Selection Enhances Osteogenic Capacity of Human Adipose-Derived Stromal Cells. TISSUE ENGINEERING: Part A. 2013

d'Aquino, Riccardo et al. 2009. "Human dental pulp stem cells: from biology to clinical applications." Journal of experimental zoology. Part B, Molecular and developmental evolution 312B(5): 408–15. Available at: http://www.ncbi.nlm.nih.gov/pubmed/19065566 [Accessed January 12, 2015].

Davies, O., Smith, A., Cooper, P., Shelton, R. &Scheven, B. The effects of cryopreservation on cells isolated from adipose, bone marrow and dental pulp tissues. Cryobiology(2014).doi:10.1016/j.cryobiol.2014.08.003

De Mendonca Costa A, Bueno DF, Martins MT, Kerkis I, Kerkis A, Fanganiello RD, et al. Reconstruction of large cranial defects in nonimmunosuppressed experimental design with human dental pulp stem cells. The Journal of craniofacial surgery. 2008 Jan;19(1):204-10.

Deng, Y. *et al.* The role of miR-31-modified adipose tissue-derived stem cells in repairing rat critical-sized calvarial defects. *Biomaterials* 34, 6717–28 (2013).

Derynck, R. &Akhurst, R. J. Differentiation plasticity regulated by TGF-beta family proteins in development and disease. *Nature cell biology* 9, 1000–4 (2007).

Dragoo JL, Choi JY, Lieberman JR, et al. Bone induction by BMP-2 transduced stem cells derived from human fat. J Orthop Res 2003;21:622-9

Egusa, H., Iida, K., Kobayashi, M., Lin, T. Y., Zhu, M., Zuk, P. a, …Nishimura, I. (2007).Downregulation of extracellular matrix-related gene clusters during osteogenic differentiation of human bone marrow- and adipose tissue-derived stromal cells. Tissue Engineering, 13(10), 2589–600.doi:10.1089/ten.2007.0080

Eskildsen, T. *et al.* MicroRNA-138 regulates osteogenic differentiation of human stromal (mesenchymal) stem cells in vivo. *Proceedings of the National Academy of Sciences*(2011).doi:10.1073/pnas.1016758108

Friedman RC, Farh KK, Burge CB, Bartel DP (2009) Most mammalian mRNAs are conserved targets of microRNAs. Genome Res 19(1):92–105. doi:10.1101/gr.082701.108

Goh BC, Thirumala S, Kilroy G, Devireddy RV, Gimble JM. Cryopreservation characteristics of adipose-derived stem cells: maintenance of differentiation potential and viability. Journal of tissue engineering and regenerative medicine 2007;1:322-4.

Guo, L., Zhao, R. & Wu, Y. The role of microRNAs in self-renewal and differentiation of mesenchymal stem cells.*Experimental hematology* 39, 608–16 (2011).

Graziano, A., d' Aquino, R., Laino, G. &Papaccio, G. Dental pulp stem cells: a promising tool for bone regeneration.Stem cell reviews 4, 21–6 (2008).

Ha, M. & Kim, V. Regulation of microRNA biogenesis. Nature reviews. Molecular cell biology 15, 509–24 (2014)

Healy, K. &Guldberg, R. Bone tissue engineering. *Journal of musculoskeletal & neuronal interactions.*2007. 7, 328–30

Holzwarth, J. & Ma, P. Biomimetic nanofibrous scaffolds for bone tissue engineering. *Biomaterials* 32, 9622–9 (2011).

Horbelt D, Denkis A, Knaus P (2012) A portrait of Transforming Growth Factor β superfamily signalling: Background matters. Int. J. Biochem. Cell Biol. 44(3), 469–74.

Huang, G., Gronthos, S. & Shi, S. Mesenchymal stem cells derived from dental tissues vs. those from other sources: their biology and role in regenerative medicine. *Journal of dental research* **88**, 792–806 (2009).

Huang, S. *et al.* Upregulation of miR-22 Promotes Osteogenic Differentiation and Inhibits Adipogenic Differentiation of Human Adipose Tissue-Derived MesenchymalStem Cells by RepressingHDAC6Protein Expression.*Stem Cells and Development*(2012).doi:10.1089/scd.2012.0014

Itoh, S. &Dijke, P. Negative regulation of TGF-β receptor/Smad signal transduction.*Current Opinion in Cell Biology* 19, 176184 (2007).

James, Aaron W et al. 2011. "Deleterious effects of freezing on osteogenic differentiation of human adipose-derived stromal cells in vitro and in vivo." Stem cells and development 20(3): 427–439.

Jeziorska, M. Transforming growth factor-βs and CD105 expression in calcification and bone formation in human atherosclerotic lesions. *Zeitschrift for Kardiologie* 90, III23III26 (2001).

Jiang, Ting et al. 2010. "Potent in vitro chondrogenesis of CD105 enriched human adipose-derived stem cells." Biomaterials 31: 3564–3571.

Jin H, Park S, Oh W, Yang Y, Kim S, Choi S. Down-regulation of CD105 is associated with multi-lineage differentiation in human umbilical cord blood-derived mesenchymal stem cells.Biochemical and biophysical research communications 2009; 381 (4): 676–81.

Kern, S., Eichler, H., Stoeve, J., Klüter, H. &Bieback, K. Comparative Analysis of Mesenchymal Stem Cells from Bone Marrow, Umbilical Cord Blood, or Adipose Tissue. Stem Cells (2006).doi:10.1634/stemcells.2005-0342

Kolf, C., Cho, E. & Tuan, R. Mesenchymal stromal cells. Biology of adult mesenchymal stem cells: regulation of niche, self-renewal and differentiation. Arthritis Research & Therapy 9, 204 (2007)

Krol, J., Loedige, I. &Filipowicz, W. The widespread regulation of microRNA biogenesis, function and decay. Naturereviews. Genetics 11, 597–610 (2010).

Laino G, d'Aquino R, Graziano A, Lanza V, Carinci F, Pirozzi G, Naro F, Papaccio G. 2005. Dental pulp stem cells can be detected in aged humans: an useful source for living autologous fibrous bone tissue (LAB). J Bone Miner Res 20:1394–1402.

Laino G, Graziano A, d'Aquino R, Pirozzi G, Lanza V, Valiante S, De Rosa A, Naro F, Vivarelli E, Papaccio G. 2006. An approachable human adult stem cell source for hard-tissue

Levi B, James AW, Nelson ER, Vistnes D, Wu B, Lee M, et al. Human adipose derived stromal cells heal critical size mouse calvarial defects. 2010. PLoSOne.5(6):e11177.

Levi, B., Wan, D., Glotzbach, J., Hyun, J., Januszyk, M., Montoro, D., Sorkin, M., et al. (2011). CD105 protein depletion enhances human adipose-derived stromal cell osteogenesis through reduction of transforming growth factor β1 (TGF-β1) signaling. The Journal of biological chemistry, 286(45), 39497–509.doi:10.1074/jbc.m111.256529

Lewis, B. P., Burge, C. B. &Bartel, D. P. Conserved seed pairing, often flanked by adenosines, indicates that thousands of human genes are microRNA targets. *Cell*120, 15–20 (2005).

Li C, Guo B, Ding S, Rius C, Langa C, Kumar P, *et al* . TNF alpha down-regulates CD105 expression in vascular endothelial cells: a comparative study with TGF beta 1. *Anticancer research* 23, 1189–96

Li, Z. *et al.* A microRNA signature for a BMP2-induced osteoblast lineage commitment program. *Proceedings of the National Academy of Sciences* 105, 13906–13911 (2008).

Lu, J. et al. MicroRNA expression profiles classify human cancers. Nature 435, 834–838 (2005)

Luzi, E. *et al.* Osteogenic differentiation of human adipose tissue-derived stem cells is modulated by the miR-26a targeting of the SMAD1 transcription factor. *Journal of bone and mineral research : the official journal of the American Society for Bone and Mineral Research*23, 287–95 (2008).

Maeda, S., Hayashi, M., Komiya, S., Imamura, T. &Miyazono, K. Endogenous TGF-β signaling suppresses maturation of osteoblasticmesenchymal cells. *The EMBO Journal* **23,** 552–563 (2004).

Massagué, J. TGFbeta in Cancer. *Cell* 134,215–30 (2008).

Mayo, V., Sawatari, Y., Huang, C. & Garcia-Godoy, F. Neural crest-derived dental stem cells—Where we are and where we are going. *Journal of Dentistry* 42, 10431051 (2014).

Mitchell, James B et al. 2006. "Immunophenotype of human adipose-derived cells: temporal changes in stromal-associated and stem cell-associated markers." Stem cells (Dayton, Ohio) 24(2): 376–85. Available at: http://www.ncbi.nlm.nih.gov/pubmed/16322640 [Accessed November 28, 2014].

Miura M, Gronthos S, Zhao M, Lu B, Fisher LW, Robey PG, et al. SHED: stem cells from human exfoliated deciduous teeth. Proceedings of the National Academy of Sciences of the United States of America. 2003 May 13;100(10):5807-12.

Mizuno, Hiroshi, MorikuniTobita, and A. CagriUysal. 2012. "Concise Review: Adipose-Derived Stem Cells as a Novel Tool for." Stem cells Regenerative Medicine 30: 804–810.

Miyazono, K. Positive and negative regulation of TGF-beta signaling. *Journal of cell science* 113 (Pt 7), 1101–9 (2000).

Papaccio, Gianpaolo et al. 2006. "Long-Term Cryopreservation of Dental Pulp Stem Cells (SBP-DPSCs) and Their Differentiated Osteoblasts : A Cell Source for Tissue Repair." 325(December 2005): 319–325.

Pevsner-Fischer, M., Levin, S. &Zipori, D.The origins of mesenchymal stromal cell heterogeneity. *Stem cell reviews* **7,** 560–8 (2011).

Pfaffl MW. A new mathematical model for relative quantification in real-time RT-PCR. Nucleic Acids Res. 2001;29(9):e45. Epub 2001/05/09. PubMed PMID: 11328886.

Phinney, D. Functional heterogeneity of mesenchymal stem cells: Implications for cell therapy. *Journal of Cellular Biochemistry***113,** 2806–2812 (2012).

Satija, Neeraj Kumar et al. 2007. "Mesenchymal stem cells: molecular targets for tissue engineering." Stem cells and development 16: 7–23.

Siddappa, R, H Fernandes, J Liu, C van Blitterswijk, et al. 2007. "The response of human mesenchymal stem cells to osteogenic signals and its impact on bone tissue engineering." Curr Stem Cell Res Ther 2: 209–220.

Slezak-Prochazka, Izabella, JoostKluiver, Debora de Jong, Gertrud Kortman, Nancy Halsema, SibrandPoppema, Bart-Jan Kroesen, and Anke van den Berg. 2013. "Cellular Localization and Processing of Primary Transcripts of Exonic microRNAs." PloS One 8 (9): e76647. doi:10.1371/journal.pone.0076647.

Stark, MS. SonikaTyagi, Derek J. Nancarrow, Glen M. Boyle, Anthony L. Cook, David C. Whiteman, Peter G. Parsons, Christopher Schmidt, Richard A. Sturm, Nicholas K. Hayward. Characterization of the Melanoma miRNAome by Deep Sequencing.PLOS March 2010 | Volume 5 | Issue 3 | e9685

Stefani, G. & Slack, F. J. Small non-coding RNAs in animal development. *Nature reviews. Molecular cell biology* 9, 219–30 (2008).

Tholpady SS, Llull R, Ogle RC, Rubin JP, Futrell JW, Katz AJ. Adipose tissue: stem cells and beyond. *Clinics in plastic surgery* 2006; 33 (1): 55–62, vi.

Trubiani O, G Orsini, S Caputi and A Piatelli. (2006). Adult mesenchymal stem cells in dental research: a new approach for tissue engineering. Int J ImmunopatholPharmacol 19:451–460.

Valencia-Sanchez, M., Liu, J., Hannon, G. & Parker, R. Control of translation and mRNA degradation by miRNAs and siRNAs. *Genes &Development*(2006).doi:10.1101/gad.1399806

Vandesompele J, De Preter K, Pattyn F, Poppe B, Van Roy N, De Paepe A, et al. Accurate normalization of real-time quantitative RT-PCR data by geometric averaging of multiple internal control genes. Genome Biol. 2002;3(7):RESEARCH0034. Epub 2002/08/20. PubMed PMID: 12184808.

Wang, Q., Cai, J., Cai, X.-H. & Chen, L. miR-346 regulates osteogenic differentiation of human bone marrow-derived mesenchymal stem cells by targeting the Wnt/β-catenin pathway. *PloS one* 8, e72266 (2013).

Wang. Y. Chen, M. Tao, Z. Hua, Q. Chen, S. Xiao, B. Identification of predictive biomarkers for early diagnosis of larynx carcinoma based on microRNAs expression data.Cancer Genetics 206 (2013) 340e346.

Yan, X., Liu, Z. & Chen, Y. Regulation of TGF-β signaling by Smad7. *ActaBiochimicaetBiophysicaSinica* 41, 263–272 (2009).

Zuk PA, Zhu M, Mizuno H, Huang J, Futrell JW, Katz AJ, et al. Multilineage cells from human adipose tissue: implications for cell-based therapies. Tissue engineering. 2001 Apr;7(2):211-28.

Xiao YT, Xiang LX, Shao JZ (2007) Bone morphogenetic protein. Biochem. Biophys. Res. Commun. 362(3), 550–3.

Schematic Conclusion

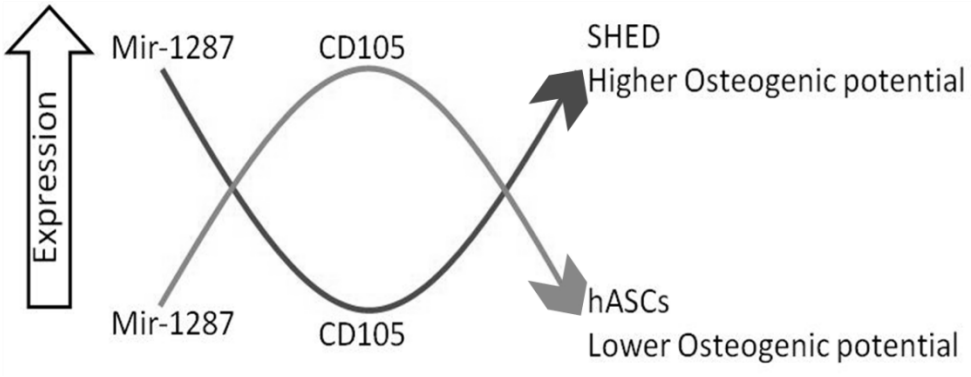

Table S1

Target	NM	Forward primer	Reverse Primer
RUNX2 (Runt-related transcription factor 2)	NM_001024630.3	agtggacgaggcaagagtttc	gttcccgaggtccatctactg
*ALP (*Alkaline phosphatase)	NM_000478.4	gatacaagcactcccacttcatctg	ctgttcagctcgtactgcatgtc
*DLX5 (*Distal-less homeobox 5)	NM_005221	accagccagaagaagtgac	ccttctctgtaatgcggcca
CD105 (Endoglin)	NM_001144950	tgcacttggcctacaattcca	agctgcccactcaaggatct
*BGLAP (*Osteocalcin*)*	NM_199173	ggcgctacctgtatcaatgg	gtggtcagccaactcgtca
ACTB (Endogenous Control)	NM_001101	tgaagtgtgacgtggacatc	ggaggagcaatgatcttgat
TBP (Endogenous Control)	NM_001172085	gtgacccagcatcactgtttc	gcaaaccagaaacccttgcg
HMBS (Endogenous control)	NM_001024382	agcttgctcgcatacagacg	agctccttggtaaacaggctt

Table S1. Primers used for Real-Time PCR experiments.

Figure S1

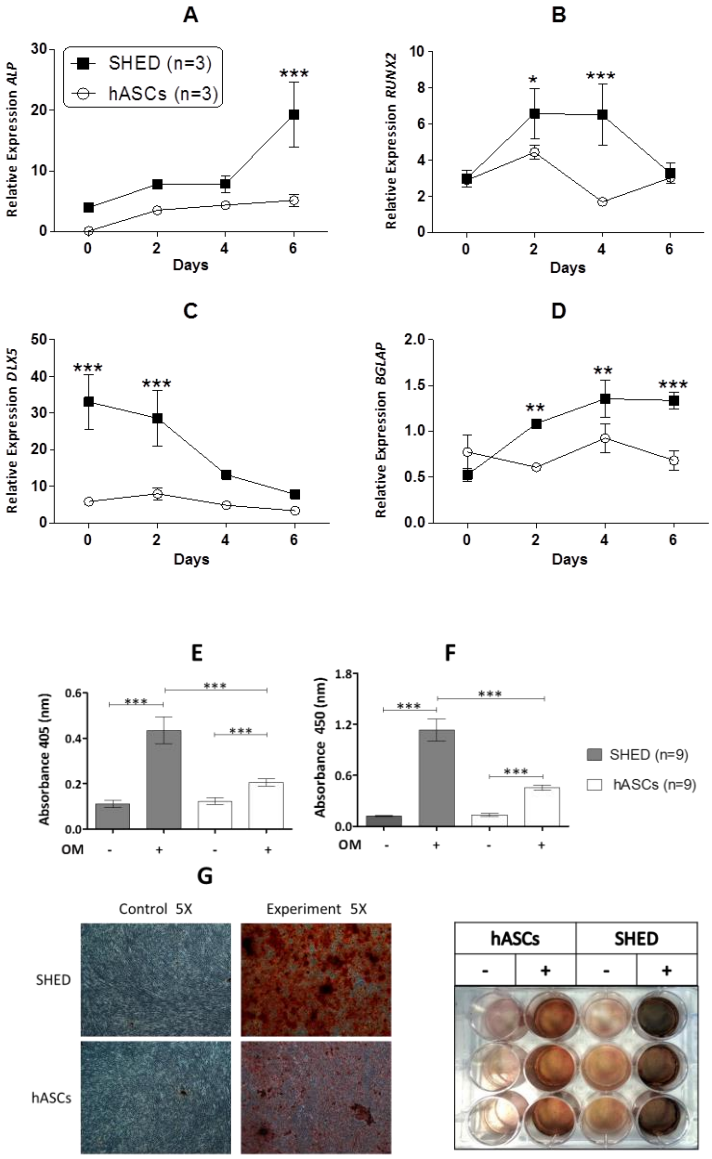

Figure S1: Relative expression of osteoblastogenic markers through qRT-PCR during in vitro osteoblastogenic differentiation at 0, 2, 4 and 6 days in SHED and hASCs (n=3 per cell type) A- ALP (alkaline Phosphatase), B- RUNX2 (runt-related transcription factor 2), C- DLX5 (distal-less homeobox 5) and D- BGLAP (osteocalcin). ACTb, TBP and HMBS were used as endogenous control. Tests with $p<0.05$ were considered to be statistically significant (* $p<0.05$, ** $p<0.01$, *** $p<0.001$). E. Quantification of Alkaline Phosphatase activity (absorbance at 405 nm) after 9 days of in vitro osteogenic differentiation in SHED and hASCs (n=9 per cell type). F. Quantification of extracellular matrix mineralization (absorbance at 450 nm) after 21 days of in vitro osteogenic differentiation in SHED and hASCs (n=9 per cell type). G. Pictures of Alizarin Red S staining after 21 days of osteogenic differentiation in SHED and hASCs. Bars represent mean absorbance with respective standard deviations (OM- osteogenic media). Tests with $p<0.05$ were considered to be statistically significant (* $p<0.05$, ** $p<0.01$, *** $p<0.001$).

Figure S2

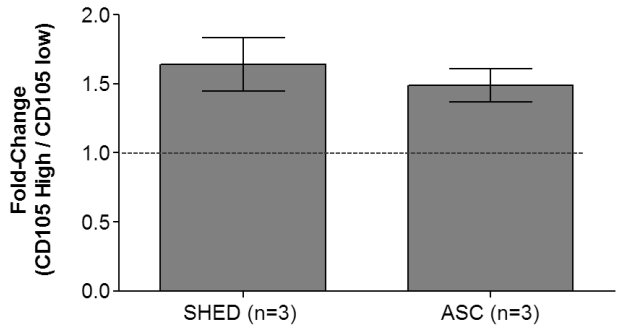

Figure S2: Fold-Change of CD105 of subpopulations sorted for CD105low/high in SHED and hASCs (n=3). ACTb, TBP and HMBS were used as endogenous control. Tests with $p<0.05$ were considered to be statistically significant

Figure S3

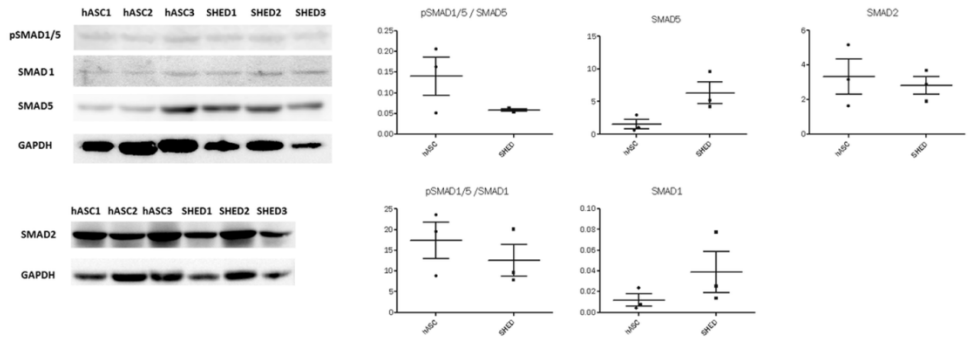

Figure S3: Western Blotting experiments quantifying the expression of SMADs and pSMADs in SHED and hASCs (n=3). GAPDH was used as endogenous control.

CHAPTER IV

Improvement of *In Vitro* Osteogenic Potential though Differentiation of Induced Pluripotent Stem Cells from Human Exfoliated Dental Tissue towards Mesenchymal-like Stem Cells

Hindawi Publishing Corporation
Stem Cells International
Volume 2015, Article ID 249098, 9 pages
http://dx.doi.org/10.1155/2015/249098

Hindawi

Research Article

Improvement of *In Vitro* Osteogenic Potential through Differentiation of Induced Pluripotent Stem Cells from Human Exfoliated Dental Tissue towards Mesenchymal-Like Stem Cells

Felipe Augusto Andre Ishiy,[1] Roberto Dalto Fanganiello,[1] Karina Griesi-Oliveira,[1] Angela May Suzuki,[1] Gerson Shigeru Kobayashi,[1] Andressa Gois Morales,[1] Luciane Portas Capelo,[2] and Maria Rita Passos-Bueno[1]

[1] *Department of Genetics and Evolution, Institute of Bioscience, University of Sao Paulo, 05508-090 Sao Paulo, SP, Brazil*
[2] *Science and Technology Institute, Federal University of Sao Paulo, 12247-014 Sao Jose dos Campos, SP, Brazil*

Correspondence should be addressed to Maria Rita Passos-Bueno; passos@ib.usp.br

Received 30 September 2014; Revised 19 December 2014; Accepted 29 December 2014

Academic Editor: Jack Parent

Copyright © 2015 Felipe Augusto Andre Ishiy et al. This is an open access article distributed under the Creative Commons Attribution License, which permits unrestricted use, distribution, and reproduction in any medium, provided the original work is properly cited.

Constraints for the application of MSCs for bone reconstruction include restricted self-renewal and limited cell amounts. iPSC technology presents advantages over MSCs, providing homogeneous cellular populations with prolonged self-renewal and higher plasticity. However, it is unknown if the osteogenic potential of iPSCs differs from that of MSCs and if it depends on the iPSCs originating cellular source. Here, we compared the *in vitro* osteogenesis between stem cells from human deciduous teeth (SHED) and MSC-like cells from iPSCs from SHED (iPS-SHED) and from human dermal fibroblasts (iPS-FIB). MSC-like cells from iPS-SHED and iPS-FIB displayed fibroblast-like morphology, downregulation of pluripotency markers and upregulation of mesenchymal markers. Comparative *in vitro* osteogenesis analysis showed higher osteogenic potential in MSC-like cells from iPS-SHED followed by MSC-like cells from iPS-FIB and SHED. CD105 expression, reported to be inversely correlated with osteogenic potential in MSCs, did not display this pattern, considering that SHED presented lower CD105 expression. Higher osteogenic potential of MSC-like cells from iPS-SHED may be due to cellular homogeneity and/or to donor tissue epigenetic memory. Our findings strengthen the rationale for the use of iPSCs in bone bioengineering. Unveiling the molecular basis behind these differences is important for a thorough use of iPSCs in clinical scenarios.

1. Introduction

Clinical demand for bone tissue is evident to supplant bony structures lost due to trauma, disease, or congenital malformation. Cell replacement therapies represent a promising strategy for bone engineering, and human mesenchymal stem cells (MSCs) isolated from various adult tissues have been extensively investigated as a potential cell source for bone regenerative treatments [1, 2]. However, large-scale applications are constrained since MSCs are found in limited amounts, are highly heterogeneous, and their long-term in vitro expansion can lead to senescence and spontaneous differentiation [3, 4]. Additionally, the differentiation potential of MSCs may vary depending on the tissue of origin [5].

Generation of human induced pluripotent stem cells (hiPSCs) was first achieved using dermal fibroblasts [6, 7]. Thereafter, hiPSCs have been derived from an ample variety of starting cells, including MSCs. Reprogramming MSCs to hiPSC is an attractive approach to circumvent issues associated with the direct use of MSCs since it allows the production of cells with robust *in vitro* self-renewal capacity and with differentiation multipotential. Controlling differentiation cues *in vivo* is a significant challenge and direct transplantation of pluripotent stem cells may result in tumor formation [8]. Therefore, derivation of MSC-like cells from

pluripotent stem cells has been pursued by a number of researchers [9–11].

Most types of MSCs are not easily obtained using minimally invasive procedures. Stem cells from human exfoliated deciduous teeth (SHED) can be easily isolated from a readily accessible tissue source, expanded under simple culture conditions, and banked. Even though SHED have been reported to be especially useful to restore bone [12, 13], as mentioned above, their inherent population heterogeneity and limited expansion capacity restrict their use for therapeutic purposes. While hiPSCs have been generated from SHED (iPS-SHED) [14], there is no report exploring the *in vitro* osteogenic potential of MSC-like cells derived from iPS-SHED populations. Therefore, the goal of this study is threefold: (1) to verify if MSC-like cells from iPS-SHED and SHED isolated from the same donors exhibit similar *in vitro* osteogenic potential; (2) to compare the osteogenic potential of MSC-like cells from iPS-SHED with MSC-like cells from hiPSCs derived from mature dermal fibroblasts (iPS-FIB), considered the most accessible cell source for iPSC generation; (3) to compare the expression of CD105 between these cellular populations, which has been inversely correlated with an increased osteogenic potential [15].

2. Materials and Methods

2.1. Isolation of Stem Cells from Human Exfoliated Dental Tissue (SHED), Human Dermal Fibroblasts, and Generation of Human Induced Pluripotent Stem Cells (hiPSCs). SHED were obtained from teeth of 6 independent subjects by enzymatic digestion of pulp from deciduous teeth as described in Miura et al., 2003 [12]. Human adult dermal fibroblasts, the most accessible and feasible cell source for iPSC generation [14], were obtained according to the protocol detailed in Aasen and Belmonte 2010, adapted for fibroblast isolation [16]. hiPSCs were obtained from SHED from 2 independent subjects (3 clones derived from each) and fibroblast cell populations from 3 independent subjects (2 clones each). *SOX2*, *c-MYC*, *OCT4*, and *KLF4* ectopic expression were induced through retroviral transduction, as originally reported in Takahashi et al., 2007 [6]. Two days after transduction, SHED and fibroblasts were cocultivated with irradiated murine embryonic fibroblasts (Millipore) in embryonic stem cell medium Dulbecco's modified Eagle/F12 medium (DMEM/F12) supplemented with 2 mM GlutaMAX-I, 0.1 mM nonessential amino acids, 55 uM 2-mercaptoethanol, 30 ng/mL of bFGF, and 20% of knockout serum replacement all provided by Life Technologies. Typical hiPSC colonies formed on feeder cells were transferred to matrigel (BD-Biosciences) coated plates and expanded in Essential 8 Medium (Life Technologies) supplemented with 100 ug/mL of normocin (Invivogen). hiPSCs displayed embryonic stem cell-like morphology, expressed pluripotency markers (*NANOG, OCT3, OCT4*), and displayed trilineage differentiation potential after embryoid body differentiation and *in vivo* teratoma formation (see Supplementary Figure 1 in Supplementary Material available online at http://dx.doi.org/10.1155/2015/249098). This project was approved by the local ethical committee (Protocol number 121/2001-FR. 435054).

2.2. Derivation of MSC-Like Cells from iPS-SHED and iPS-FIB. iPS-SHED and iPS-FIB colonies from confluent plates were detached with accutase (Life Technologies). hiPSC colonies were partially dissociated via manual pipetting and the cells were plated onto matrigel-coated tissue culture dishes at 1×10^4 cells/cm^2 in MSC differentiation culture medium (Dulbecco's modified Eagle medium High Glucose—DMEM with 10% fetal bovine serum, 1% penicillin/streptomycin, 1% nonessential amino acids, and 5 ng/mL of bFGF) for 14 days with media changes every 3 days. For subsequent passages, single-cell suspensions were prepared using TrypLE reagent (Life Technologies) and cells were passaged with a 1 : 3 split ratio in standard culture flasks (Corning) without matrigel coating.

2.3. Characterization of MSC-Like Cells from iPS-SHED and from iPS-FIB. SHED and MSC-like cells from iPS-SHED and from iPS-FIB were harvested and resuspended to 10^5 cells in 100 uL of PBS containing 1% BSA. Cells were separately labeled with FITC, PE, PE-Cy5, PERCP-Cy5.5, or APC-H7 conjugated rat anti-human antibodies CD29, CD31 (Biolegend), CD34, CD45, CD73, CD90 CD105, and CD166 (Becton Dickinson) on ice and protected from light for 40 min. An isotype-matched mAb was used as a control (Becton Dickinson). Data were acquired and analyzed with the FACSAria II cytometer and CellQuest software (Becton Dickinson). Multipotential differentiations of MSC-like cells from iPS-SHED and from iPS-FIB were performed as previously described by de Mendonça Costa et al., 2008 [13], and representative pictures of adipogenesis, osteogenesis, and chondrogenesis were included as supplementary Figure 2.

2.4. Real-Time Quantitative PCR. Total RNA was obtained from cell populations with the use of Nucleospin RNA II extraction kit (Macherey-Nagel) following manufacturer's recommendations. Briefly, one microgram of total RNA was converted into cDNA using Superscript II (Life Technologies), according to the manufacturer's recommendations. Real-time quantitative PCR reactions were performed with 2x SYBR Green PCR Master Mix (Life Technologies) and 25 nM–200 nM of each primer. Fluorescence was detected using ABI Prism 7500 Sequence Detection System, under standard temperature protocol. Primer pairs were designed with Primer-BLAST (http://www.ncbi.nlm.nih.gov/tools/primer-blast/; primer sequences are listed in Table 1, and their amplification efficiencies (E) were determined by serial cDNA dilutions $\log_{10}$-plotted against Ct values, in which $E = 10^{-1/\text{slope}}$. Expression of target genes was assessed relative to a calibrator cDNA (ΔCt). Finally, GeNorm v3.4 [17] was used to determine the most stable endogenous controls (among *ACTB, TBP, and HMBS*) and calculate normalization factors for each sample. The final expression values were determined based on a previous method [18], dividing $E^{-\Delta Ct}$ by the corresponding normalization factor.

2.5. In Vitro Osteogenic Induction. For osteogenic induction, MSC-like cells from iPS-SHED and from iPS-FIB were plated in 12-well plates (4×10^4 cells per well) and after

Table 1: Primers used for real-time quantitative PCR experiments.

Target	NM	Forward primer	Reverse primer
OCT3 (pluripotency)	NM_001173531.1	gtggtcagccaactcgtca	ccaaaaaccctggcacaaact
OCT4 (pluripotency)	NM_002701.3	cctcacttcactgcactgta	caggttttctttccctagct
NANOG (pluripotency)	NM_024865	tggacactggctgaatccttc	cgttgattaggctccaaccat
RUNX2	NM_001024630.3	agtggacgaggcaagagtttc	gttcccgaggtccatctactg
ALP	NM_000478.4	gatacaagcactcccacttcatctg	ctgttcagctcgtactgcatgtc
BGLAP	NM_199173	ggcgctacctgtatcaatgg	gtggtcagccaactcgtca
COL1A1	NM_000088.3	gggccaagacgaagacat	caacacccttgccgttgtcg
DLX5	NM_005221	accagccagaagaagtgac	ccttctctgtaatgcggcca
CD105 (*ENG*)	NM_001144950	tgcacttggcctacaattcca	agctgcccactcaaggatct
ACTB (endogenous control)	NM_001101	tgaagtgtgacgtggacatc	ggaggagcaatgatcttgat
TBP (endogenous control)	NM_001172085	gtgacccagcatcactgtttc	gcaaaccagaaaacccttgcg
HMBS (endogenous control)	NM_001024382	agcttgctcgcatacagacg	agctccttggtaaacaggctt

3 days, medium was replaced with osteogenic induction medium (Stem Pro Osteogenesis Kit-Life Technologies). Culture medium was changed every 2-3 days and cultures were maintained for 21 days. After 9 days of osteogenic induction, alkaline phosphatase activity was quantified through a biochemical assay: cells were treated with phosphatase substrate (Sigma-Aldrich), and the resulting p-nitrophenol was quantified colorimetrically using a Multiskan EX ELISA plate reader (Thermo Scientific) at 405 nm. After 21 days mineralization of extracellular matrix was assessed through alizarin red staining. Briefly, cells were washed three times with PBS, fixed with a 70% ethanol solution for 30 minutes at room temperature, followed by three distilled water washes, and finally stained with a 0.2% alizarin red S solution (Sigma-Aldrich) for 30 minutes at room temperature. After three washes with PBS, plates were air-dried at room temperature; pictures were taken. Staining was removed with 20% methanol/10% acetic acid solution and measured colorimetrically using a Multiskan EX ELISA plate reader (Thermo Scientific) at 450 nm. von Kossa staining was also performed after 14 and 21 days of osteogenic induction: cell cultures were washed once with PBS, a 1% silver nitrate solution was added, and the plate was exposed to UV light for 40 minutes. After UV light exposure the plate was rinsed with distilled water. Sodium thiosulfate (3%) was added for 5 minutes, the plates were then rinsed in water, and Van Gieson solution was added for 5 minutes. Plates were washed with 100% ethanol and air-dried for image analysis.

2.6. Statistical Analysis. All experiments were performed in triplicate. Unpaired Student's t-test was used for single comparisons. Error bars in bar graphs represent standard deviation. The level of statistical significance was set at $P < 0.05$.

3. Results

After 12 days of induction of iPS-SHED and iPS-FIB with MSC medium under feeder-free conditions, MSC-like cells derived from iPS-SHED and from iPS-FIB achieved 80% confluence in 25 cm^2 flasks and showed a spindle-shaped fibroblast-like morphology (Figure 1(a)). *OCT3*, *OCT4*, *NANOG*, and *ALP* mRNAs were significantly downregulated in MSC-like cells from iPS-SHED and from iPS-FIB when compared with the original hiPSC populations ($P < 0.05$, Figures 1(b′) and 1(b″)). Moreover MSC-like cells from iPS-SHED and from iPS-FIB expressed high levels of mesenchymal markers (CDs 29, 73, 90, and 105 and CD 166) and low levels of endothelial (CD 31) and hematopoietic (CDs 34 and 45) markers (Figure 2).

Next, we assessed the *in vitro* osteogenic potential of MSC-like cells from iPS-SHED, MSC-like cells from iPS-FIB and SHED during early *in vitro* osteogenesis by quantifying gene expression of key osteogenesis markers (*DLX5* and *RUNX2*, two early transcription factors associated with osteogenesis, *ALP* and *COL1A1*, two early osteoblast markers, and *BGLAP*, a late osteoblast marker). *ALP* gene expression was upregulated in all cellular populations from day 2 to day 6 but showed higher expression in days 4 and 6 in MSC-like cells from iPS-SHED and from iPS-FIB in comparison with SHED ($P < 0.001$). *DLX5* peaked at day 2 in MSC-like cells from iPS-SHED and from iPS-FIB and was upregulated in SHED at all time points ($P < 0.001$). *RUNX2* was also upregulated in SHED until day 6 of osteogenic induction, in comparison with MSC-like cells from iPS-SHED and from iPS-FIB ($P < 0.001$). *COL1A1* was upregulated in MSC-like cells from iPS-SHED and in SHED from day 2 to day 6 ($P < 0.001$) but showed no significant upregulation in MSC-like cells from iPS-FIB during this period. *BGLAP* was not upregulated during this early stage of osteoinduction in any cellular population, as expected for a late osteoblast marker (Figure 3(a)).

ALP enzymatic activity was higher in MSC-like cells from iPS-SHED when compared with MSC-like cells from iPS-FIB (2.3-fold increase, $P < 0.01$) and with SHED (2.54-fold increase, $P < 0.001$) after 9 days of *in vitro* osteoinduction (Figure 3(b)). Alizarin red S staining revealed more matrix mineralization in MSC-like cells from iPS-SHED when compared with SHED (4.36- fold increase, $P < 0.001$) and with MSC-like cells from iPS-FIB (1.45-fold increase, $P < 0.01$) after 21 days of osteoinduction

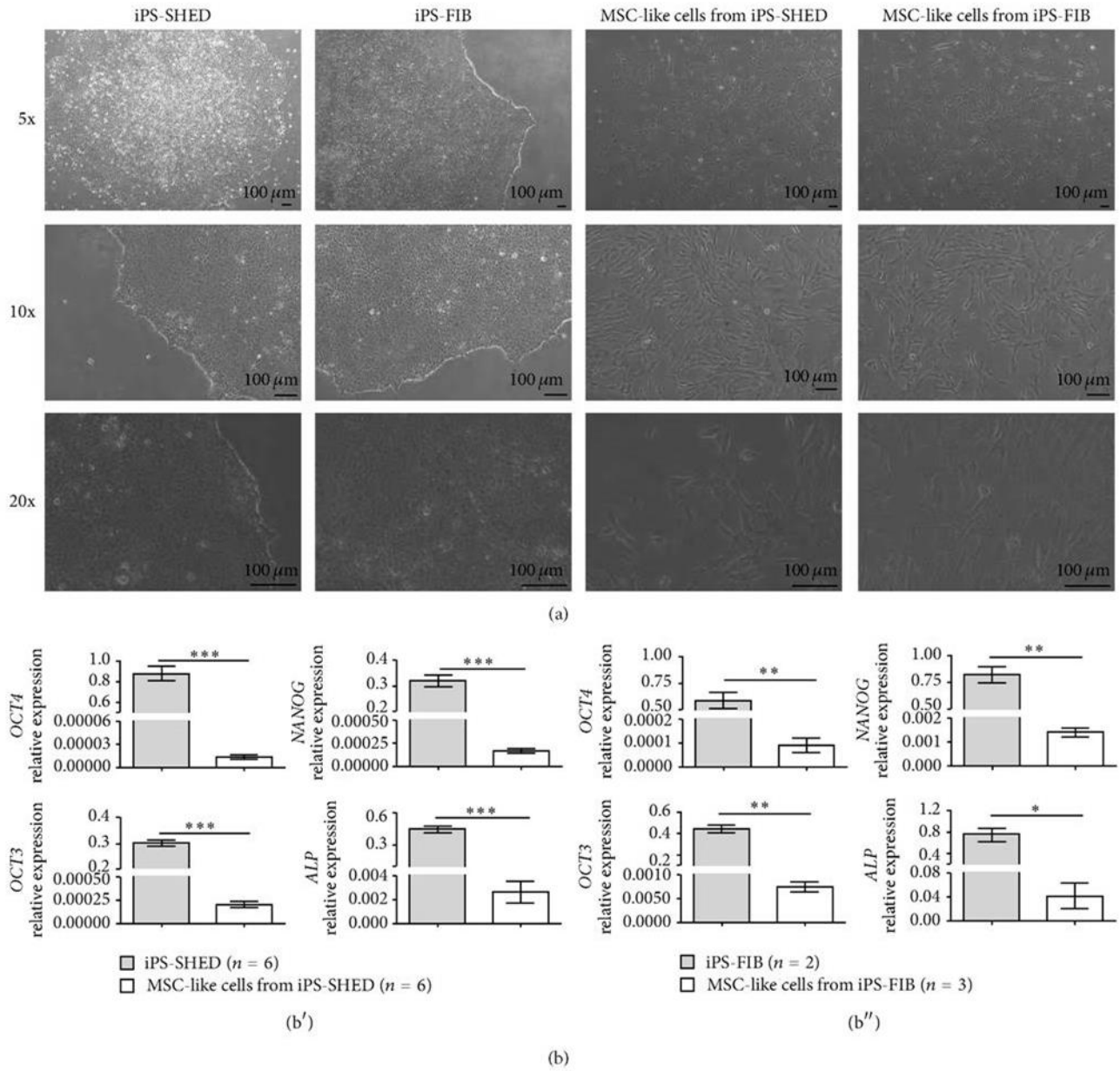

FIGURE 1: (a) Morphology of undifferentiated hiPSC colonies cultured on matrigel and MSC-like cells from iPS-SHED and iPS-FIB after 12 days of *in vitro* mesenchymal induction. Scale bar = 100 um. (b) Real-time quantitative PCR analysis of pluripotency markers in undifferentiated hiPSCs ((b′) SHED and (b″) fibroblasts) and in MSC-like cells from iPS-SHED and from iPS-FIB. *ACTB*, *TBP*, and *HMBS* were used as endogenous controls. Values represent means +/− SD, $P < 0.05$ (*), $P < 0.01$ (**), and $P < 0.001$ (***).

(Figure 3(c)). In this time point, MSC-like cells from iPS-FIB showed a 2.99-fold increase ($P < 0.001$) in mineralized matrix production when compared with SHED. These data were validated by von Kossa staining after 14 and 21 days of *in vitro* osteogenesis (Figure 3(e)).

Finally, we compared the expression of *CD105* mRNAs between SHED, MSC-like cells from iPS-SHED and from iPS-FIB and found a lower expression of this gene in SHED when compared with the latter cellular populations ($P < 0.001$, Figure 3(d)).

4. Discussion

iPSC technology has gained attention to engender cellular populations to be used in tissue engineering, displaying self-renewal, pluripotency, and differentiation plasticity similar to embryonic stem cells. Furthermore, the use of hiPSCs is not hindered by the ethical issues associated with the use of human embryos and permits the generation of therapeutically relevant cell types genetically compatible to patients, evading rejection drawbacks that may follow transplantation of nonautologous cells [19].

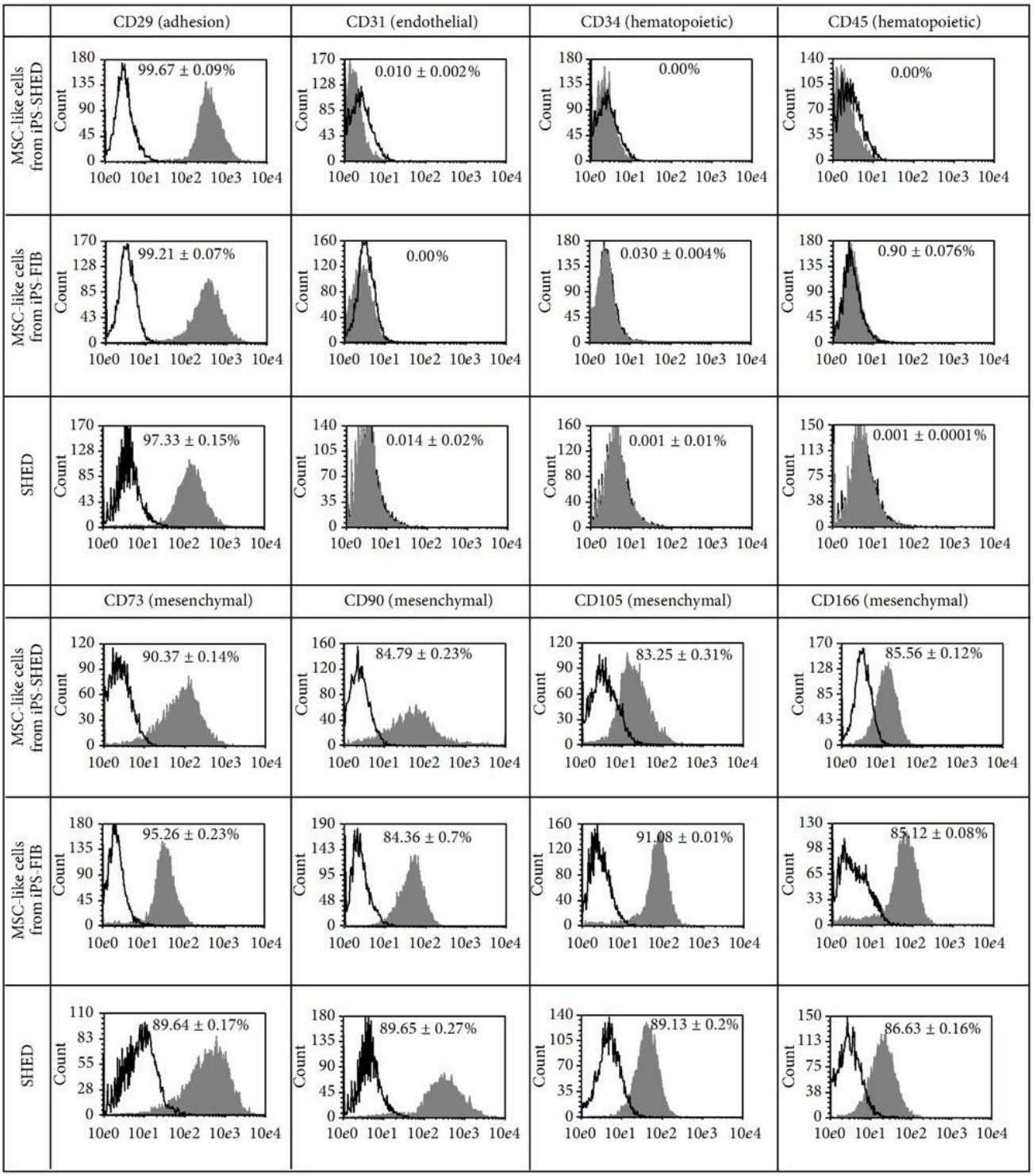

FIGURE 2: Representative surface antigen profiling of SHED, MSC-like cells from iPS-SHED and from iPS-FIB labeled with antibodies against mesenchymal, endothelial, and hematopoietic antigens. White histograms represent isotype controls and grey histograms represent the fluorescence of conjugated antibodies for each antigen. Mean expression rates are indicated above each graph and displayed as mean +/− SD.

There is an increasing interest in investigating iPSCs for bone regenerative therapies and a series of studies have generated murine iPSCs and assessed their direct differentiation towards osteoblasts [20–23]. From a safety point of view, the use of progenitor cells instead of undifferentiated iPSCs for therapeutic purposes is advantageous since progenitor cells are already primed for a specific differentiation pathway and tumor formation risk is reduced [24]. Moreover, recent

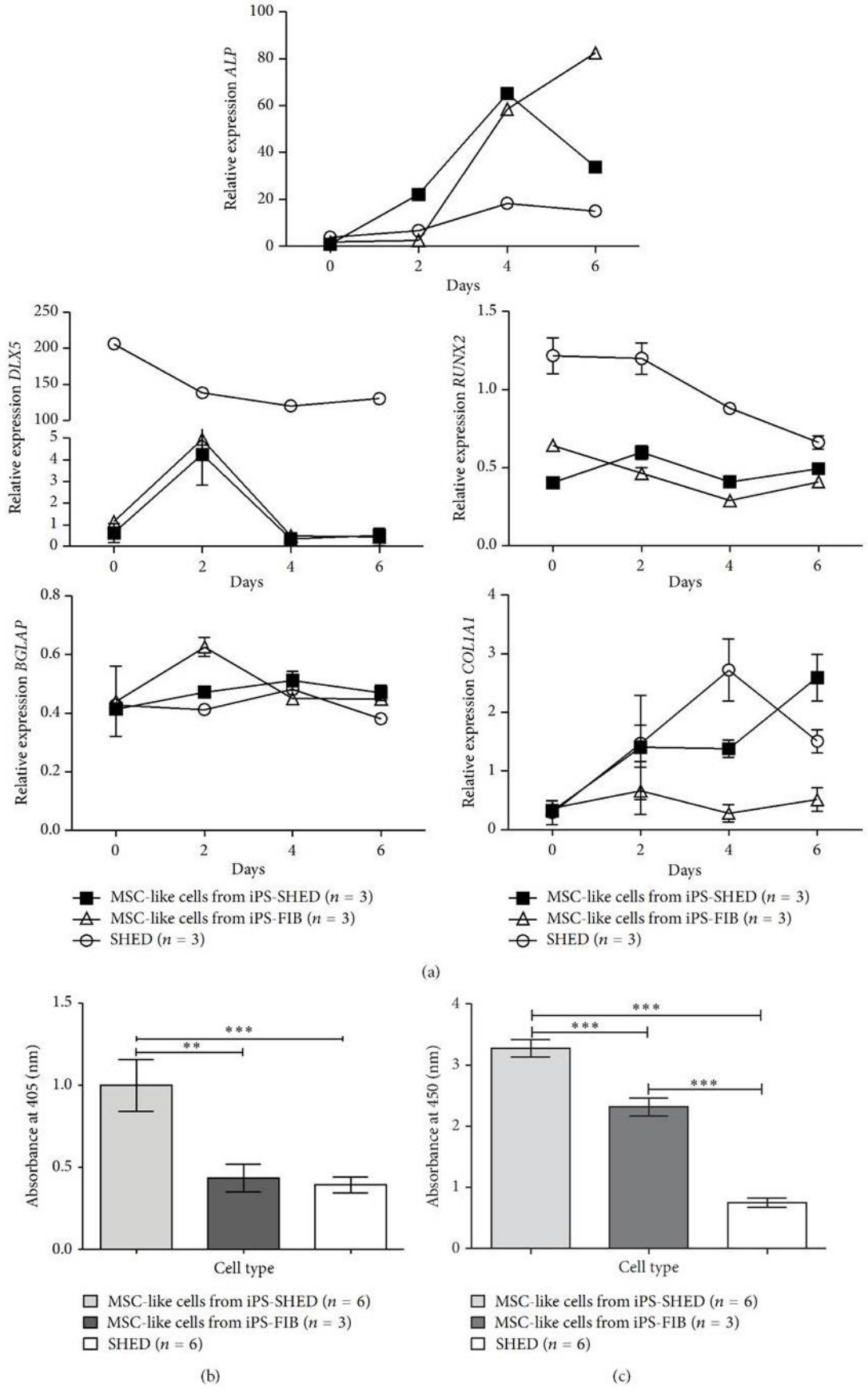

FIGURE 3: Continued.

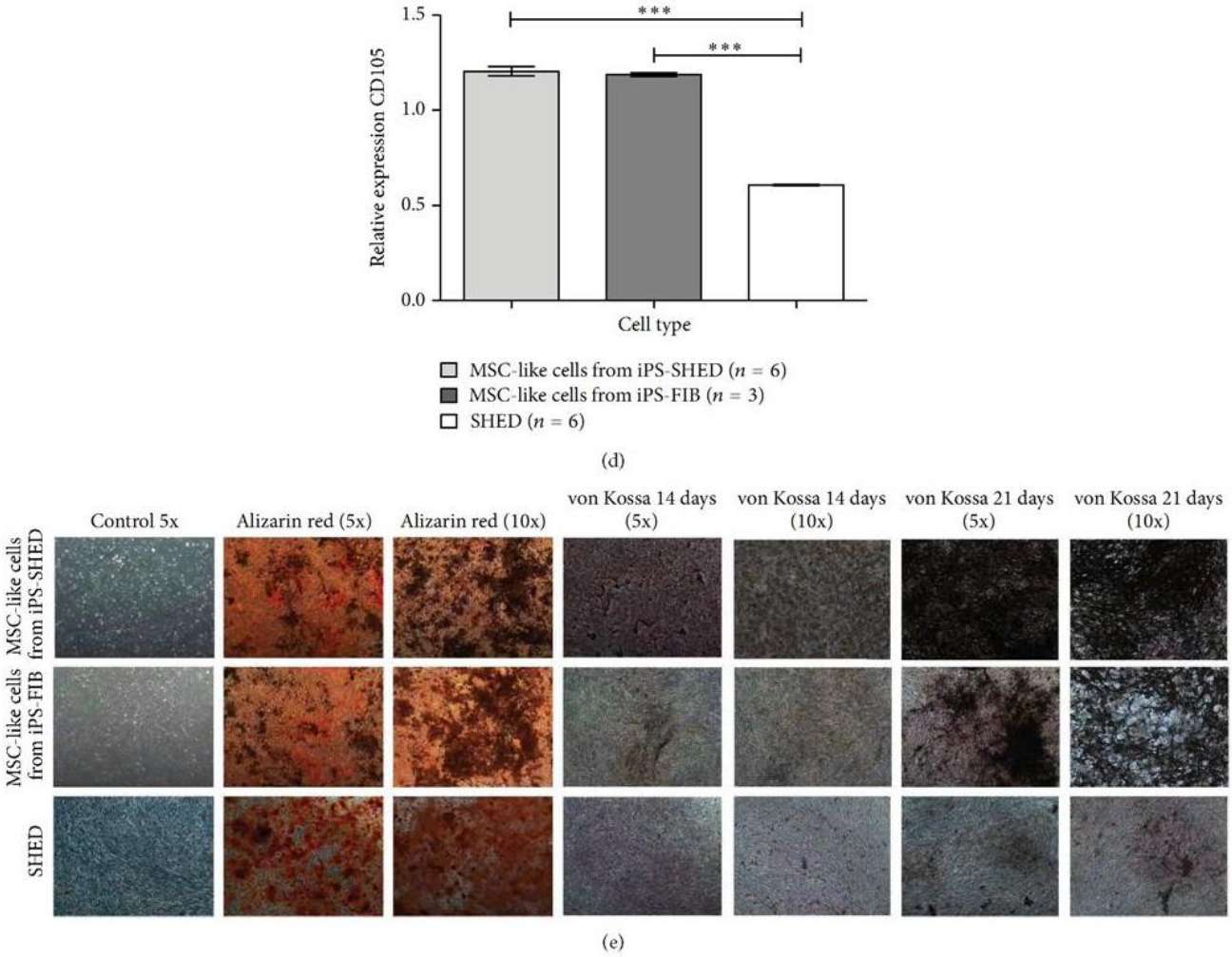

FIGURE 3: (a) Real-time quantitative PCR analysis of alkaline phosphatase (*ALP*), *DLX5*, *RUNX2*, *BGLAP*, and *COL1A1* in MSC-like cells from iPS-SHED, MSC-like cells from iPS-FIB and SHED. *ACTB*, *TBP*, and *HMBS* were used as endogenous controls. (b) Alkaline phosphatase activity quantification in cells cultured for 9 days in osteogenic medium. Values represent means +/− SD, $P < 0.01$ (**), and $P < 0.001$ (***). (c) Alizarin red S staining quantification in cells cultured for 21 days in osteogenic medium. Values represent means +/− SD, $P < 0.001$ (***). (d) Real-time quantitative PCR analysis of CD105 in undifferentiated SHED and MSCs from iPS-SHED and from iPS-FIB. *ACTB*, *TBP*, and *HMBS* were used as endogenous controls. Values represent means +/− SD, $P < 0.001$ (***). (e) Representative pictures of alizarin red S (after 21 days of *in vitro* osteoinduction, with 5 and 10x magnification) and von Kossa staining (after 14 and 21 of *in vitro* osteogenic induction, with 5 and 10x magnification) of mineralized deposits in MSC-like cells from iPS-SHED, MSC-like cells from iPS-FIB and SHED. Basal growth medium free of osteoinduction factors was used in the control group (with 5x magnification).

reports suggest that some of the reparative effects associated with MSC transplantation are not mediated by cellular differentiation per se but by paracrine factors secreted by them [25]; Fanganiello et al., submitted.

The MSC differentiation from hiPSCs seemed to be successful as both MSC-like cells from iPS-SHED and from iPS-FIB displayed typical mesenchymal cell morphology, downregulation of pluripotency markers and similar cell surface antigen profiles and multipotential when compared with SHED. After *in vitro* osteoinduction, upregulation of osteogenesis markers *DLX5* and *RUNX2* in SHED in comparison with MSC-like cells from iPS-SHED and from iPS-FIB may indicate a previous commitment of this cell population towards the osteogenic lineage. However, in days 4 and 6 of osteoinduction, MSC-like cells from iPS-SHED and from iPS-FIB presented upregulation of *ALP*, a metalloenzyme known as a key early marker of osteogenesis. MSC-like cells from iPS-SHED also had more ALP enzymatic activity when compared with MSC-like cells from iPS-FIB and with SHED in midstage osteogenesis. MSC-like cells from iPS-SHED and from iPS-FIB produced significantly more mineralized extracellular matrix when compared with SHED. Overall, MSC-like cells from iPS-SHED were able to undergo induced *in vitro* osteogenesis in a more efficient fashion than MSCs from iPS-FIB or from the originating SHED populations.

One of the factors that could explain the higher efficiency of the *in vitro* osteogenesis in MSC-like cells from iPS-SHED and iPS-FIB in comparison with SHED might be related to

the presence of a more homogeneous cellular population attributed to the direct plating protocol adopted. We have decided to choose the iPSC direct plating method over the embryoid body (EB) protocol since EBs are known to contain a heterogeneous mixture of cells with different degrees of multipotency that may limit their net osteogenic potential [26–28]. Accordingly, enhanced osteogenic differentiation has been associated with direct plating [29–32], and this method has been proposed to yield uniform batches of osteoprogenitor cells [31].

We also tested if the difference in osteogenic potential between the MSC-like cells from iPS-SHED from iPS-FIB and SHED is related to CD105 expression, as its lower expression has been associated with a higher osteogenic potential in MSCs harvested from human adipose tissue (hASCs) when compared with MSCs with higher CD105 expression [15]. Interestingly we found CD105 expression to be significantly lower in SHED when compared with both MSC-like cells from iPS-SHED and from iPS-FIB. Therefore, the higher osteogenic potential in this case may be due to other factors.

The difference in osteogenic potential here reported between MSC-like cells from iPS-SHED and from-iPS-FIB may possibly be related to a somatic epigenetic memory of the tissue of origin [33]. Derivation of pure populations of functionally differentiated cells from iPSCs is still challenging and different cell types show variable susceptibility to reprogramming. In fact, MSCs derived from iPSC lines from different tissues have been shown to exhibit variability in their differentiation profiles. Hynes et al. 2014 reported that MSC-like cells from iPSCs generated from periodontal ligament displayed higher osteogenic capacity both *in vitro* and *in vivo* when compared to MSC-like cells from iPSCs generated from lung and gingival fibroblasts, which was attributed to epigenetic memory of the donor tissue [34]. In another study, Sanchez-Freire et al. 2014 reported higher cardiac differentiation efficiency in MSC-like cells derived from iPSCs generated from cardiac progenitors in comparison with dermal fibroblasts from the same donor, which was demonstrated to be due to the retention of residual methylation signatures of the tissue of origin [35].

5. Conclusions

Our findings provide an important argument towards the use of iPSCs in tissue bioengineering since MSC-like cells from iPS-SHED and from iPS-FIB displayed higher osteogenic potential than SHED. We also suggest that cellular homogeneity and tissue of origin are important factors to be considered when planning to use iPSCs in bone regenerative medicine. CD105 does not seem to be a main factor involved in these differences. The dissection of the molecular basis of osteogenic differentiation in MSC-like cells from iPSC-derived cells may furnish insights into the clinical usefulness of iPSCs from different sources.

Conflict of Interests

The authors declare that there is no conflict of interests regarding the publication of this paper.

Authors' Contribution

Felipe Augusto Andre Ishiy and Roberto Dalto Fanganiello contributed equally to this work.

Acknowledgments

The authors are grateful to the subjects who participated in this work. They thank Simone Gomes Ferreira and Patricia Semedo Kuriki for technical assistance and Constancia Gotto Urbani for secretarial assistance. This work was supported by grants from the Brazilian Ministry of Health, the Foundation for Research Support of the State of Sao Paulo (FAPESP), and the National Council for Scientific and Technological Development (CNPq).

References

[1] D. Marolt, M. Knezevic, and G. V. Novakovic, "Bone tissue engineering with human stem cells," *Stem Cell Research & Therapy*, vol. 1, no. 2, article 10, 2010.

[2] X. Wang, Y. Wang, W. Gou, Q. Lu, J. Peng, and S. Lu, "Role of mesenchymal stem cells in bone regeneration and fracture repair: a review," *International Orthopaedics*, vol. 37, no. 12, pp. 2491–2498, 2013.

[3] M. Pevsner-Fischer, S. Levin, and D. Zipori, "The origins of mesenchymal stromal cell heterogeneity," *Stem Cell Reviews and Reports*, vol. 7, no. 3, pp. 560–568, 2011.

[4] K. Stenderup, J. Justesen, C. Clausen, and M. Kassem, "Aging is associated with decreased maximal life span and accelerated senescence of bone marrow stromal cells," *Bone*, vol. 33, no. 6, pp. 919–926, 2003.

[5] P. G. Robey, "Cell sources for bone regeneration: the good, the bad, and the ugly (But Promising)," *Tissue Engineering Part B: Reviews*, vol. 17, no. 6, pp. 423–430, 2011.

[6] K. Takahashi, K. Tanabe, M. Ohnuki et al., "Induction of pluripotent stem cells from adult human fibroblasts by defined factors," *Cell*, vol. 131, no. 5, pp. 861–872, 2007.

[7] W. E. Lowry, L. Richter, R. Yachechko et al., "Generation of human induced pluripotent stem cells from dermal fibroblasts," *Proceedings of the National Academy of Sciences of the United States of America*, vol. 105, no. 8, pp. 2883–2888, 2008.

[8] Y. Jung, G. Bauer, and J. A. Nolta, "Concise review: induced pluripotent stem cell-derived mesenchymal stem cells: progress toward safe clinical products," *Stem Cells*, vol. 30, no. 1, pp. 42–47, 2012.

[9] Q. Lian, Y. Zhang, J. Zhang et al., "Functional mesenchymal stem cells derived from human induced pluripotent stem cells attenuate limb ischemia in mice," *Circulation*, vol. 121, no. 9, pp. 1113–1123, 2010.

[10] T. Barberi, L. M. Willis, N. D. Socci, and L. Studer, "Derivation of multipotent mesenchymal precursors from human embryonic stem cells," *PLoS Medicine*, vol. 2, no. 6, article e161, 2005.

[11] L. G. Villa-Diaz, S. E. Brown, Y. Liu et al., "Derivation of mesenchymal stem cells from human induced pluripotent stem

cells cultured on synthetic substrates," *Stem Cells*, vol. 30, no. 6, pp. 1174–1181, 2012.

[12] M. Miura, S. Gronthos, M. Zhao et al., "SHED: Stem cells from human exfoliated deciduous teeth," *Proceedings of the National Academy of Sciences of the United States of America*, vol. 100, no. 10, pp. 5807–5812, 2003.

[13] A. de Mendonça Costa, D. F. Bueno, M. T. Martins et al., "Reconstruction of large cranial defects in nonimmunosuppressed experimental design with human dental pulp stem cells," *Journal of Craniofacial Surgery*, vol. 19, no. 1, pp. 204–210, 2008.

[14] X. Yan, H. Qin, C. Qu, R. S. Tuan, S. Shi, and G. T.-J. Huang, "iPS cells reprogrammed from human mesenchymal-like Stem/Progenitor cells of dental Tissue Origin," *Stem Cells and Development*, vol. 19, no. 4, pp. 469–480, 2010.

[15] B. Levi, D. C. Wan, J. P. Glotzbach et al., "CD105 protein depletion enhances human adipose-derived stromal cell osteogenesis through reduction of transforming growth factor beta1 (TGF-beta1) signaling," *The Journal of Biological Chemistry*, vol. 286, no. 45, pp. 39497–39509, 2011.

[16] T. Aasen and J. C. I. Belmonte, "Isolation and cultivation of human keratinocytes from skin or plucked hair for the generation of induced pluripotent stem cells," *Nature Protocols*, vol. 5, no. 2, pp. 371–382, 2010.

[17] J. Vandesompele, K. de Preter, F. Pattyn et al., "Accurate normalization of real-time quantitative RT-PCR data by geometric averaging of multiple internal control genes," *Genome Biology*, vol. 3, no. 7, Article ID RESEARCH0034, 2002.

[18] M. W. Pfaffl, "A new mathematical model for relative quantification in real-time RT-PCR," *Nucleic Acids Research*, vol. 29, no. 9, article e45, 2001.

[19] I. de Lázaro, A. Yilmazer, and K. Kostarelos, "Induced pluripotent stem (iPS) cells: a new source for cell-based therapeutics?" *Journal of Controlled Release*, vol. 185, no. 1, pp. 37–44, 2014.

[20] H. Egusa, H. Kayashima, J. Miura et al., "Comparative analysis of mouse-induced pluripotent stem cells and mesenchymal stem cells during osteogenic differentiation *in vitro*," *Stem Cells and Development*, vol. 23, no. 18, pp. 2156–2169, 2014.

[21] K. Tashiro, M. Inamura, K. Kawabata et al., "Efficient adipocyte and osteoblast differentiation from mouse induced pluripotent stem cells by adenoviral transduction," *Stem Cells*, vol. 27, no. 8, pp. 1802–1811, 2009.

[22] C.-L. Kao, L.-K. Tai, S.-H. Chiou et al., "Resveratrol promotes osteogenic differentiation and protects against dexamethasone damage in murine induced pluripotent stem cells," *Stem Cells and Development*, vol. 19, no. 2, pp. 247–257, 2010.

[23] T. Hayashi, H. Misawa, H. Nakahara et al., "Transplantation of osteogenically differentiated mouse iPS cells for bone repair," *Cell Transplantation*, vol. 21, no. 2-3, pp. 591–600, 2012.

[24] C. Karlsson, K. Emanuelsson, F. Wessberg et al., "Human embryonic stem cell-derived mesenchymal progenitors—potential in regenerative medicine," *Stem Cell Research*, vol. 3, no. 1, pp. 39–50, 2009.

[25] A. I. Caplan and J. E. Dennis, "Mesenchymal stem cells as trophic mediators," *Journal of Cellular Biochemistry*, vol. 98, no. 5, pp. 1076–1084, 2006.

[26] G. Bilousova, D. H. Jun, K. B. King et al., "Osteoblasts derived from induced pluripotent stem cells form calcified structures in scaffolds both *in vitro* and *in vivo*," *Stem Cells*, vol. 29, no. 2, pp. 206–216, 2011.

[27] J. M. Karp, L. S. Ferreira, A. Khademhosseini, A. H. Kwon, J. Yeh, and R. S. Langer, "Cultivation of human embryonic stem cells without the embryoid body step enhances osteogenesis *in vitro*," *Stem Cells*, vol. 24, no. 4, pp. 835–843, 2006.

[28] A. Nasu, M. Ikeya, T. Yamamoto et al., "Genetically matched human iPS cells reveal that propensity for cartilage and bone differentiation differs with clones, not cell type of origin," *PLoS ONE*, vol. 8, no. 1, Article ID e53771, 2013.

[29] D. A. Shimko, C. A. Burks, K. C. Dee, and E. A. Nauman, "Comparison of *in vitro* mineralization by murine embryonic and adult stem cells cultured in an osteogenic medium," *Tissue Engineering*, vol. 10, no. 9-10, pp. 1386–1398, 2004.

[30] V. Sottile, A. Thomson, and J. McWhir, "*In vitro* osteogenic differentiation of human ES cells," *Cloning and Stem Cells*, vol. 5, no. 2, pp. 149–155, 2003.

[31] Y. Dogaki, S. Y. Lee, T. Niikura et al., "Efficient derivation of osteoprogenitor cells from induced pluripotent stem cells for bone regeneration," *International Orthopaedics*, vol. 38, no. 9, pp. 1779–1785, 2014.

[32] L. Duplomb, M. Dagouassat, P. Jourdon, and D. Heymann, "Differentiation of osteoblasts from mouse embryonic stem cells without generation of embryoid body," *In Vitro Cellular & Developmental Biology—Animal*, vol. 43, no. 1, pp. 21–24, 2007.

[33] K. Kim, A. Doi, B. Wen et al., "Epigenetic memory in induced pluripotent stem cells," *Nature*, vol. 467, no. 7313, pp. 285–290, 2010.

[34] K. Hynes, D. Menicanin, K. Mrozik, S. Gronthos, and P. M. Bartold, "Generation of functional mesenchymal stem cells from different induced pluripotent stem cell lines," *Stem Cells and Development*, vol. 23, no. 10, pp. 1084–1096, 2014.

[35] V. Sanchez-Freire, A. S. Lee, S. Hu et al., "Effect of human donor cell source on differentiation and function of cardiac induced pluripotent stem cells," *Journal of the American College of Cardiology*, vol. 64, no. 5, pp. 436–448, 2014.

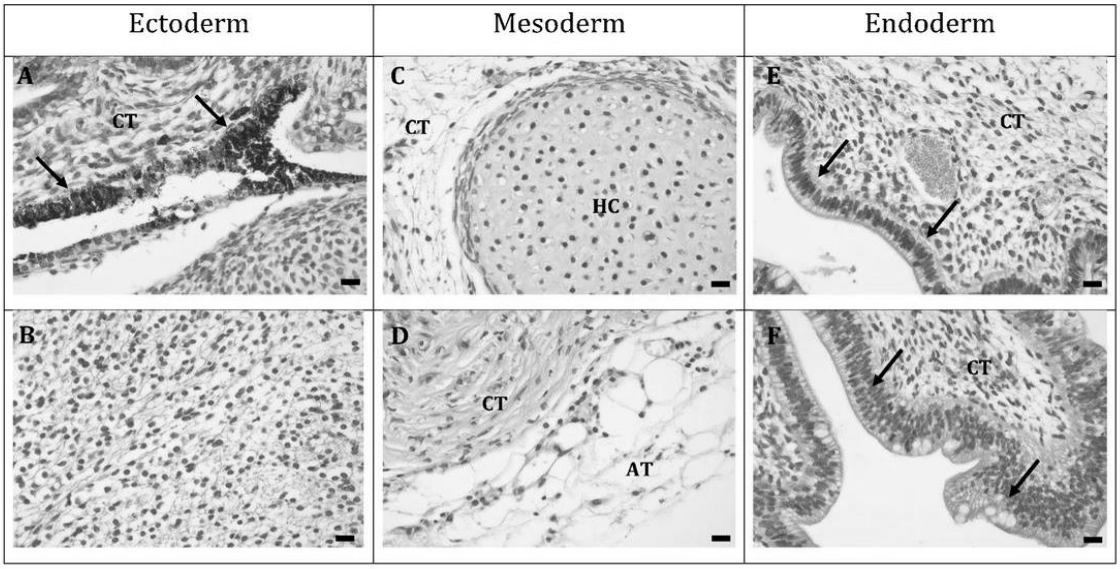

Supplementary figure 1: Hematoxylin and eosin staining of histopathological sections of the iPSC-derived teratoma, containing tissues from the three germ layers. The representative ectodermal tissues include (A) pigment epithelium containing melanin granules and (B) glial cells. The representative mesodermal tissues include (C) hyaline cartilage (HC), connective tissue (CT) and (D) adipose tissue (AT). The representative endodermal tissues include (E) respiratory ciliated epithelium and (F) gastro-intestinal-like epithelium. (A-F) Scale bar= 100ìm (40x magnification). Arrows indicate epithelial tissue.

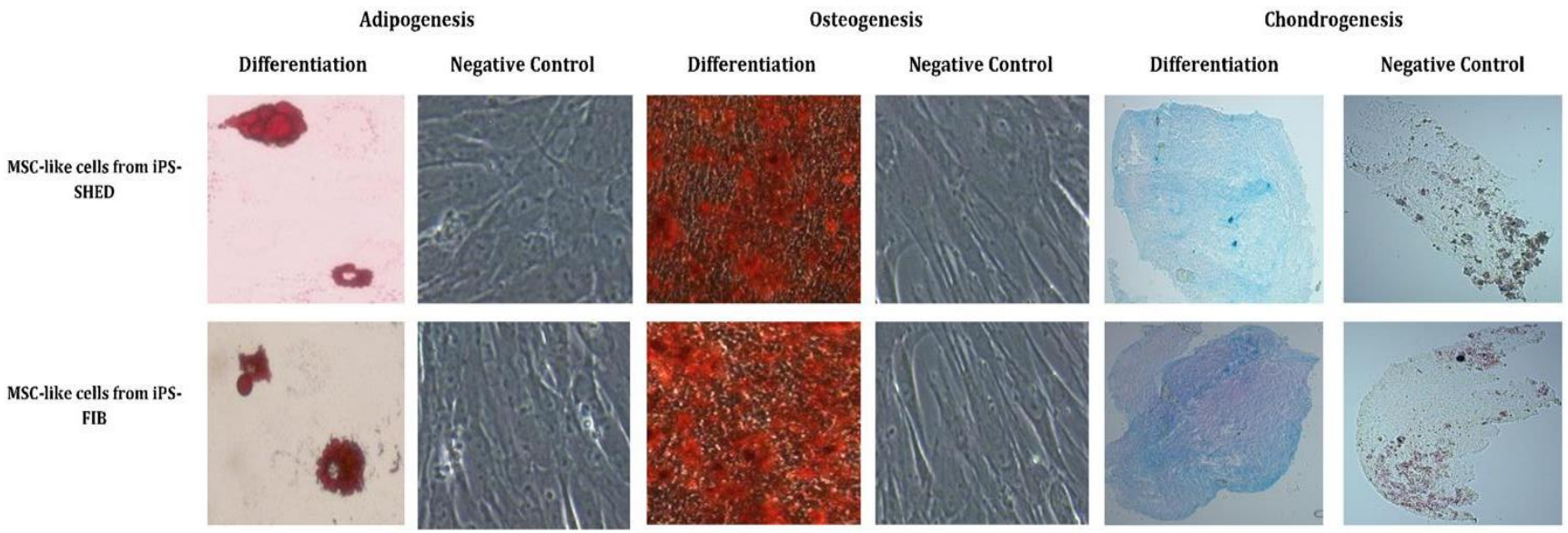

Supplementary figure 2: Representative pictures of adipogenesis (Oil-Red O staining after 14 days of in vitro induction, 20X of magnification), osteogenesis (Alizarin Red S after 21 days of in vitro induction, 20X of magnification) and chondrogenesis (Alcian blue staining after 21 of in vitro induction, 10X of magnification) of MSC-like cells from iPS-SHED and from iPS-FIB.

CHAPTER V

Neural crest-derived mesenchymal cells in the aetiology of Treacher Collins syndrome

Neural crest-derived mesenchymal cells in the aetiology of Treacher-Collins syndrome

Felipe A. A. Ishiy, Gerson S. Kobayashi, Camila M. Musso, Luiz C. Caires, Ernesto Goulart, Roberto D. Fanganiello, Patrícia Semedo-Kuriki, Naila Lourenço, Karina Griesi-Oliveira, Ângela M. Suzuki, Maria Rita Passos-Bueno.

Abstract

Apoptosis of pre-migratory cranial neural crest cells is considered to be the major phenotypic driver of Treacher Collins syndrome (TCS), a mandibulofacial dysostosis caused by loss-of-function mutations in *TCOF1*. However, the effect of these mutations on post-migratory, neural crest-derived mesenchymal cells and their skeletogenic fate remains elusive. To address this question, we report the establishment and phenotype assessment of neural crest-derived mesenchymal cells (nMSCs) from TCS iPSCs. We show that TCS nMSCs display both increased apoptosis and aberrant osteo-chondrogenic profiles *in vitro*. In comparison to controls, TCS cells showed changes in osteogenic potential and dysregulated expression of chondrogenesis markers during osteogenic and chondrogenic differentiation. These results suggest that cellular properties of neural crest-derived mesenchymal cells are impacted by *TCOF1* loss of function, providing additional clues to unravel the pathogenesis of TCS.

INTRODUCTION

Treacher Collins Syndrome (TCS1, OMIM #154500; TCS2, OMIM#613717; TCS3, OMIM #248390) is a rare mandibulofacial dysostosis present in 1:50,000 live births. Despite showing overlap with other craniofacial syndromes, the clinical presentation of TCS is very typical and includes hypoplasia of facial bones, particularly the zygomatic bones and the mandible, external ear anomalies and conductive hearing loss (Trainor et al., 2009). Genetic alterations in the genes *TCOF1*, *POLR1C* and *POLR1D* are the currently established underlying causes of TCS. Loss-of-function mutations in *TCOF1*, responsible for the vast majority of cases (Splendore et al., 2000), result in haploinsufficiency of its encoded protein, Treacle, which is involved in ribosome biogenesis (Gonzales et al., 2005); concurrently, *POLR1C* and *POLR1D* mutations are also linked to deficiency in ribosome biogenesis due to impairment of RNA polymerase I/III (Dauwerse et al., 2011; Trainor and Merrill, 2014).

Human craniofacial development is a multi-stage process in which neural crest cells (NCCs) play a major role. Initially, cranial NCCs emerge from the neuroepithelium at the foremost region of the neuraxis and migrate to constitute the mesenchyme of the pharyngeal arches. Subsequently, the neural crest-derived mesenchymal cells undergo proliferation and

differentiation to generate a range of craniofacial components, including facial bones, cartilage, and connective tissue (Bhatt et al., 2013; Gong et al., 2014; Twigg & Wilkie, 2015). During this process, *TCOF1* loss of function is considered to impair ribosome biogenesis leading to increased apoptosis and proliferation deficit of NCCs, ultimately resulting in hypoplasia of facial bone and cartilage, as reported in animal models (Dixon et al., 1997; Jones et al., 1999; Dixon et al., 2006; Jones et al., 2008; Weiner et al., 2012). Still, the direct impact exerted by *TCOF1* pathogenic mutations in human post-migratory craniofacial mesenchymal cells is not well characterised, nor is its effects on their differentiation properties.

Induced pluripotent stem cells (iPSCs) stand as an invaluable tool to model human disease, as patient-specific iPSCs can be generated and differentiated towards affected cell types. This possibility has recently embraced craniofacial diseases, as directed generation of neural crest cells (iNCCs) from iPSCs is now attainable. iNCC cultures can, in turn, be induced towards iNCC mesenchymal derivatives, such as osteoblasts, chondrocytes and adipocytes, expanding possibilities for investigating disease-related phenotypes (Menendez et al., 2013; Fukuta et al., 2014, Matsumoto et al., 2015). Although multipotent post-migratory neural crest-derived mesenchymal cells have been successfully isolated from mouse embryos and studied *in vitro* (Zhao et al., 2006), mouse neural crest development possess intrinsic features not observed in other species (Barriga et al., 2015) and may not faithfully represent human craniofacial development in every aspect. Furthermore, studies exploring the properties of NCC-derived mesenchymal cells are scarce, especially regarding the effect of mutations associated with craniofacial syndromes.

Here, we investigated cellular phenotypes of neural crest-derived mesenchymal cells from TCS patients. These cells were obtained by inducing TCS iPSCs towards a neural crest stage, in an attempt to recapitulate human craniofacial development *in vitro*. Our results show the effectiveness of this approach in investigating craniofacial phenotypes, and they provide insight into the impact of *TCOF1* loss of function in human neural crest-derived craniofacial mesenchymal cells.

RESULTS

Generation of TCS and control iPSCs

All iPSC cultures displayed embryonic stem cell-like morphology and expressed pluripotency markers *NANOG, OCT3/4, ALPL*, and SSEA-4 (Fig. S1A), and subtelomeric MLPA assays showed no chromosomal imbalances in either control or TCS iPSCs (Fig. S1B). Both TCS subjects had been molecularly characterised in another work (Masotti et al., 2009) and harboured the following genotypes: subject F2441-1 - c.4344dupA (p.Arg1448fs); subject F2625-1 - c.431delC (p.Thr144fs). We generated 5 independent iPSC clones from the TCS iPSCs (F2441-1c1-c2; F2625-1c1-c3). Control samples comprised 3 individuals and a total of 6 clones (F7405-1-c1-c3, F7007-1c1-c2, and F9048-1c1; Table SI); albeit F9048-1 was reprogrammed with episomal vectors, it showed no differences in expression of pluripotency markers in comparison to the other iPSCs, and it was therefore included in the experiments described herein. Reduced expression of *TCOF1* mRNA was confirmed in TCS iPSCs, as compared to controls (Fig. 1).

iPSC-derived neural crest cells express neural crest markers

iPSC-derived neural crest cells (iNCCs) were induced from TCS and control iPSCs with a methodology based on TGF-β/Activin pathway blockade and WNT pathway activation (Menendez et al., 2013; Fukuta et al., 2014). After differentiation, TCS and control iNCC populations displayed typical neural crest cell morphology and expressed neural crest markers p75(NTR) and HNK1. Of note, the TCS iNCCs displayed decreased HNK1 expression, and the proportion of $HNK1^{+}$ cells varied between 43.7% and 66.9%% (Fig. 2A). RT-qPCR assays revealed upregulation of neural crest markers *PAX3*, *TFAP2A*, *ZIC1* and *SOX10*, and downregulation of pluripotency markers *OCT3/4*, *NANOG*, and *ALPL*, when compared with the originating iPSCs (Fig 2B). Finally, reduction of *TCOF1* transcript expression (~25% reduction) was confirmed in TCS iNCCs, when compared to controls (Fig 1).

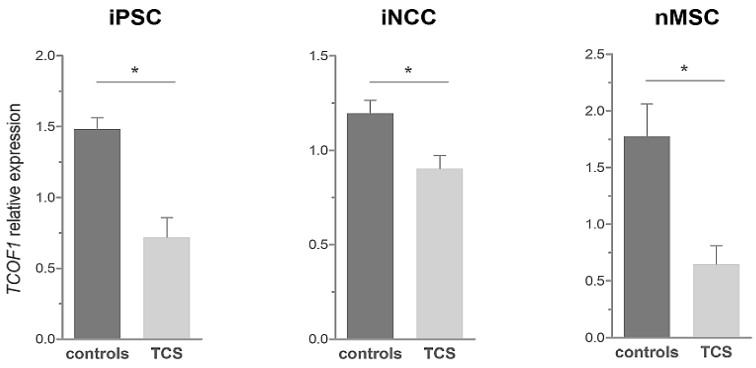

Figure 1: Characterisation of *TCOF1* expression in TCS cells. RT-qPCR assessment of *TCOF1* transcript abundance in iPSCs, iNCCs and nMSCs from controls and TCS subjects.(*) $p < 0.05$; Student's t-test.

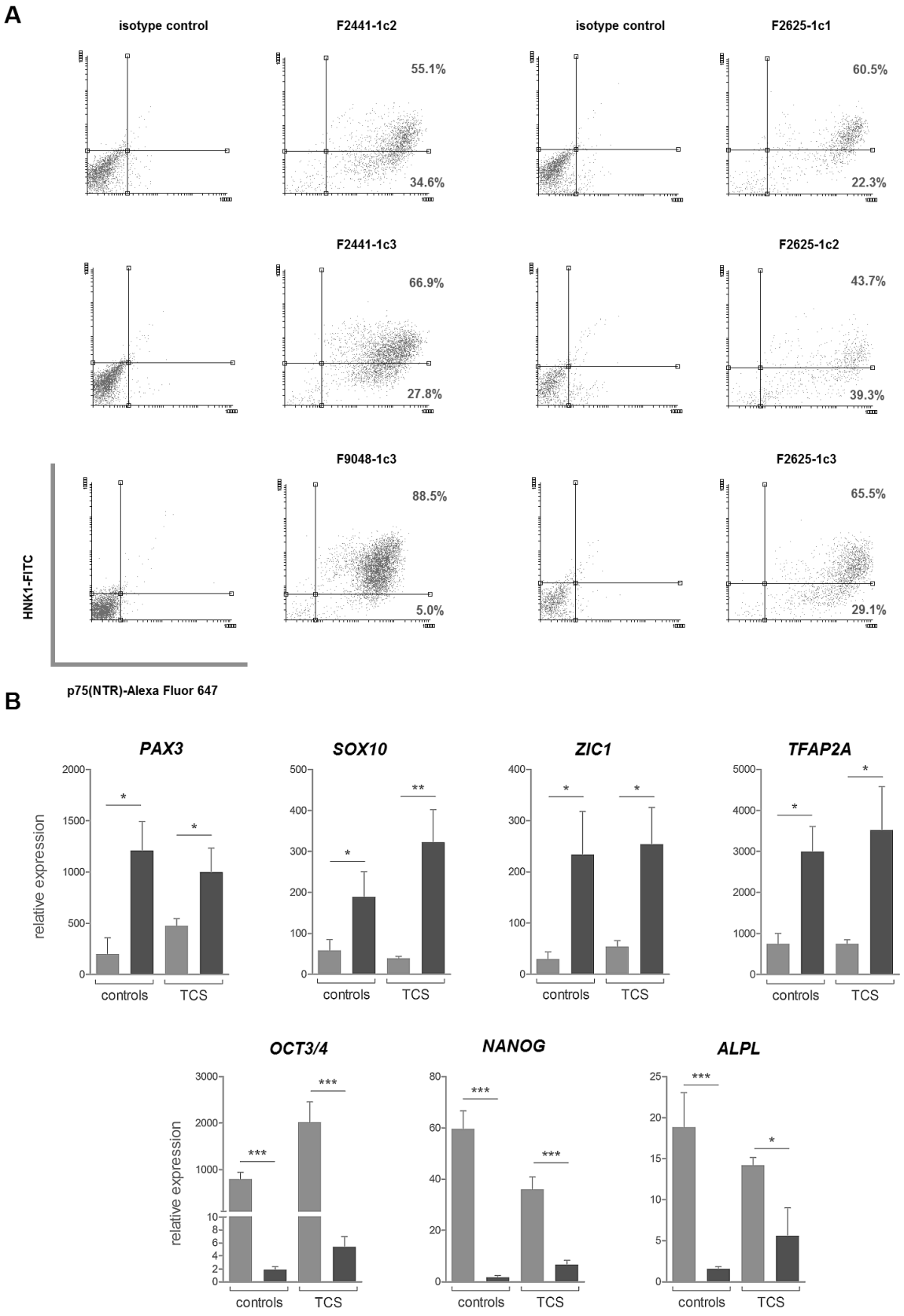

Figure 2: Characterisation of iNCCs. A) Biparametric flow cytometry dot plots for HNK1 and p75(NTR) expression in TCS and a representative control. Values in represent p75(NTR)$^{+}$ cell fractions either positively (upper right) or negatively (lower right) stained for HNK1. **B)** RT-qPCR assessment of neural crest (upper panel) and pluripotency marker (lower panel) expression between iNCCs and the originating iPSCs.(*) $p< 0.05$; (**) $p< 0.01$; (***) $p< 0.001$; Student's t-test.

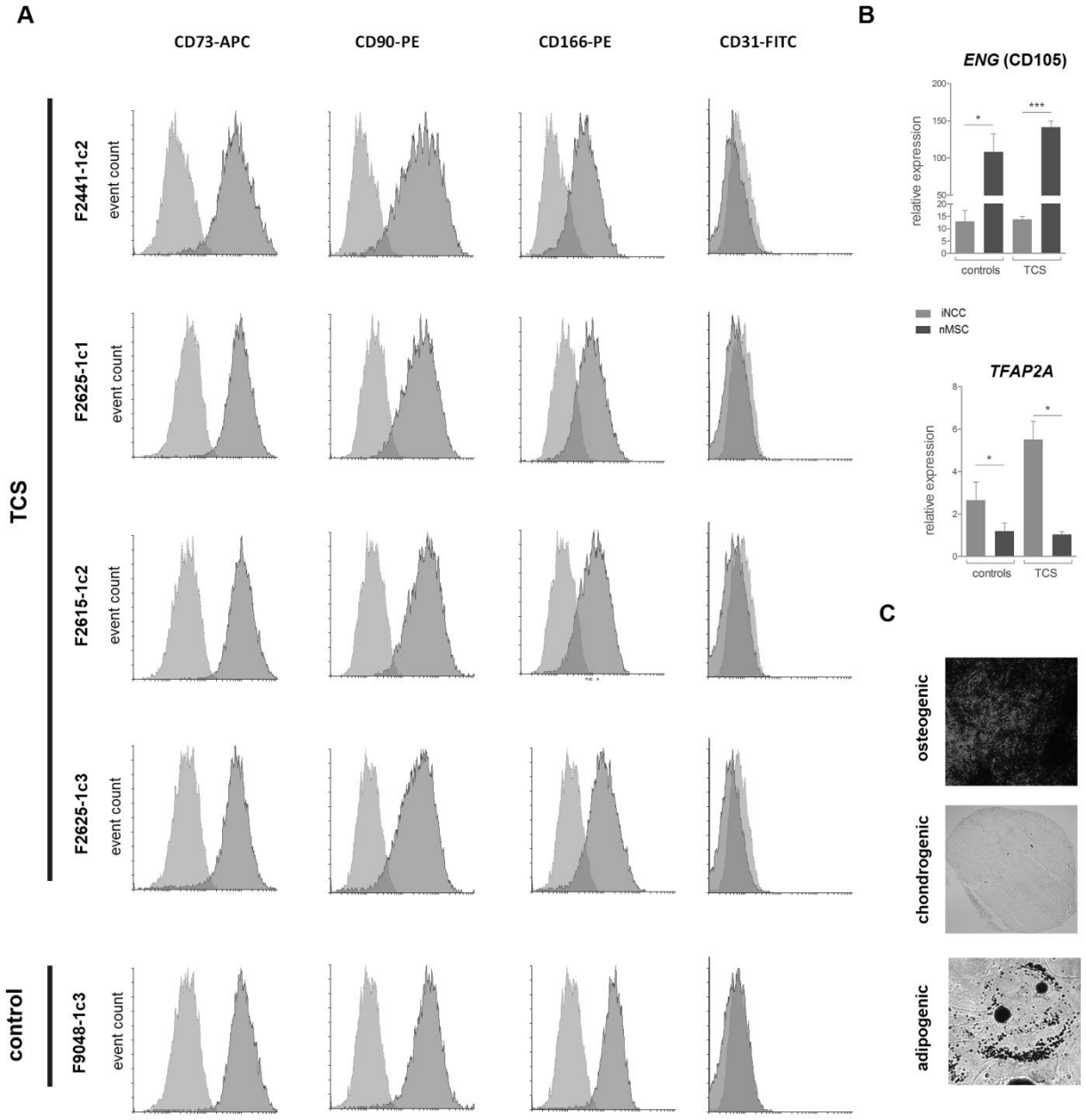

Figure 3:Characterisation of nMSCs. A) Flow cytometry immunophenotype profiling of nMSCs showing positive staining for mesenchymal markers CD73, CD90 and CD166, and negative staining for endothelial marker CD31. Histograms represent event count (y-axis) vs. fluorescence (x-axis). Experimental data (blue) were plotted in overlay with data from isotype controls (light blue). **B)** RT-qPCR assays showing upregulation of mesenchymal marker *ENG* (CD105) and downregulation of neural crest marker *TFAP2A* in nMSCs compared to iNCCs; (***) $p<0.001$; (*) $p<0.05$; Student's t-test. **C)** Example of osteogenic, chondrogenic, and adipogenic differentiation of nMSCs, detected with Alizarin Red, Alcian Blue, and Oil Red staining, respectively.

Multipotent neural crest-derived mesenchymal stem-like cells (nMSCs) can be efficiently generated from TCS iNCCs

In spite of the lower HNK1 expression in TCS iNCCs, they were submitted to differentiation towards the mesenchymal lineage. Both TCS and control nMSC populations

showed spindle-shaped fibroblast-like morphology (data not shown), and notably, surface antigen profiling revealed a homogeneous mesenchymal immunophenotype, with positively stained cells for mesenchymal markers CD73, CD166 and CD90, and negative staining for endothelial marker CD31 (Fig. 3A). In agreement, nMSCs showed downregulation of *OCT3/4*, *NANOG* and *ALPL* and upregulation of mesenchymal marker *ENG* (CD105), when compared with the original iPSCs (Fig. 3B). These cells also displayed tri-lineage potential, being able to undergo osteogenic, chondrogenic and adipogenic *in vitro* differentiation (Fig. 3C). Strikingly, *TCOF1* mRNA expression was greatly reduced in TCS nMSCs (~64% reduction) as compared to controls (Fig. 1).

TCS nMSCs exhibit alterations in osteogenic and chondrogenic potential

During the first 6 days of osteoinduction, all nMSCs showed the expected transcriptional behaviour, with upregulation of early osteogenesis markers *RUNX2*, *ALPL* and *COL1A1,* and downregulation of late osteoblast marker *BGLAP* (Fig. S2). Further examination of *in vitro* osteogenic differentiation revealed increased osteopotential in TCS nMSC populations: in comparison to controls, these cells displayed higher alkaline phosphatase (ALP) activity after 9 days of osteoinduction and more deposition of mineralised matrix after 21 days (Fig. 4A; Fig. S2).

During chondrogenic differentiation, we observed altered expression of key transcripts involved in chondrogenesis in TCS nMSCs, which exhibited upregulation of *ACAN* and *COL2A1* in comparison to controls at day 9 (Fig. 4B). Alcian blue staining of extracellular glycosaminoglycans after 21 days of *in vitro* chondrogenic differentiation did not reveal pronounced differences between TCS and control nMSCs (data not shown).

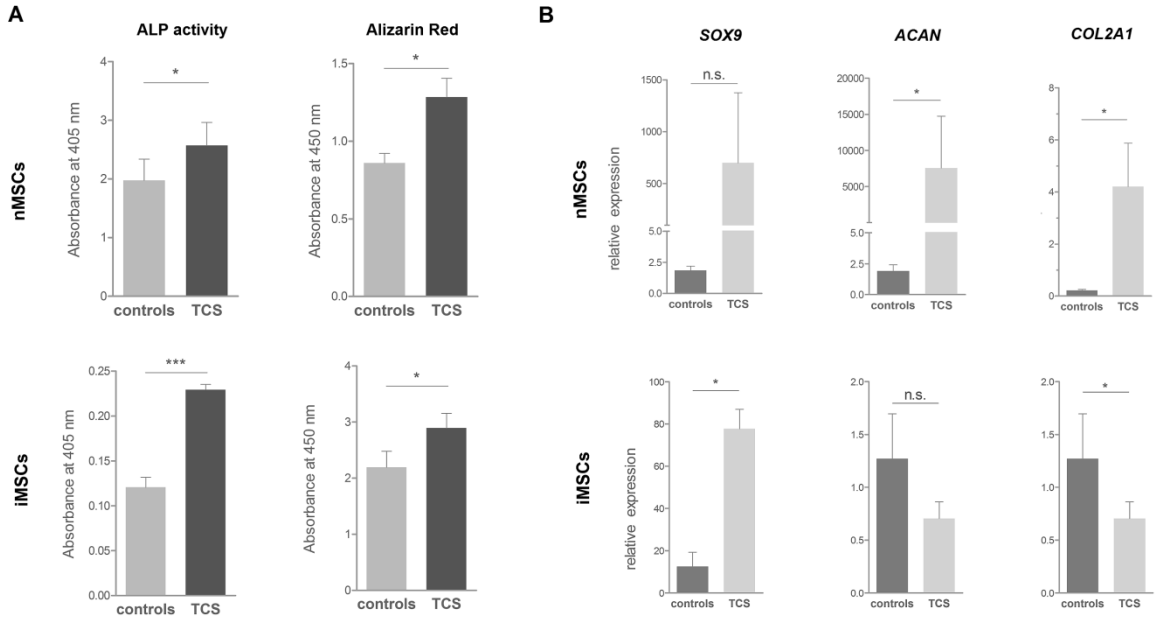

Figure 4: TCS nMSCs and iMSCs show alterations in osteogenic and chondrogenic potential, in comparison to controls. A) Colorimetric quantification of alkaline phosphatase (ALP) activity after 9 days and matrix mineralisation after 21 days of osteogenic differentiation. **B)** RT-PCR assays showing the transcriptional profile of chondrogenesis-associated transcripts after 9 days of chondrogenic differentiation. (***) $p<0.001$; (**) $p<0.01$; (*) $p<0.05$; Student's t-test; n.s. = not significant.

Basal apoptosis is increased in TCS nMSCs

Since increased apoptosis of NCCs is regarded as a major driver of the craniofacial phenotypes seen in TCS (Dixon et al., 2006), we sought for differences in apoptotic events between TCS and control iNCCs and nMSCs, as proof-of-principle evidence to support our cellular model. While apoptosis in TCS iNCCs did not deviate from control iNCCs, augmented early and late apoptosis was observed in TCS nMSCs. Unexpectedly, this observation was not associated with detectable changes in proliferative potential of these cells, in relation to controls (Fig. 5).

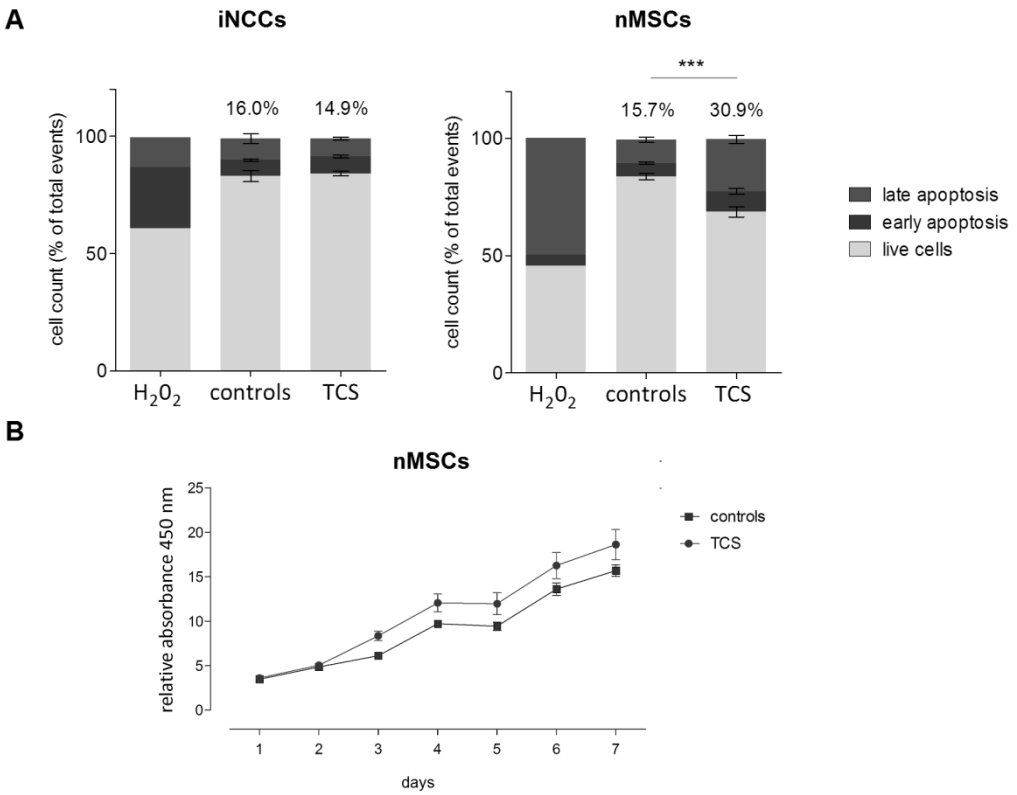

Figure 5: Increased apoptosis in TCS nMSCs. A) 7-AAD/Annexin V flow cytometry results depicting the fraction of live cells, and cells undergoing early and late apoptosis in nMSCs and iNCCs. Percentages represent the sums of early and late apoptotic events. H_2O_2-treated cells were used as positive staining controls. (***) $p<0.001$; Student's t-test. **B)** XTT assay depicting the proliferation profile of control and TCS nMSCs. No statistically significant differences were observed; two-way ANOVA with Bonferroni post-tests.

TCS non-neural crest mesenchymal cells partially reproduce the TCS nMSC phenotype

To evaluate if subjecting patients' cells through a neural crest stage is necessary to generate mesenchymal cells displaying disease-relevant phenotypes, we sought to replicate the results obtained thus far in mesenchymal stem-like cells directly induced from iPSCs (iMSCs). Akin to nMSCs, iMSCs possessed a characteristic and homogeneous mesenchymal immunophenotype (positive for CD105, CD73 and CD90; negative for CD31, CD34 and CD45; Fig. S3A); also, iMSCs showed transcriptional upregulation of *ENG* (CD105) and downregulation of pluripotency markers *OCT3/4*, *NANOG* and *ALPL*, upon differentiation from iPSCs (Fig. S3B). TCS iMSCs showed a 34% reduction in *TCOF1* expression, when compared with controls (Fig. S3C).

Osteogenic differentiation assays performed on iMSCs showed comparable results in relation to nMSCs. ALP enzymatic activity and mineralised matrix deposition were significantly

higher in TCS iMSCs at days 9 and 21 of osteoinduction, respectively (Fig. 4A). Furthermore, the transcriptional profile of genes involved in chondrogenesis at day 9 of differentiation also deviated from controls, with diminished *COL2A1* expression and increased *SOX9* expression in TCS iMSCs (Fig. 4B).

Finally, no differences in either basal apoptosis or proliferation were detected between TCS and control iMSCs (Fig. S3 D,E).

DISCUSSION

The development of iPSC technology has opened new possibilities to study human craniofacial diseases, as neural crest-derived, patient-specific cell types harbouring pathogenic mutations can be generated and studied *in vitro* under controlled conditions. Several studies in animal models have consistently appointed insufficient NCC migration due to apoptosis as the main determinant of the TCS phenotype (Dixon et al., 1997; Jones et al., 1999; Dixon et al., 2006; Jones et al., 2008; Weiner et al., 2012). Here, we used iPSCs to generate an *in vitro* equivalent of human neural crest-derived mesenchymal cells in order to evaluate the phenotypical outcomes of *TCOF1* haploinsufficiency on this cell type. We successfully generated iPSCs from TCS patients, which, akin to control iPSCs, had no signs of chromosomal imbalances and displayed high expression of pluripotency-associated genes; further, they demonstrated the ability to give rise to iNCCs and nMSCs, and to be directly differentiated into iMSCs. Hence, diminished *TCOF1* expression had no apparent effect on iPSC generation.

The properties of the iNCCs and nMSCs reported here are congruent with the expected neural crest and mesenchymal phenotypes, as shown in other works (Menendez et al., 2011; Menendez et al., 2013; Fukuta et al., 2014; Kreitzer et al., 2014). All iNCCs displayed transcriptional upregulation of neural crest markers in comparison to the iPSCs. Of note, iNCC cultures from TCS patients comprised a $p75(NTR)^{+}/HNK1^{-}$ cell fraction, in contrast to the double-positive control iNCCs here and to a TCS iNCC line reported elsewhere (Menendez et al., 2013); still, other works have reported generation of iPSC-derived neural crest cells solely based on p75(NTR) readout (Fukuta et al., 2014; Kreitzer et al., 2014), indicating that HNK1 expression is not entirely crucial to characterise this cell type. Nevertheless, we showed that the mixed TCS iNCC populations here can be successfully converted to nMSCs: all nMSCs displayed *bona fide* mesenchymal stem cell characteristics, possessed homogeneous immunophenotype with high expression of mesenchymal markers, and showed plasticity to generate osteoblasts, chondrocytes and adipocytes *in vitro*. These results show that the nMSCs reported here are suitable for assessment of mesenchymal differentiation and other cellular

parameters, and they suggest that lower HNK1 expression in iNCCs is not a limiting factor to generate neural crest-derived mesenchymal cells *in vitro*.

According to previous observations in animal models (Dixon et al., 1997; Jones et al., 1999; Dixon et al., 2006; Jones et al., 2008; Weiner et al., 2012), one expected finding for *TCOF1*-deficient NCCswould be augmented apoptosis, but no deviations in this parameter were detected when comparing TCS iNCCs to control iNCCs. This observation could be related to the lower HNK1 expression detected in TCS iNCCs. HNK1 is an *in vitro* neural crest marker solely found expressed in migratory NCCs in animal models (Bronner-Fraser, 1987; Sadaghiani & Vielkind, 1990; Del Barrio & Nieto, 2004; Giovannone et al., 2015), arguably implying that the mixture of $HNK1^{+}$/$HNK1^{-}$ iNCCs from TCS patients comprises migratory and non-migratory iNCCs, which may show different apoptosis rates in face of *TCOF1* haploinsufficiency. In agreement, in $Tcof1^{+/-}$ mice, migratory NCCs are viable, while increased apoptosis is confined to the neuroepithelial, pre-migratory NCCs (Dixon et al., 2006). Alternatively, since apoptosis was assessed in iNCCs grown under normal culture conditions, differences in apoptosis between TCS and control iNCCs may only be detectable after subjecting cells to additional challenges or inductive signals.

The greater amount of apoptotic cells detected in TCS nMSCs here associates *TCOF1* haploinsufficiency with cell death in neural crest-derived mesenchymal cells. The pathogenic mechanism proposed for TCS predicts that insufficiency of *TCOF1* transcripts upon high demand for ribosome synthesis leads to cellular stress and apoptosis (Dixon et al., 2006). As neural crest-derived mesenchymal cells must undergo rapid proliferation before differentiation (Achileos & Trainor, 2012; Twigg & Wilkie, 2015), these results suggest that mesenchymal apoptosis may occur prior to differentiation within the embryonic craniofacial complex. However, such inference must be assimilated with caution, as increased apoptosis did not result in observable proliferation deficits in TCS nMSCs, and whether the apoptosis rates observed are sufficiently high to project measurable differences in proliferation remains to be determined. Accordingly, akin to iNCCs, apoptosis was assessed in nMSCs under regular culture conditions, which may not produce enough apoptotic cells to result in proliferation changes in TCS samples. Nonetheless, it will be interesting to see if viability of *TCOF1*-deficient neural crest-derived mesenchymal cells is compromised under high proliferative demand *in vitro* or in TCS animal models.

The mesenchymal differentiation assays showed dissimilarities in the osteogenic and chondrogenic potential between control and TCS samples, both in nMSCs and iMSCs. Although

no peak expression of osteogenesis markers was observed in TCS cells within the first 6 days of osteoinduction, ALP activity and matrix mineralisation were unmistakably increased in TCS nMSCs and iMSCs, indicating enhanced osteopotential with peak expression of these markers likely occurring beyond the assessed time window. Transcriptional dysregulation of key genes involved in chondrogenesis was observed in TCS nMCs and iMSCs as compared to controls, albeit with an apparent lack of difference in alcian blue-stained chondrocyte pellets. This finding might be related to the limited sensitivity of the technique (Solchaga et al., 2011), and more studies are necessary to confirm if the transcriptional alterations of chondrogenesis-associated genes results in differences between TCS and control samples. Still, although NCC apoptosis has been considered to be the major contributor to the craniofacial manifestations of TCS, our results indicate association between mesenchymal differentiation and *TCOF1*/Treacle function in humans. There is an unequivocal cross-talk between ribosome biogenesis and osteo-chondrogenesis due to interactions amongst members of both pathways (Trainor & Merril, 2014). For example, *Runx2*, a key transcription factor involved in osteo-chondral differentiation, has been shown to interact with UBF-1 to downregulate rRNA synthesis and cell proliferation during differentiation (Trainor & Merril, 2014; Pratap et al., 2003; Galindo et al., 2005; Ali et al., 2008); notably, Treacle co-localises with UBF-1 and RNA polymerase I in nucleolar regions (Valdez et al., 2004), further suggesting that functional impairment of Treacle may influence osteo-chondral differentiation. Hence, better understanding the relationship between *TCOF1* haploinsufficiency and mesenchymal differentiation not only provides insight into craniofacial development, but may also be invaluable for the surgical rehabilitation of TCS patients, which often lacks long-term stable results after mandibular distraction osteogenesis (Stelnicki et al., 2002; Gursoy et al., 2008).

Our results suggest that recapitulating craniofacial development by transitioning iPSCs through a neural crest stage may be advantageous to study TCS and other Mendelian craniofacial dysmorphologies. Increased apoptosis was only observed in nMSCs derived from iNCCs, whilst the number of apoptotic cells in TCS iMSC cultures directly differentiated from iPSCs was similar to that in controls; therefore, *TCOF1* mutations may specifically affect neural crest-derived mesenchymal cells *in vitro*. This is supported by the broader difference in *TCOF1* mRNA expression detected between TCS patients and control subjects for nMSCs (~64%) in comparison to iMSCs here (~34%) and adult mesenchymal cells described in a previous work (~31%) (Masotti et al., 2009). The reasons for such dramatic reduction of *TCOF1* transcripts in TCS nMSCs as compared to other types of mesenchymal cells are unclear, but they may include compensatory expression from the non-mutated allele, as previously proposed for TCS adult

cells (Isaac et al., 2000), or cell type-specific differential expression of the mutated allele due to epigenetic, environmental, or stochastic factors (Kaern et al., 2005; Gimelbrant et al., 2007). Either way, the greater reduction in the amount of *TCOF1* transcripts in TCS nMSCs suggest that disruption of neural crest-derived mesenchymal cell development might play a role in the aetiology of TCS in humans, attesting the importance of considering this cell type when investigating craniofacial phenotypes.

In summary, here we describe an *in vitro* model for studying neural crest-derived mesenchymal cells from TCS syndrome patients. Our findings suggest apoptosis as a phenotypical outcome of *TCOF1* haploinsufficiency in neural crest-derived mesenchymal cells and they suggest that mesenchymal differentiation towards osteoblast and chondrocyte lineages may be altered in TCS. Future studies should focus on further dissecting how reduced amounts of Treacle affect proliferation and differentiation of neural crest-derived mesenchymal cells undergoing osteo-chondrogenic specification *in vitro* and *in vivo*.

METHODS

Biological samples and ethics statement

Facial periosteum fragments were obtained from TCS subjects submitted to reconstructive plastic surgery at Hospital das Clínicas, University of São Paulo, Brazil. Punch biopsy skin fragments were obtained from 2 healthy control subjects from the lower back region, under local anaesthesia. The study was approved by the ethical committee of Instituto de Biociências, University of São Paulo, Brazil (accession number 39478314.8.0000.5464), and informed consent was obtained from both patients and control subjects or from their legal guardians. Periosteal fibroblasts were extracted according to a previously published protocol (Fanganiello et al., 2007). Dermal fibroblasts were isolated according to the methods described in Aasen & Belmonte (2010).

Generation of human induced pluripotent stem cells (iPSCs)

Fibroblasts from two TCS patients were reprogrammed via *SOX2*, *c-MYC*, *OCT4* and *KLF4* retroviral transduction, as originally reported in Takahashi et al, 2007. Two control fibroblasts had also been reprogrammed with this method, as described elsewhere (Ishiy et al., 2014). One additional control fibroblast sample was reprogrammed with the use of episomal vectors (pCXLE-hOCT3/4-shP53-F, addgene plasmid 27077; pCXLE-hSK, addgene plasmid 27078; pCXLE-hUL, addgene plasmid 27080), as described in Okita et al (2011), with the use of

Amaxa Nucleofector II (program U-020) and NHDF nucleofection kit (Lonza), according to manufacturer's recommendations. Two days after transduction/nucleoporation, fibroblasts were co-cultivated with irradiated murine embryonic fibroblasts (Millipore) in embryonic stem cell medium (DMEM/F12 supplemented with 2mM GlutaMAX-I, 0.1mM non-essential aminoacids, 100uM 2-mercaptoethanol, 30ng/ml of bFGF and 20% of knockout serum replacement; all provided by Life Technologies). Typical iPSC colonies formed on feeder cells were transferred to matrigel (BD-Biosciences)-coated plates and expanded in Essential 8™ Medium (Life Technologies) supplemented with 100ug/mL of Normocin (Invivogen). pCXLE-hOCT3/4-shP53-F, pCXLE-hSK, and pCXLE-hUL were a gift from Shinya Yamanaka.

MLPA assays

Total DNA was extracted from iPSC cultures with the use of NucleoSpin Tissue (Macherey-Nagel), following supplier's instructions. Multiplex Ligation-dependent Probe Amplification (MLPA) analysis was performed with subtelomeric kits (P036 and P070; MRC-Holland) to detect chromosomal imbalances, as previously described (Jehee et al., 2011).

Differentiation of iNCCs from iPSCs

Procedures for iNCC derivation were based on previously published methodology (Menendez et al., 2013; Fukuta et al., 2014). Before differentiation, iPSC colonies were adapted to single-cell passaging by rinsing cells with PBS followed by dissociation with Accutase (Life Technologies) for up to 5 minutes at room temperature, centrifugation at 200 g for 4 min and seeding onto Matrigel-coated dishes. After 2 subcultures, single cells were seeded onto 60-mm Matrigel-coated dishes at $5x10^4$ cells/cm^2. Two days post-seeding, medium was changed to iNCC differentiation medium, composed of Essential 6™ Medium (Life Technologies) supplemented with 8ng/mL bFGF (Life Technologies), 20uM SB431542 (Sigma-Aldrich), 1uM CHIR99021 (Sigma-Aldrich), and 100ug/mL Normocin; differentiation medium was changed daily. After ~2-4 days, neural crest-like cells were seen detaching from colony borders. Before reaching confluence, cultures were rinsed once with PBS and briefly incubated with Accutase at room temperature until differentiated cells detached and most undifferentiated colonies were left on the dish. Cell suspensions were centrifuged at 200 g for 4 minutes and re-seeded onto new Matrigel-coated dishes in fresh iNCC differentiation medium. With this method, passaging was performed whenever necessary, for 15 days, whereby morphologically homogeneous iNCC cultures were obtained. Differentiated iNCCs were cultivated for up to 8 passages in iNCC differentiation medium, replenished daily. In all procedures involving single-cell passaging, media were supplemented with 5uM Rock inhibitor

(Sigma-Aldrich) upon seeding and maintained for 24 hours; after about 10 days of iNCC differentiation, Rock inhibitor was no longer needed to maintain cell viability.

Differentiation of nMSCs from iNCCs

nMSC populations were obtained through incubation of iNCCs with mesenchymal stem cell medium, as previously described (Menendez et al., 2011). In brief, iNCCs were seeded at $2x10^4$ cells/cm^2 onto non-coated 60-mm tissue culture dishes in nMSC medium (DMEM/F12 supplemented with 10% FBS, 2mM GlutaMAX-I, 0.1mM non-essential aminoacids, and 100ug/mL Normocin) containing 5uM Rock inhibitor. Cells were differentiated for 6 days and passaged with TrypLE™ Express (Life Technologies) when needed. nMSC cultures were expanded in nMSC medium for up to 6 passages, with medium changes every 3 days.

Direct derivation of iMSCs from iPSCs

iMSCs were generated following published methods (Ishiy et al., 2015). Briefly, iPSC colonies were treated with Accutase and cells were plated onto Matrigel-coated tissue culture dishes at $1×10^4$ cells/cm^2 in iMSC differentiation medium (DMEM/High Glucose with 10% FBS, 1% penicillin/streptomycin, 1% nonessential amino acids, and 5ng/mL of bFGF) for 14 days, with media changes every 3 days. For subsequent passages, single-cell suspensions were prepared using TrypLE Express and cells were passaged with a 1:3 split ratio in standard culture flasks (Corning) without Matrigel coating.

Chondrogenic, osteogenic and adipogenic differentiation

For the osteogenic induction, cells were seeded in 12-well plates ($4x10^4$ cells per well), and after 3 days, medium was replaced with osteogenic induction medium (StemPro Osteogenesis Kit; Life Technologies). Differentiation medium was changed every 2-3 days. After 9 days, alkaline phosphatase activity was quantified through incubation with phosphatase substrate (Sigma-Aldrich), and the resulting p-nitrophenol was quantified colorimetrically using a Multiskan EX ELISA plate reader (Thermo Scientific) at 405 nm. After 21 days, extracellular matrix mineralisation was assessed through alizarin red staining. Briefly, cells were washed three times with PBS, fixed in 70% ethanol for 30 minutes at room temperature, washed 3x with distilled water, and finally stained with a 0.2% Alizarin Red S solution (Sigma-Aldrich) for 30 minutes at room temperature. After three washes with PBS, plates were air dried at room temperature. Staining was removed with a 20% methanol / 10% acetic acid solution and colorimetrically assessed using a Multiskan EX ELISA plate reader (Thermo Scientific) at 450nm.

For chondrogenesis, $1x10^5$ cells/well were plated into 6-well plates and after 3 days growth medium was replaced with chondrogenic medium (StemPro Chondrogenesis Kit; Life Technologies). To quantify chondrogenic markers, total RNA was extracted after 9 days of differentiation. Chondrocyte pellets were produced by centrifuging 3×10^5 cells at 500g and incubating pellets in nMSC medium for 24 hours before switching to chondrogenic medium. After 21 days, pellets were fixed and frozen in Tissue-Tek O.C.T (Sakura), 5um cryosections were performed, sections were fixed with 4% paraformaldehyde and stained with Alcian Blue 0.1% in 0.1 N HCl.

Adipogenic differentiation was performed on $1x10^5$ cells/well seeded into 6-well plates. After cells achieved 80% confluence, growth medium was replaced with adipogenesis medium (StemPro Adipogenesis Kit; Life Technologies). Cells were differentiated for 21 days, after which Oil red staining was performed. Cells were washed with PBS, fixed in 4% paraformaldehyde and stained with Oil Red 0.5% in isopropanol. Pictures were taken using an Axiovision microscope (Zeiss).

Apoptosis and proliferation Assays

For the apoptosis assays, a total of $1x10^5$ cells/well was seeded into 6-well culture plates. On the next day, apoptotic activity was measured with a kit based on Annexin V and 7-AAD staining (Guava Nexin Reagent), following manufacturer's instructions. Cells treated with 10uM H_2O_2 for 30 minutes were used as staining controls. Subpopulations were ascertained in a Guava flow cytometer (EMD Millipore) as follows: non-apoptotic cells: Annexin V(-) and 7-AAD(-); early apoptotic cells: Annexin V(+) and 7-AAD(-); late-stage apoptotic and dead cells: Annexin V(+) and 7-AAD(+).

Cell proliferation was assessed with the use of an XTT assay (Cell Proliferation Kit II; Roche), following supplier's instructions. Briefly, cells were seeded into 96-well culture plates at $2x10^3$ cells/well, in quadruplicates. To quantify metabolically active cells, medium was changed to DMEM/F12 without phenol red (Life Technologies), a solution of XTT was added, and cells were incubated at 37°C for 3 hours. Immediately, plates were colorimetrically assessed in a microplate spectrophotometer (Epoch; BioTek) at 450nm.

Flow cytometry

To assess the immunophenotype of iNCCs, cells were detached with Accutase, and washed twice with 2 volumes of blocking solution (4% BSA in PBS without Ca^{2+} and Mg^{2+}).

iNCCs were incubated with the conjugated antibodies in blocking solution in the dark for 1 hour at 4°C, washed twice with PBS, and fixed in 1% paraformaldehyde/PBS. The following antibodies were used: IgM k FITC Mouse Anti-Human CD57 (anti-HNK1; BD Pharmingen 561906), IgG1 k Alexa Fluor 647 Mouse Anti-Human CD271 (anti-p75NTR; BD Pharmingen 560877), FITC Mouse IgM k isotype control (BD Pharmingen 555583), and Alexa Fluor 647 Mouse IgG1 k isotype control (BD Pharmingen 557714). Antibody concentrations followed manufacturer's recommendations. A minimum of 5,000 events were acquired in a FACS Aria II flow cytometer (BD Biosciences) and analysed on Flowing software (v2.5).

nMSCs and iMSCs were dissociated with TrypLE Express and washed twice with 2 volumes of blocking solution (1% BSA in PBS without Ca^{2+} and Mg^{2+}). Cells were incubated in the aforementioned conditions with the following conjugated antibodies: FITC Mouse Anti-Human CD31 (BD Pharmingen 555445), APC Mouse Anti-Human CD73 (BD Pharmingen 560847), PE Mouse Anti-Human CD90 (BD Pharmingen 555596), FITC Mouse Anti-Human CD105 (BD Pharmingen 551443), PE Mouse Anti-Human CD166 (BD Pharmingen 559263), and FITC, PE and APC Mouse IgG1 κ Isotype Controls (BD Pharmingen 555748, 554681 and 555749, respectively). Antibody concentrations followed manufacturer's recommendations. At least 5,000 events were acquired in a FACS Aria II equipment and analysed on the Flowing software (v2.5) and Guava Express PRO (Millipore).

RNA extraction and Real-time quantitative PCR (RT-qPCR)

Total RNA was obtained from cell populations with the use of Nucleospin RNA II extraction kit (Macherey-Nagel) following manufacturer's recommendations. Briefly, 1ug of total RNA was converted into cDNA using Superscript II (Life Technologies) and oligo-dT primers according to manufacturer's recommendations. Real-Time quantitative PCR reactions were performed with 2X Fast SYBR Green PCR Master Mix (Life Technologies) and 50nM–400nM of each primer. Fluorescence was detected using the 7500 Fast Real-Time PCR System (Life Technologies), under standard temperature protocol. Primer pairs were either designed with Primer-BLAST (http://www.ncbi.nlm.nih.gov/tools/primer-blast/) or retrieved from PrimerBank (http://pga.mgh.harvard.edu/primerbank/; primers are listed in Table SII), and their amplification efficiencies (E) were determined by serial cDNA dilutions $\log_{10}$-plotted against Ct values, in which $E=10^{-1/slope}$. Gene expression was assessed relative to a calibrator cDNA (ΔCt). Finally, NormFinder (Andersen et al., 20014) was used to determine the most stable endogenous control (among *ACTB*, *TBP*, *HMBS*, *GAPDH*, or *HPRT1*), and calculate normalization factors ($E^{-\Delta Ct}$) for each sample. The final relative expression values were determined based on a previous method (Pfaffl et al., 2001), by dividing $E^{-\Delta Ct}$ of target genes by

$E^{-\Delta Ct}$ of the endogenous control. All relative expression values were log-transformed for analysis and graphed in linear scale, unless stated otherwise. Primers were supplied by Exxtend.

Statistical analysis:

All experiments were performed in triplicates, unless stated otherwise herein. Statistical comparisons were performed on the Graphpad Prism software. Values were represented as means ± standard error. The level of statistical significance was set at $p<0.05$.

Web Resources

OMIM – Online Mendelian Inheritance in Men - http://www.omim.org/

Primer-BLAST - http://www.ncbi.nlm.nih.gov/tools/primer-blast/

Primer Bank - https://pga.mgh.harvard.edu/primerbank/

SUPPLEMENTARY FIGURES

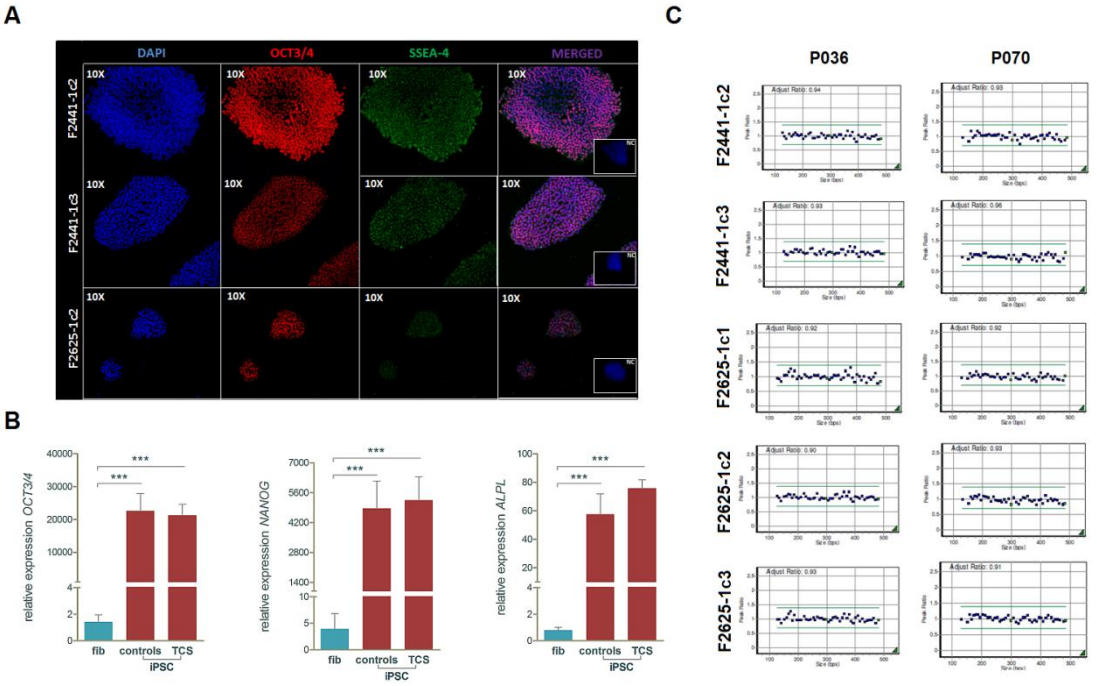

Figure S1: iPSC characterisation. A) Immunofluorescence micrographs showing expression of pluripotency markers OCT3/4 and SSEA-4 in TCS iPSCs. NC=negative control **B)** RT-qPCR showing transcriptional upregulation of pluripotency-associated genes *OCT3/4*, *NANOG*, and *ALPL* in controls and TCS samples. Graphs were plotted relative to expression data of 2 adult fibroblasts (F2625-1 and F2441-1); (***) *p*-value < 0.001; Student's t-test. **C)** MLPA analysis with peak ratios for subtelomeric probes (blue dots) and control probes (green dots) with the use of 2 kits, showing no chromosomal imbalances. Control iPSCs had been previously characterised in Chapter III and Ishiy et al (2015).

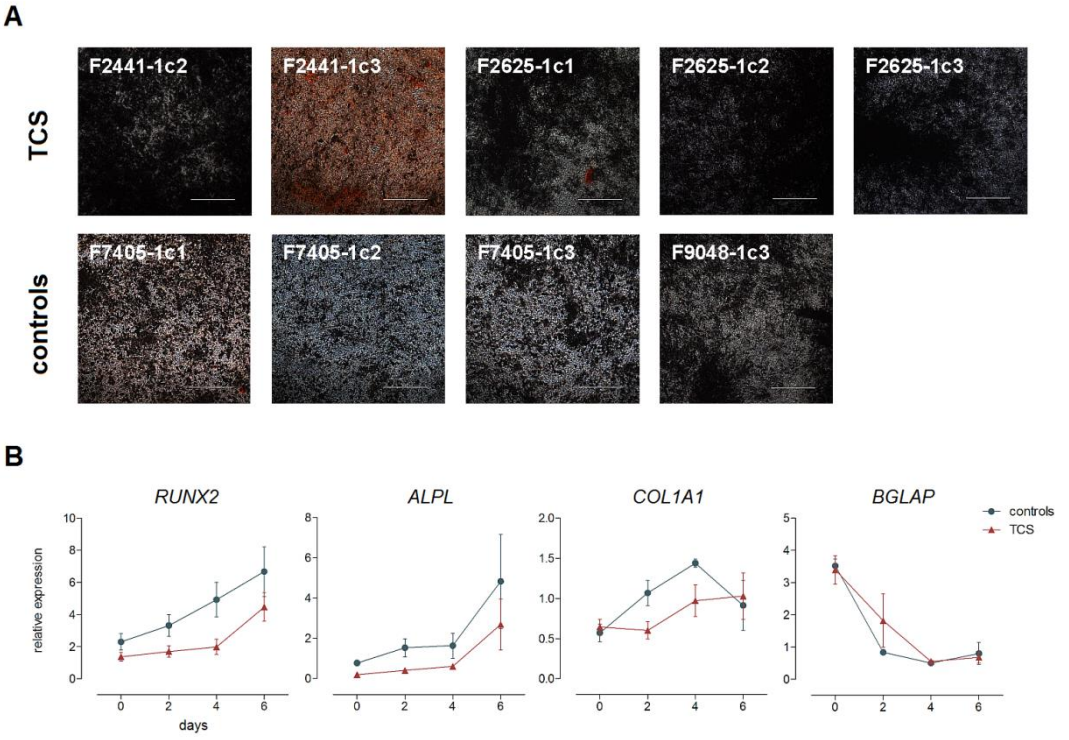

Figure S2: Osteogenic differentiation of control and TCS nMSCs. A) Alizarin Red staining showed increased matrix mineralisation in TCS samples as compared to controls. Scale bars=500um **B)** Transcriptional profile of osteogenesis-associated genes during the initial 6 days of osteoinduction. No statistically significant differences were observed; two-way ANOVA with Bonferroni post-tests.

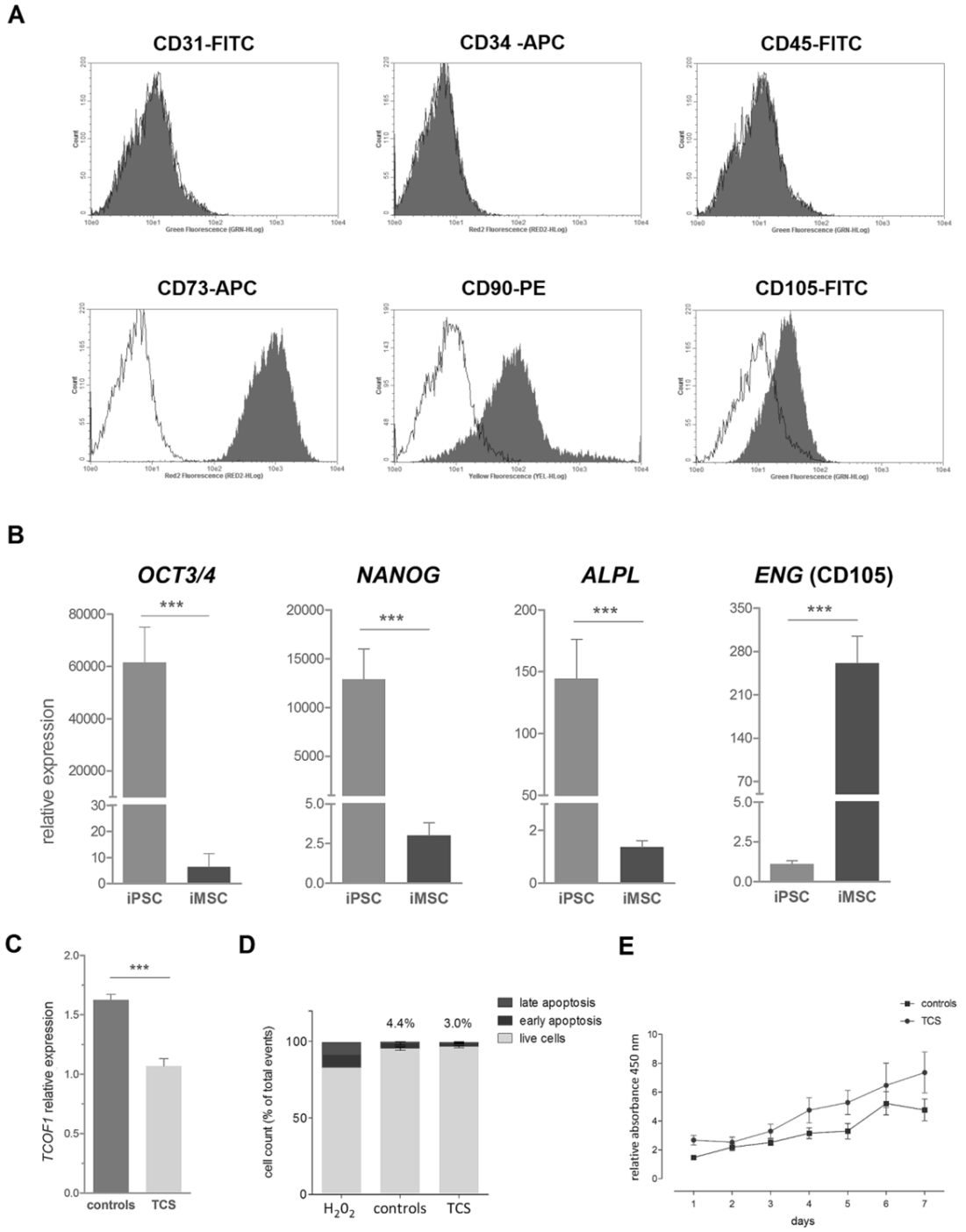

Figure S3: Characterisation and phenotype assessment of TCS iMSCs. A) Representative flow cytometry histograms showing staining for mesenchymal cell markers CD73, CD90 and CD105, and non-mesenchymal markers CD31, CD34 and CD45. **B)** RT-qPCR assessment of pluripotency markers *OCT3/4,*NANOG, and *ALPL,* and mesenchymal marker *ENG* in iMSCs compared to the originating iPSCs. **C)** *TCOF1* transcript expression between control and TCS iMSCs. **D)** 7-AAD/Annexin V flow cytometry results depicting the fraction of live cells, and cells undergoing early and late apoptosis in iMSCs. Percentages represent the sums of early and late apoptotic events. H_2O_2-treated cells were used as positive staining controls. **E)** XTT assay depicting the proliferation profile of control and TCS iMSCs.

SUPPLEMENTARY TABLES

Table SI: Sample information.

Subject	Clinical status	Age*	Gender	Parental somatic cell	Reprogramming method	Clone	iPSC- derived cell type
F7405-1	control	27	male	dermal fibroblasts	retroviral	F7405-1c1	iNCC/nMSC/iMSC
						F7405-1c2	iNCC/nMSC/iMSC
						F7405-1c3	iNCC/nMSC/iMSC
F7007-1	control	23	male	dermal fibroblasts	retroviral	F7007-1c2	iMSC
						F7007-1c4	iMSC
F9048-1	control	20	male	dermal fibroblasts	episomal	F9048-1c3	iNCC/nMSC
F2441-1	TCS	9	female	periosteal fibroblasts	retroviral	F2441-1c2	iNCC/nMSC/iMSC
						F2441-1c3	iNCC/nMSC/iMSC
F2625-1	TCS	30	female	periosteal fibroblasts	retroviral	F2625-1c1	iNCC/nMSC/iMSC
						F2625-1c2	iNCC/nMSC/iMSC
						F2625-1c3	iNCC/nMSC/iMSC

* Age upon collection of tissue sample

Table SII: Primer sequences used in RT-qPCR.

Target	Forward primer (5'-3')	Reverse Primer (5'-3')
ACTB	TGAAGTGTGACGTGGACATC	GGAGGAGCAATGATCTTGAT
GAPDH	ATCACCATCTTCCAGGAGCG	GGGCAGAGATGATGACCCTTT
HPRT1	CCTGGCGTCGTGATTAGTGAT	AGACGTTCAGTCCTGTCCATAA
HMBS	AGCTTGCTCGCATACAGACG	AGCTCCTTGGTAAACAGGCTT
TBP	GTGACCCAGCATCACTGTTTC	GCAAACCAGAAACCCTTGCG
OCT3/4	GTGGTCAGCCAACTCGTCA	CCAAAAACCCTGGCACAAACT
NANOG	TGGACACTGGCTGAATCCTTC	CGTTGATTAGGCTCCAACCAT
TCOF1	GCCCCTGGAAAAGTTGTCACT	GGTTTCTCACTGGTGGCTTCAC
PAX3	AAGCCCAAGCAGGTGACAAC	CTCGGATTTCCCAGCTGAAC
ZIC1	AAGGTCCACGAATCCTCCTC	TTGTGGTCGGGTTGTCTG
TFAP2A	CTCCGCCATCCCTATTAACAAG	GACCCGGAACTGAACAGAAGA
SOX10	CCTCACAGATCGCCTACACC	CATATAGGAGAAGGCCGAGTAGA
ENG	TGCACTTGGCCTACAATTCCA	AGCTGCCCACTCAAGGATCT
SOX9	AGCGAACGCACATCAAGAC	CTGTAGGCGATCTGTTGGGG
ACAN	TTTCAAGAAGGCGAGGCGTCCG	TGGCTGAAGGCAAGCCTGGT
COL2A1	GGCAATAGCAGGTTCACGTACA	CGATAACAGTCTTGCCCCACTT
RUNX2	AGTGGACGAGGCAAGAGTTTC	GTTCCCGAGGTCCATCTACTG
ALPL	GATACAAGCACTCCCACTTCATCTG	CTGTTCAGCTCGTACTGCATGTC
COL1A1	GGGCCAAGACGAAGACAT	CAACACCCTTGCCGTTGTCG
BGLAP	GGCGCTACCTGTATCAATGG	GTGGTCAGCCAACTCGTCA

REFERENCES

Aasen, T. e J. C. Izpisua Belmonte. Isolation and cultivation of human keratinocytes from skin or plucked hair for the generation of induced pluripotent stem cells. Nat Protoc, v.5, n.2, Feb, p.371-82. 2010.

Achilleos, A. e P. A. Trainor. Neural crest stem cells: discovery, properties and potential for therapy. Cell Res, v.22, n.2, Feb, p.288-304. 2012.

Ali, S. A., S. K. Zaidi, et al. Phenotypic transcription factors epigenetically mediate cell growth control. Proc Natl Acad Sci U S A, v.105, n.18, May 6, p.6632-7. 2008.

Barriga, E. H., P. A. Trainor, et al. Animal models for studying neural crest development: is the mouse different? Development, v.142, n.9, May 1, p.1555-60. 2015.

Bhatt, S., R. Diaz, et al. Signals and switches in Mammalian neural crest cell differentiation. Cold Spring Harb Perspect Biol, v.5, n.2, Feb. 2013.

Bronner-Fraser, M. Perturbation of cranial neural crest migration by the HNK-1 antibody. Dev Biol, v.123, n.2, Oct, p.321-31. 1987.

Dauwerse, J. G., J. Dixon, et al. Mutations in genes encoding subunits of RNA polymerases I and III cause Treacher Collins syndrome. Nat Genet, v.43, n.1, Jan, p.20-2. 2011.

Del Barrio, M. G. e M. A. Nieto. Relative expression of Slug, RhoB, and HNK-1 in the cranial neural crest of the early chicken embryo. Dev Dyn, v.229, n.1, Jan, p.136-9. 2004.

Dixon, J., K. Hovanes, et al. Sequence analysis, identification of evolutionary conserved motifs and expression analysis of murine tcof1 provide further evidence for a potential function for the gene and its human homologue, TCOF1. Hum Mol Genet, v.6, n.5, May, p.727-37. 1997.

Dixon, J., N. C. Jones, et al. Tcof1/Treacle is required for neural crest cell formation and proliferation deficiencies that cause craniofacial abnormalities. Proc Natl Acad Sci U S A, v.103, n.36, Sep 5, p.13403-8. 2006.

Fanganiello, R. D., A. L. Sertie, et al. Apert p.Ser252Trp mutation in FGFR2 alters osteogenic potential and gene expression of cranial periosteal cells. Mol Med, v.13, n.7-8, Jul-Aug, p.422-42. 2007.

Fukuta, M., Y. Nakai, et al. Derivation of mesenchymal stromal cells from pluripotent stem cells through a neural crest lineage using small molecule compounds with defined media. PLoS One, v.9, n.12, p.e112291. 2014.

Galindo, M., J. Pratap, et al. The bone-specific expression of Runx2 oscillates during the cell cycle to support a G1-related antiproliferative function in osteoblasts. J Biol Chem, v.280, n.21, May 27, p.20274-85. 2005.

Gimelbrant, A., J. N. Hutchinson, et al. Widespread monoallelic expression on human autosomes. Science, v.318, n.5853, Nov 16, p.1136-40. 2007.

Giovannone, D., B. Ortega, et al. Chicken trunk neural crest migration visualized with HNK1. Acta Histochem, v.117, n.3, Apr, p.255-66. 2015.

Gong, S. G. Cranial neural crest: migratory cell behavior and regulatory networks. Exp Cell Res, v.325, n.2, Jul 15, p.90-5. 2014.

Gonzales, B., D. Henning, et al. The Treacher Collins syndrome (TCOF1) gene product is involved in pre-rRNA methylation. Hum Mol Genet, v.14, n.14, Jul 15, p.2035-43. 2005.

Gursoy, S., J. Hukki, et al. Five year follow-up of mandibular distraction osteogenesis on the dentofacial structures of syndromic children. Orthod Craniofac Res, v.11, n.1, Feb, p.57-64. 2008.

Isaac, C., K. L. Marsh, et al. Characterization of the nucleolar gene product, treacle, in Treacher Collins syndrome.Mol Biol Cell, v.11, n.9, Sep, p.3061-71. 2000.

Ishiy, F. A., R. D. Fanganiello, et al. Improvement of In Vitro Osteogenic Potential through Differentiation of Induced Pluripotent Stem Cells from Human Exfoliated Dental Tissue towards Mesenchymal-Like Stem Cells. Stem Cells Int, v.2015, p.249098. 2015.

Jehee, F. S., J. T. Takamori, et al. Using a combination of MLPA kits to detect chromosomal imbalances in patients with multiple congenital anomalies and mental retardation is a valuable choice for developing countries. Eur J Med Genet, v.54, n.4, Jul-Aug, p.e425-32. 2011.

Jones, N. C., P. G. Farlie, et al. Detection of an appropriate kinase activity in branchial arches I and II that coincides with peak expression of the Treacher Collins syndrome gene product, treacle. Hum Mol Genet, v.8, n.12, Nov, p.2239-45. 1999.

Jones, N. C., M. L. Lynn, et al. Prevention of the neurocristopathy Treacher Collins syndrome through inhibition of p53 function. Nat Med, v.14, n.2, Feb, p.125-33. 2008.

Kaern, M., T. C. Elston, et al. Stochasticity in gene expression: from theories to phenotypes. Nat Rev Genet, v.6, n.6, Jun, p.451-64. 2005.

Kreitzer, F. R., N. Salomonis, et al. A robust method to derive functional neural crest cells from human pluripotent stem cells. Am J Stem Cells, v.2, n.2, p.119-31. 2013.

Masotti, C., C. C. Ornelas, et al. Reduced transcription of TCOF1 in adult cells of Treacher Collins syndrome patients. BMC Med Genet, v.10, p.136. 2009.

Matsumoto, Y., M. Ikeya, et al. New Protocol to Optimize iPS Cells for Genome Analysis of Fibrodysplasia Ossificans Progressiva. Stem Cells, v.33, n.6, Jun, p.1730-42. 2015.

Menendez, L., M. J. Kulik, et al. Directed differentiation of human pluripotent cells to neural crest stem cells. Nat Protoc, v.8, n.1, Jan, p.203-12. 2013.

Menendez, L., T. A. Yatskievych, et al. Wnt signaling and a Smad pathway blockade direct the differentiation of human pluripotent stem cells to multipotent neural crest cells. Proc Natl Acad Sci U S A, v.108, n.48, Nov 29, p.19240-5. 2011.

Okita, K., T. Yamakawa, et al. An efficient nonviral method to generate integration-free human-induced pluripotent stem cells from cord blood and peripheral blood cells. Stem Cells, v.31, n.3, Mar, p.458-66. 2012.

Pfaffl, M. W. A new mathematical model for relative quantification in real-time RT-PCR. Nucleic Acids Res, v.29, n.9, May 1, p.e45. 2001.

Pratap, J., M. Galindo, et al. Cell growth regulatory role of Runx2 during proliferative expansion of preosteoblasts. Cancer Res, v.63, n.17, Sep 1, p.5357-62. 2003.

Sadaghiani, B. e J. R. Vielkind.Distribution and migration pathways of HNK-1-immunoreactive neural crest cells in teleost fish embryos.Development, v.110, n.1, Sep, p.197-209. 1990.

Solchaga, L. A., K. J. Penick, et al. Chondrogenic differentiation of bone marrow-derived mesenchymal stem cells: tips and tricks. Methods Mol Biol, v.698, p.253-78. 2011.

Splendore, A., E. O. Silva, et al. High mutation detection rate in TCOF1 among Treacher Collins syndrome patients reveals clustering of mutations and 16 novel pathogenic changes. Hum Mutat, v.16, n.4, Oct, p.315-22. 2000.

Stelnicki, E. J., W. Y. Lin, et al. Long-term outcome study of bilateral mandibular distraction: a comparison of Treacher Collins and Nager syndromes to other types of micrognathia. Plast Reconstr Surg, v.109, n.6, May, p.1819-25; discussion 1826-7. 2002.

Takahashi, K., K. Tanabe, et al. Induction of pluripotent stem cells from adult human fibroblasts by defined factors. Cell, v.131, n.5, Nov 30, p.861-72. 2007.

Trainor, P. A., J. Dixon, et al. Treacher Collins syndrome: etiology, pathogenesis and prevention. Eur J Hum Genet, v.17, n.3, Mar, p.275-83. 2009.

Trainor, P. A. e A. E. Merrill. Ribosome biogenesis in skeletal development and the pathogenesis of skeletal disorders. Biochim Biophys Acta, v.1842, n.6, Jun, p.769-78. 2014.

Twigg, S. R. e A. O. Wilkie.New insights into craniofacial malformations. Hum Mol Genet, Jun 17. 2015.

Valdez, B. C., D. Henning, et al. The Treacher Collins syndrome (TCOF1) gene product is involved in ribosomal DNA gene transcription by interacting with upstream binding factor. Proc Natl Acad Sci U S A, v.101, n.29, Jul 20, p.10709-14. 2004.

Weiner, A. M., N. L. Scampoli, et al. Fishing the molecular bases of Treacher Collins syndrome. PLoS One, v.7, n.1, p.e29574. 2012.

Zhao, H., P. Bringas, Jr., et al. An in vitro model for characterizing the post-migratory cranial neural crest cells of the first branchial arch. Dev Dyn, v.235, n.5, May, p.1433-40. 2006.

CHAPTER VI

General Discussion and Conclusions

6 - General Discussion and Conclusions

In this work, through the use of different approaches such as microarray expression analysis and molecular surface sorting, we have shown that mesenchymal stem cells, most particularly those derived from dental pulp of human exfoliated teeth (SHED), present an efficient *in vitro* osteogenesis and that at least two factors seem to contribute to the regulation of this process. We also have shown the advantages of the use of iPSCs with the derivation of MSC-like cells that exhibited higher osteogenesis *in vitro* as compared to adult stem mesenchymal cells, and their use in the genetic field through the obtainment of iPSCs to model Treacher Collins syndrome.

We first described that SHED present an increased osteogenic potential as compared to hASCs. In order to answer which factors could be regulating these differences, we performed microarray expression analysis to investigate the osteogenesis in adult MSCs. We observed that *IGF2* were upregulated in SHED when compared to hASCs. We hypothesized that this marker could be directly associated with the higher osteogenic potential in SHED, and through a treatment/supplementation with exogenous *IGF2* and *IGF2* inhibitor (chromeceptin) we observed a positive correlation of this marker with *in vitro* osteogenesis, supporting our hypothesis. We also have shown that imprinting is involved in the regulation of IGF2 expression in SHED. Thus we propose *IGF2* as an osteogenic biomarker in MSCs, which can be used to pre-select cells to be used in bone tissue engineering or alternatively, the use of IGF2 to induce better osteogenesis could be explored.

We do not expect that *IGF2* expression it is the only factor contributing to the *in vitro* osteogenesis differences between SHEDand hASCs. In order to address this question, we choose to use other approach to study the differences of *in vitro* osteogenesis in SHED and

hASCs. Using transcriptional analysis and cell sorting we demonstrated that SHED presented lower expression of CD105 when compared to hASCs and that the low levels of CD105 in SHED contribute to its *in vitro* osteogenic potential. Through *in silico* analysis and gain/loss function assays we showed that the microRNA 1287 is a promising candidate in CD105 regulation in SHED and hASCs and that *IGF2* is not apparently involved in CD105 expression levels regulation. These results thus show that inverse correlation of CD105 expression with osteogenic potential is not specific to hASC (Levi et al., 2011) and it is cell-specific regulated.

Based on the above-mentioned findings, we reinforce that the regulation of the osteogenic potential in adult MSCs is a multifactorial process and our work has contributed to the identification of two factors involved in this regulation. Further studies are required to evaluate if each of these factors alone or in combination in cell culture assays would contribute to a more efficient osteogenesis in adult MSC.

Further, we observed that the cell source used to reprogram and derive iPSCs is an important factor to achieve a better *in vitro* osteogenesis, as MSC-like from SHED presented higher osteogenesis compared to MSC-like from fibroblasts and from adult SHED. Our findings thus strength the importance of cell type/source selection to derive iPSCs and depending on the purpose or tissue to be obtained the cell type/source could be a limiting factor and influence the final results. Neither *IGF2* nor CD105 seemed to be involved with the increased osteogenic potential of the MSC-like. Finally, in the last chapter we describe an *in vitro* model to Treacher-Collins syndrome. Using different methods, we have compared derived neural crest cells (iNCCs), neural crest-derived mesenchymal cells (nMSCs) and MSC-like cells from iPSC, which allow us to recapitulate different stages of craniofacial development. We observed alteration of osteogenesis/chondrogenesis in MSC-like cells derived from patients. nMSCs from Treacher-Collins subjects presented a higher apoptosis rate, consistent with the findings in the literature using animal models to Treacher-Collins syndrome. Therefore, through several

analyses, we have shown that we obtained reliable iNCC, nMSCs and iMSCs from patients and controls and these cell types can thus be used to model TCS. Through the use of pluripotent cells of patients with bone genetic disorders, we expect to better understand craniofacial bone development and identify new pathways critical to this process that could recapitulate *in vitro* bone formation. We expect that this approach may also contribute to better bone reconstruction therapies in the future.

CHAPTER VII

Additional publications and participations in Conferences/Meetings

8 -Appendix: Additional publicationsand participations in Conferences/Meetings

PARTICIPATIONS IN CONFERENCES/MEETINGS

Ishiy, FAA; Ornelas, CM; Fanganiello, RD; Griesi-Oliveira, K; Sdrigotti, MA; Calcaterra, N; Passos-Bueno, MR. Induced pluripotent stem cells to model treacher collins syndrome in a dish.13th international society of stem cell research.**2015**. Stockholm, Sweden. **Poster Presentation**

Ishiy, FAA; Fanganiello, RD; Capelo, LP; Kuriki, PS; Morales, AG; Passos-Bueno, Mr. CD105 expression as a marker to explain osteogenic potential differences of mesenchymal stem cells of different sources. 12th international society of stem cell research.**2014**. Vancouver, Canada. **Poster Presentation**

Fanganiello R.D., **Ishiy FAA,** Yumi D., Capelo L.P., Passos-Bueno M.R. Differentially expressed genes associated to higher osteogenic potential of human mesenchymal stem cells. International Society of Stem Cells Research Meeting.**2013**. Boston, Massachussetts, EUA. **Poster Presentation**

FanganielloRD, **Ishiy FAA,** Capelo LP, Aguena M, Bueno DF, Almada, BP, Martins MT, Passos-Bueno MR. Comparison of the osteogenic potential of adult stem cells from different sources. The American Society of Human Genetics.**2012**. San Francisco, California, EUA. **Poster Presentation**

Ishiy FAA, FanganielloRD, Kobayashi GS, Sunaga DY, Capelo LP, Passos-Bueno MR.Gene expression analysis of mesenchymal stem cells during initial osteoblastogenic differentiation.VII Brazilian Congress on Stem Cells and Cell Therapy.**2012**. São Paulo, SP, Brazil. Hospital Sírio-Libanês and FeComércio. **Poster Presentation**

FanganielloRD, Capelo LP, **Ishiy FAA,** , Almada, BP, Aguena M, Bueno DF, Martins MT, Passos-Bueno MR. Comparison of the osteogenic potential of adult stem cells from different sources. American Society of Human Genetics Meeting.**2012.** San Francisco, California, EUA. **Poster presentation**

PUBLICATIONS – ORIGINAL ARTICLES

Modeling Treacher-Collins Syndrome using iPSCs. **Ishiy FAA**, Gerson S. Kobayashi, Camila M. Musso, Luiz C. Caires, Ernesto Goulart, Andressa G. Morales, Karina Griesi-Oliveira, Patrícia Semedo-Kuriki, Fanganiello RD, Maria Rita Passos-Bueno.(*preparation*).

Modelling Richieri-Costa-Pereira syndrome with iPSC-derived neural crest cells.Gerson S. Kobayashi, **Ishiy FAA**, Camila M. Musso, Luiz C. Caires, Ernesto Goulart, Andressa G. Morales, Karina Griesi-Oliveira, Patrícia Semedo-Kuriki, Maria Rita Passos-Bueno. (*preparation*).

hsa-miR-1287 regulates *in vitro* osteogenic potential of SHED through downregulation of CD105.**Ishiy FAA**, Fanganiello RD, Kobayashi GS, Kuriki PS, Passos-Bueno MR. (*preparation*).

Cnbp ameliorates Treacher Collins Syndrome craniofacial anomalies through a pathway that involves redox-responsive genes.de Peralta, M. S. P., Mouguelar, V. S., Sdrigotti, M. A., **Ishiy, FAA**, Fanganiello, R. D., Passos-Bueno, M. R., ... & Calcaterra, N. B. (2016). Cell Death & Disease, 7(10), e2397.**doi: 10.1038/cddis.2016.299**.

Non-specific FGFR2 ligands, FGF19 and FGF10, lead to abnormal cellular behavior in Apert syndrome-derived fibroblast and stem cells. Yeh E, Atique R, Fanganiello RD, Sunaga DY, **Ishiy FAA**, Passos-Bueno MR.**doi: 10.1089/scd.2016.0018. Epub 2016 Jun 23**

Increased in vitro osteopotential in SHED associated with higher IGF2 expression when compared with hASCs. Fanganiello RD, **Ishiy FAA**, Kobayashi GS, Cruz LA, Sunaga DY, Passos-Bueno MR. Stem Cell Reviews and Reports, **2015. DOI 10.1007/s12015-015-9592-x**

Improvement of In Vitro Osteogenic Potential through Differentiation of Induced Pluripotent Stem Cells from Human Exfoliated Dental Tissue towards Mesenchymal-Like Stem Cells.**Ishiy FAA**, Fanganiello RD, Griesi-Oliveira K, Suzuki AM, Kobayashi GS, Morales AG, Capelo LP, Passos-Bueno MR. Stem Cells International, 9 pages, **2015. doi: 10.1155/2015/249098**

FGFR2 Mutation confers a Less Drastic Gain of Function in Mesenchymal Stem Cells Than in Fibroblasts. Yeh E, Atique R, **Ishiy FAA**, Fanganiello RD, Alonso N, Matushita H, da Rocha KM, Passos-Bueno MR. Stem Cells Review and Reports, v.8, p. 685-695, **2012. Doi:10.1007/S12015-011-9327-6**

Optimization of Parameters for a More Efficient Use of Adipose-Derived Stem Cells in Regenerative Medicine Therapies.Aguena M, Fanganiello RD, Tissiani LAL, **Ishiy, FAA**, Atique R, Alonso N, Passos-Bueno MR. Stem Cells International, v. 2012, p. 1-7, **2012. Doi:10.1155/2012/202610**

References

Aasen, T., Raya, A., Barrero, M. J., Garreta, E., Consiglio, A., Gonzalez, F., ... & Edel, M. (2008). Efficient and rapid generation of induced pluripotent stem cells from human keratinocytes. Nature biotechnology, 26(11), 1276-1284.

Al-Nbaheen, M., Ali, D., Bouslimi, A., Al-Jassir, F., Megges, M., Prigione, A., ... & Aldahmash, A. (2013). Human stromal (mesenchymal) stem cells from bone marrow, adipose tissue and skin exhibit differences in molecular phenotype and differentiation potential. Stem Cell Reviews and Reports, 9(1), 32-43.

Alongi DJ, Yamaza T, Song Y, et al. Stem/progenitor cells from inflamed human dental pulp retain tissue regeneration potential. Regenerative medicine. 2010;5(4):617-631. doi:10.2217/rme.10.30.

Amini AR, Laurencin CT, Nukavarapu SP. Bone tissue engineering: recent advances and challenges. Crit Rev Biomed Eng 2012; 40(5): 363–408.

Ananiev, G., Williams, E. C., Li, H., & Chang, Q. (2011). Isogenic pairs of wild type and mutant induced pluripotent stem cell (iPSC) lines from Rett syndrome patients as in vitro disease model. PloS one, 6(9), e25255.

Casser-Bette, M., Murray, A.B., Closs, E.I. et al. Calcif Tissue Int (1990) 46: 46. doi:10.1007/BF02555824

Badylak, S.; Nerem, R. Progress in tissue engineering and regenerative medicine. Proceedings of the National Academy of Sciences of the United States of America, v. 107, n.8, p. 3285-3286, 2010.

Baer PC, Geiger H, "Adipose-Derived Mesenchymal Stromal/Stem Cells: Tissue Localization, Characterization, and Heterogeneity," Stem Cells International, vol. 2012, Article ID 812693, 11 pages, 2012. doi:10.1155/2012/812693

Bara, J. J., Richards, R. G., Alini, M. and Stoddart, M. J. (2014), Concise Review: Bone Marrow-Derived Mesenchymal Stem Cells Change Phenotype Following In Vitro Culture: Implications for Basic Research and the Clinic. Stem Cells, 32: 1713–1723. doi:10.1002/stem.1649

Barberi T., Willis L. M., Socci N. D., Studer L. (2005). Derivation of multipotent mesenchymal precursors from human embryonic stem cells. PLoS Med. 2:e161. 10.1371/journal.pmed.0020161

Baksh, D., Song, L., & Tuan, R. S. Adult mesenchymal stem cells: characterization, differentiation, and application in cell and gene therapy.Journal of cellular and molecular medicine. v.8, n.3, p.301-16, 2004. Retrieved from http://www.ncbi.nlm.nih.gov/pubmed/15491506

Bazley Faith A., Liu Cyndi F., Yuan Xuan, Hao Haiping, All Angelo H., De Los Angeles Alejandro, Zambidis Elias T., Gearhart John D., and Kerr Candace L.. Stem Cells and Development. November 2015, 24(22): 2634-2648. doi:10.1089/scd.2015.0100.

Bhatt, S., Diaz, R., & Trainor, P. A. (2013). Signals and switches in Mammalian neural crest cell differentiation. Cold Spring Harbor perspectives in biology, 5(2), a008326.

Bianco, P. et al. The meaning, the sense and the significance: translating the science of mesenchymal stem cells into medicine. Nat. Med. 19, 35–42 (2013).

Bielby R, Jones E, McGonagle, D. The role of mesenchymal stem cells in maintenance and repair of bone. Injury Volume 38, Issue 1, Supplement, March 2007, Pages S26-S32

Bose S, Roy M, Bandyopadhyay A. Recent advances in bone tissue engineering scaffolds. Trends Biotechnol. 2012;30(10):546–554. doi: 10.1016/j.tibtech.2012.07.005.

BOURIN P, BUNNELL BA, CASTEILLA L, et al. Stromal cells from the adipose tissue-derived stromal vascular fraction and culture expanded adipose tissue-derived stromal/stem cells: a joint statement of the International Federation for Adipose Therapeutics (IFATS) and Science and the International Society for Cellular Therapy (ISCT). Cytotherapy. 2013;15(6):641-648. doi:10.1016/j.jcyt.2013.02.006.

Boyd, N. L., Robbins, K. R., Dhara, S. K., West, F. D., & Stice, S. L. (2009). Human Embryonic Stem Cell–Derived Mesoderm-like Epithelium Transitions to Mesenchymal Progenitor Cells. Tissue Engineering Part A, 15(8), 1897-1907.

Bruder, S. P., Fink, D. J. and Caplan, A. I. (1994), Mesenchymal stem cells in bone development, bone repair, and skeletal regenaration therapy. J. Cell. Biochem., 56: 283–294. doi:10.1002/jcb.240560303

Bueno, D. F., Kerkis, I., Costa, A. M., Martins, M. T., Kobayashi, G. S., Zucconi, E., Fanganiello, R. D., Salles, FT.,Almeida, AB., do Amaral, C.E. R., Alonso, N., Passos-Bueno, MR. New source of muscle-derived stem cells with potential for alveolar bone reconstruction in cleft lip and/or palate patients. Tissue engineering. Part A. v. 15, n.2, p.427-35, 2009. doi:10.1089/ten.tea.2007.0417

Byers, B., Cord, B., Nguyen, H. N., Schüle, B., Fenno, L., Lee, P. C., ... & Palmer, T. D. (2011). SNCA triplication Parkinson's patient's iPSC-derived DA neurons accumulate α-synuclein and are susceptible to oxidative stress. PloS one, 6(11), e26159.

Cahan, Patrick, and George Q. Daley. "Origins and implications of pluripotent stem cell variability and heterogeneity." Nature reviews Molecular cell biology 14.6 (2013): 357-368.

Campagnoli C, Roberts IA, Kumar S, Bennett PR, Bellantuono I, Fisk NM. Identification of mesenchymal stem/progenitor cells in human first-trimester fetal blood, liver, and bone marrow. Blood. 2001;98(8):2396–2402. doi: 10.1182/blood.V98.8.2396.

Campisi, J., & di Fagagna, F. D. A. (2007). Cellular senescence: when bad things happen to good cells. Nature reviews Molecular cell biology, 8(9), 729-740.

Caplan, A. I. (1991), Mesenchymal stem cells. J. Orthop. Res., 9: 641–650. doi:10.1002/jor.1100090504

Caplan, A. I. and Dennis, J. E. (2006), Mesenchymal stem cells as trophic mediators. J. Cell. Biochem., 98: 1076–1084. doi:10.1002/jcb.20886

Caplan, A. I. (2007). Adult mesenchymal stem cells for tissue engineering versus regenerative medicine.Journal of cellular physiology, 213(2), 341-347.

Caplan, A. I. Why are MSCs therapeutic ? New data : new insight. Journal of Pathology. v. 217, p. 318-324, 2009. doi:10.1002/path

Chamberlain, G., Fox, J., Ashton, B. and Middleton, J. (2007), Concise Review: Mesenchymal Stem Cells: Their Phenotype, Differentiation Capacity, Immunological Features, and Potential for Homing. STEM CELLS, 25: 2739–2749. doi:10.1634/stemcells.2007-0197

Chen, Y. S., Pelekanos, R. A., Ellis, R. L., Horne, R., Wolvetang, E. J., & Fisk, N. M. (2012). Small molecule mesengenic induction of human induced pluripotent stem cells to generate mesenchymal stem/stromal cells. Stem cells translational medicine, 1(2), 83-95.

Chin, M. H., Mason, M. J., Xie, W., Volinia, S., Singer, M., Peterson, C., ... & Khvorostov, I. (2009). Induced pluripotent stem cells and embryonic stem cells are distinguished by gene expression signatures. Cell stem cell, 5(1), 111-123.

Chung MT, Liu C, Hyun JS, Lo DD, Montoro DT, Hasegawa M, Li S, Sorkin M, Rennert R, Keeney M, Yang F, Quarto N, Longaker MT, Wan DC. CD90 (Thy-1)-positive selection enhances osteogenic capacity of human adipose-derived stromal cells. Tissue Eng Part A 2013; 19: 989-997 [DOI: 10.1089/ ten.tea.2012.0370]

Cohen, J. D., Babiarz, J. E., Abrams, R. M., Guo, L., Kameoka, S., Chiao, E., ... & Kolaja, K. L. (2011). Use of human stem cell derived cardiomyocytes to examine sunitinib mediated cardiotoxicity and electrophysiological alterations. Toxicology and applied pharmacology, 257(1), 74-83.

D'Aquino, R., Graziano, A., Sampaolesi, M., Laino, G., Pirozzi, G., De Rosa, A., & Papaccio, G. Human postnatal dental pulp cells co-differentiate into osteoblasts and endotheliocytes: a pivotal synergy leading to adult bone tissue formation. Cell death and differentiation. v.14, n.6, p.1162-71, 2007. doi:10.1038/sj.cdd.4402121

D' Aquino, R., Graziano, A., Laino, G., & Papaccio, G. Dental pulp stem cells: a promising tool for bone regeneration. Stem cell reviews. v.4, n.1, p. 21-6, 2008. doi:10.1007/s12015-008-9013-5

D' Aquino, R., De Rosa, A., Lanza, V., Tirino, V., Laino, L., Graziano, A., Desiderio, V., Laino, G., Papaccio, G. Human mandible bone defect repair by the grafting of dental pulp stem/progenitor cells and collagen sponge biocomplexes. European cells & materials, v.18, p.75-83, 2009. Retrieved from http://www.ncbi.nlm.nih.gov/pubmed/19908196

Dauwerse, J. G., Dixon, J., Seland, S., Ruivenkamp, C. A., van Haeringen, A., Hoefsloot, L. H., ... & Zweier, C. (2011). Mutations in genes encoding subunits of RNA polymerases I and III cause Treacher Collins syndrome. Nature genetics, 43(1), 20-22.

Derubeis AR, Cancedda R. Bone marrow stromal cells (BMSCs) in bone engineering: limitations and recent advances. Ann Biomed Eng. 2004;32:160–165.

De Mendonça Costa A, Bueno DF, Martins MT, Kerkis I, Kerkis A, Fanganiello RD, Cerruti H, Alonso N, Passos-Bueno MR. Reconstruction of large cranial defects in nonimmunosuppressed experimental design with human dental pulp stem cells. The journal of Craniofacil Surgery.v.19, n.1, p. 204-10, 2008.

M.J. Devine, M. Ryten, P. Vodicka, A.J. Thomson, T. Burdon, H. Houlden, F. Cavaleri, M. Nagano, N.J. Drummond, J.W. Taanman, et al.

Parkinson's disease induced pluripotent stem cells with triplication of the α-synuclein locus. Nat. Commun., 2 (2011), p. 440

Diederichs, S., & Tuan, R. S. (2014). Functional comparison of human-induced pluripotent stem cell-derived mesenchymal cells and bone marrow-derived mesenchymal stromal cells from the same donor. Stem cells and development, 23(14), 1594-1610.

Dimitriou R, Tsiridis E, Giannoudis PV. Current concepts of molecular aspects of bone healing. Injury. 2005;36:1392–1404.

Dixon, J., Edwards, S. J., Anderson, I., Brass, A., Scambler, P. J., & Dixon, M. J. (1997). Identification of the complete coding sequence and genomic organization of the Treacher Collins syndrome gene. Genome research, 7(3), 223-234.

Dixon, J., Jones, N. C., Sandell, L. L., Jayasinghe, S. M., Crane, J., Rey, J. P., ... & Trainor, P. A. (2006). Tcof1/Treacle is required for neural crest cell formation and proliferation deficiencies that cause craniofacial abnormalities. Proceedings of the National Academy of Sciences, 103(36), 13403-13408.

Dominici, M., Le Blanc, K., Mueller, I., Slaper-Cortenbach, I., Marini, F., Krause, D., Deans, R., Keating, A., Prockop, DJ. and Horwitz, EM. Minimal criteria for defining multipotent mesenchymal stromal cells. The International Society for Cellular Therapy position statement.Cytotherapy. 2006.doi:10.1080/14653240600855905

Edwards, S. J., Gladwin, A. J., & Dixon, M. J. (1997). The mutational spectrum in Treacher Collins syndrome reveals a predominance of mutations that create a premature-termination codon. American journal of human genetics, 60(3), 515.

Erices, Conget & Minguell (2000) Erices A, Conget P, Minguell JJ. Mesenchymal progenitor cells in human umbilical cord blood. British Journal of Haematology. 2000;109:235–242. doi: 10.1046/j.1365-2141.2000.01986.x.

Friedenstein, A. J., S. Piatetzky, Ii e K. V. Petrakova. Osteogenesis in transplants of bone marrow cells. J Embryol Exp Morphol, v.16, n.3, Dec, p.381-90. 1966

Freyschmidt J. (1993). Skeletterkrankungen. Springer- Verlag, Berlin, Heidelberg, Germany.

Giuliani A., Manescu A., Langer M., Rustichelli F., Desiderio V., Paino F., et al. . (2013). Three graft vascularization is a critical rate-limiting step in skeletal stem cell-mediated posterolateral spinal fusion. Stem Cells Transl. Med. 2, 316–324. 10.5966/sctm.2012-0136

Gimble, Jeffrey M., Adam J. Katz, and Bruce A. Bunnell. "Adipose-derived stem cells for regenerative medicine." Circulation research 100.9 (2007): 1249-1260.

Giuliani, M., Fleury, M., Vernochet, A., Ketroussi, F., Clay, D., Azzarone, B., ... & Durrbach, A. (2011). Long-lasting inhibitory effects of fetal liver mesenchymal stem cells on T-lymphocyte proliferation. PLoS One, 6(5), e19988.

Glotzbach, J. P., Wong, V. W., Gurtner, G. C., & Longaker, M. T. Regenerative medicine. Current problems in surgery. V.48, n.3, p. 148-212. 2011 doi:10.1067/j.cpsurg.2010.11.002

Gong, S. G. (2014). Cranial neural crest: Migratory cell behavior and regulatory networks. Experimental cell research, 325(2), 90-95.

Grayson WL, Bunnell BA, Martin E et al. Stromal cells and stem cells in clinical bone regeneration. Nat rev Endocrinol 2015;11:140–150.

Gronthos, S., M. Mankani, J. Brahim, P. G. Robey e S. Shi. Postnatal human dental pulp stem cells (DPSCs) in vitro and in vivo. Proc Natl Acad Sci U S A, v.97, n.25, Dec 5, p.13625-30. 2000.

Guan M, Yao W, Liu R, et al. Directing mesenchymal stem cells to bone to augment formation and increase bone mass. Nat Med. 2012;18(3):456–62.

Gutierrez-Aranda I, Ramos-Mejia V, Bueno C, Munoz-Lopez M, Real PJ, Mácia A, Sanchez L, Ligero G, Garcia-Parez JL, Menendez P. Human induced pluripotent stem cells develop teratoma more efficiently and faster than human embryonic stem cells regardless the site of injection. Stem Cells. 2010 Sep;28(9):1568-70. doi: 10.1002/stem.471.

Guzzo, R. M., Scanlon, V., Sanjay, A., Xu, R. H., & Drissi, H. (2014). Establishment of human cell type-specific iPS cells with enhanced chondrogenic potential. Stem Cell Reviews and Reports, 10(6), 820-829.

Griesi‐Oliveira, K., Sunaga, D. Y., Alvizi, L., Vadasz, E., & Passos‐Bueno, M. R. (2013). Stem cells as a good tool to investigate dysregulated biological systems in autism spectrum disorders. Autism Research, 6(5), 354-361.

Fan He, Xiaodong Chen, and Ming Pei. Tissue Engineering Part A. December 2009, 15(12): 3809-3821. doi:10.1089/ten.tea.2009.0188.

Fanganiello, R. D., Ishiy, F. A. A., Kobayashi, G. S., Alvizi, L., Sunaga, D. Y., & Passos-Bueno, M. R. (2015). Increased In Vitro Osteopotential in SHED Associated with Higher IGF2 Expression When Compared with hASCs. Stem Cell Reviews and Reports, 11(4), 635-644.

Gonzales, B., Henning, D., So, R. B., Dixon, J., Dixon, M. J., & Valdez, B. C. (2005). The Treacher Collins syndrome (TCOF1) gene product is involved in pre-rRNA methylation. Human molecular genetics, 14(14), 2035-2043.

Gruenloh, W., Kambal, A., Sondergaard, C., McGee, J., Nacey, C., Kalomoiris, S., ...& Nolta, J. A. (2011). Characterization and in vivo testing of mesenchymal stem cells derived from human embryonic stem cells. Tissue engineering Part A, 17(11-12), 1517-1525.

Grskovic, M., Javaherian, A., Strulovici, B., & Daley, G. Q. (2011). Induced pluripotent stem cells—opportunities for disease modelling and drug discovery. Nature reviews Drug discovery, 10(12), 915-929.

Haraguchi, Y., Shimizu, T., Yamato, M., & Okano, T. (2012). Concise review: cell therapy and tissue engineering for cardiovascular disease. Stem cells translational medicine, 1(2), 136-141.

Healy KE, Guldberg, RE. Bone tissue engineering. J Musculoskelet Neuronal Interact 2007; 7(4):328-330

Hematti, P. (2011). Human embryonic stem cell-derived mesenchymal progenitors: an overview. Embryonic Stem Cell Therapy for Osteo-Degenerative Diseases: Methods and Protocols, 163-174.

Holzwarth JM, Ma PX. Biomimetic nanofibrous scaffolds for bone tissue engineering.Biomaterials. 2011 Dec; 32(36): 9622–9629.

Hosoya, A., Hiraga, T., Ninomiya, T., Yukita, A., Yoshiba, K., Yoshiba, N., ...& Nakamura, H. (2012). Thy-1-positive cells in the subodontoblastic layer possess high potential to differentiate into hard tissue-forming cells. Histochemistry and cell biology, 137(6), 733-742.

Hossini, A. M., Megges, M., Prigione, A., Lichtner, B., Toliat, M. R., Wruck, W., ... & Zoubouliss, C. C. (2015). Induced pluripotent stem cell-derived neuronal cells from a sporadic Alzheimer's disease donor as a model for investigating AD-associated gene regulatory networks. BMC genomics, 16(1), 1.

Huang, G. T.-J., Gronthos, S., & Shi, S. Mesenchymal stem cells derived from dental tissues vs. those from other sources: their biology and role in regenerative medicine. Journal of dental research. v.88, n.9, p.792-806, 2009. doi:10.1177/0022034509340867

Huang GX, Arany, PR, Mooney DJ. Modeling and Validation of Multilayer Poly(Lactide-Co-Glycolide) Scaffolds for In Vitro Directed Differentiation of Juxtaposed Cartilage and Bone Tissue Eng Part A. 2015 Aug 1; 21(15-16): 2228–2240

Hwang, N. S., Varghese, S., & Elisseeff, J. (2008). Controlled differentiation of stem cells. *Advanced drug delivery reviews*, *60*(2), 199-214.

Hynes, K., Menicanin, D., Han, J., Marino, V., Mrozik, K., Gronthos, S., & Bartold, P. M. (2013). Mesenchymal stem cells from iPS cells facilitate periodontal regeneration. Journal of dental research, 0022034513498258.

Israel, M. A., Yuan, S. H., Bardy, C., Reyna, S. M., Mu, Y., Herrera, C., ... & Carson, C. T. (2012). Probing sporadic and familial Alzheimer/'s disease using induced pluripotent stem cells. Nature, 482(7384), 216-220.

in 'tAnker, P. S., Scherjon, S. A., Kleijburg-van der Keur, C., Noort, W. A., Claas, F. H. J., Willemze, R., et al (2003). Amniotic fluid as a novel source of mesenchymal stem cells for therapeutic transplantation. Blood, 102, 1548–1549.

Jones, N. C., Lynn, M. L., Gaudenz, K., Sakai, D., Aoto, K., Rey, J. P., ... & Dixon, M. J. (2008). Prevention of the neurocristopathy Treacher Collins syndrome through inhibition of p53 function. Nature medicine, 14(2), 125-133.

Jones, N. C., Lynn, M. L., Gaudenz, K., Sakai, D., Aoto, K., Rey, J. P., ... & Dixon, M. J. (2008). Prevention of the neurocristopathy Treacher Collins syndrome through inhibition of p53 function. Nature medicine, 14(2), 125-133.

Jones, N. C., Lynn, M. L., Gaudenz, K., Sakai, D., Aoto, K., Rey, J. P., ... & Dixon, M. J. (2008). Prevention of the neurocristopathy Treacher Collins syndrome through inhibition of p53 function. Nature medicine, 14(2), 125-133.

Jung, Y., Bauer, G. and Nolta, J. A. (2012), Concise Review: Induced Pluripotent Stem Cell-Derived Mesenchymal Stem Cells: Progress Toward Safe Clinical Products. STEM CELLS, 30: 42–47. doi:10.1002/stem.727

Jung, Y., Bauer, G., & Nolta, J. A. (2012). Concise review: induced pluripotent stem cell ‐ derived mesenchymal stem cells: progress toward safe clinical products. Stem cells, 30(1), 42-47.

Kadiyala S, Young RG, Thiede MA, Brude, SP. Culture expanded canine mesenchymal stem cells possess osteochondrogenic potential in vivo and in vitro. Cell Transplantation Volume 6, Issue 2, March–April 1997, Pages 125-134

Kim, D., Kim, C. H., Moon, J. I., Chung, Y. G., Chang, M. Y., Han, B. S., ... & Kim, K. S. (2009). Generation of human induced pluripotent stem cells by direct delivery of reprogramming proteins. Cell stem cell, 4(6), 472.

Katsara, O., Mahaira, L. G., Iliopoulou, E. G., Moustaki, A., Antsaklis, A., Loutradis, D., ... & Perez, S. A. (2011). Effects of donor age, gender, and in vitro cellular aging on the phenotypic, functional, and molecular characteristics of mouse bone marrow-derived mesenchymal stem cells. Stem cells and development, 20(9), 1549-1561.

Kerkis, I., Kerkis, A., Dozortsev, D., Stukart-Parsons, G. C., Gomes Massironi, S. M., Pereira, L. V., Caplan, A. I., Cerruti, HF. Isolation and characterization of a population of immature dental pulp stem cells expressing OCT-4 and other embryonic stem cell markers. Cells, tissues, organs, v.184, n.3-4, p.105-16, 2006. doi:10.1159/000099617

Kern, S., Eichler, H., Stoeve, J., Klüter, H., & Bieback, K. (2006). Comparative analysis of mesenchymal stem cells from bone marrow, umbilical cord blood, or adipose tissue. Stem cells, 24(5), 1294-1301.

Ksiazek, K. (2009). A comprehensive review on mesenchymal stem cell growth and senescence. Rejuvenation research, 12(2), 105-116.

Kobus, K., & Wójcicki, P. (2006). Surgical treatment of Treacher Collins syndrome. Annals of plastic surgery, 56(5), 549-554.

Laino, G., D'Aquino, R., Graziano, A., Lanza, V., Carinci, F., Naro, F., Pirozzi, G., et al. (2005). A New Population of Human Adult Dental Pulp Stem Cells: A Useful Source of Living Autologous Fibrous Bone Tissue (LAB). Journal of bone and mineral research : the official journal of the American Society for Bone and Mineral Research, 20(8), 1454-61. doi:10.1359/JBMR.050325

Laino, Gregorio, Carinci, F., Graziano, A., Aquino, R., Lanza, V., Rosa, A. D., Naro, F., Vivarelli, E., Papaccio, G. Scientific Studies In Vitro Bone Production Using Stem Cells Derived From Human Dental Pulp. Journal of Craniofacial Surgery, p.511-515, 2006.

Langer, R., & Vacanti, J. P. ARTICLES Tissue Engineering. Science. v. 260, 14 maio 1993

Lian, Q., Zhang, Y., Zhang, J., Zhang, H. K., Wu, X., Zhang, Y., ... & Au, K. W. (2010). Functional mesenchymal stem cells derived from human induced pluripotent stem cells attenuate limb ischemia in mice. Circulation, 121(9), 1113-1123.

Liu, Y., Goldberg, A. J., Dennis, J. E., Gronowicz, G. A., & Kuhn, L. T. (2012). One-step derivation of mesenchymal stem cell (MSC)-like cells from human pluripotent stem cells on a fibrillar collagen coating. PloS one, 7(3), e33225.

Lendeckel, Stefan, et al. "Autologous stem cells (adipose) and fibrin glue used to treat widespread traumatic calvarial defects: case report." Journal of Cranio-Maxillofacial Surgery 32.6 (2004): 370-373.

Levi B, James AW, Nelson ER, Vistnes D, Wu B, Lee M, et al. Human adipose derived stromal cells heal critical size mouse calvarial defects. 2010. PLoS One.5(6):e11177.

Levi, B., Wan, D. C., Glotzbach, J. P., Hyun, J., Januszyk, M., Montoro, D., Sorkin, M., et al. (2011). CD105 protein depletion enhances human adipose-derived stromal cell osteogenesis through reduction of transforming growth factor β1 (TGF-β1) signaling. The Journal of biological chemistry, 286(45), 39497-509. doi:10.1074/jbc.M111.256529

Loh, Y. H., Agarwal, S., Park, I. H., Urbach, A., Huo, H., Heffner, G. C., ... & Daley, G. Q. (2009). Generation of induced pluripotent stem cells from human blood. Blood, 113(22), 5476-5479.

Loh, Y. H., Hartung, O., Li, H., Guo, C., Sahalie, J. M., Manos, P. D., ... & Lensch, M. W. (2010). Reprogramming of T cells from human peripheral blood. Cell stem cell, 7(1), 15.

Lv, F. J., Tuan, R. S., Cheung, K., & Leung, V. Y. (2014). Concise review: the surface markers and identity of human mesenchymal stem cells. Stem cells, 32(6), 1408-1419.

Machado, C. O. F., Griesi-Oliveira, K., Rosenberg, C., Kok, F., Martins, S., Passos-Bueno, M. R., & Sertie, A. L. (2016). Collybistin binds and inhibits mTORC1 signaling: a potential novel mechanism contributing to intellectual disability and autism. European Journal of Human Genetics, 24(1), 59-65.

McCarthy, J. G., & Hopper, R. A. (2002). Distraction osteogenesis of zygomatic bone grafts in a patient with Treacher Collins syndrome: a case report. Journal of Craniofacial Surgery, 13(2), 279-283.

Maeda S., Hayashi M., Komiya S., Imamura T., Miyazono K. (2004) EMBO J. 23, 552–56

Maehr, R., Chen, S., Snitow, M., Ludwig, T., Yagasaki, L., Goland, R., ...& Melton, D. A. (2009). Generation of pluripotent stem cells from patients with type 1 diabetes. Proceedings of the National Academy of Sciences, 106(37), 15768-15773.

Megges, M., Geissler, S., Duda, G. N., & Adjaye, J. (2015). Generation of an iPS cell line from bone marrow derived mesenchymal stromal cells from an elderly patient. Stem cell research, 15(3), 565-568.

Menendez, L., Kulik, M. J., Page, A. T., Park, S. S., Lauderdale, J. D., Cunningham, M. L., & Dalton, S. (2013). Directed differentiation of human pluripotent cells to neural crest stem cells. Nature protocols, 8(1), 203-212.

Mesimäki, Karri, et al. "Novel maxillary reconstruction with ectopic bone formation by GMP adipose stem cells." International journal of oral and maxillofacial surgery 38.3 (2009): 201-209.

McIntosh, K., Zvonic, S., Garrett, S., Mitchell, J. B., Floyd, Z. E., Hammill, L., ... & Goh, B. (2006). The immunogenicity of human adipose‐derived cells: temporal changes in vitro. Stem cells, 24(5), 1246-1253.

Miller, J. D., Ganat, Y. M., Kishinevsky, S., Bowman, R. L., Liu, B., Tu, E. Y., ... & Taldone, T. (2013). Human iPSC-based modeling of late-onset disease via progerin-induced aging. Cell stem cell, 13(6), 691-705.

Mitchell, J. B., McIntosh, K., Zvonic, S., Garrett, S., Floyd, Z. E., Kloster, A., ... & Wu, X. (2006). Immunophenotype of Human Adipose‐Derived Cells: Temporal Changes in Stromal‐Associated and Stem Cell–Associated Markers. Stem cells, 24(2), 376-385.

Mittman, D. L., & Rodman, O. G. (1992). Mandibulofacial dysostosis (Treacher Collins syndrome): a case report. Journal of the national medical association, 84(12), 1051.

Miura, M., Gronthos, S., Zhao, M., Lu, B., & Fisher, L. w. SHED: Stem cells from human exfoliated deciduous teeth. PNAS. V.100, n.10, p.598-605, 2003. doi:10.3109/14653249.2010.542462

Miura K, Okada Y, Aoi T, Okada A, Takahashi K, Okita K, Nakagawa M, Koyanagi M, Tanabe K, Ohnuki M, Ogawa D, Ikeda E, Okano H, Yamanaka S. Variation in the safety of induced pluripotent stem cell lines. Nat Biotechnol. 2009 Aug;27(8):743-5. doi: 10.1038/nbt.1554. Epub 2009 Jul 9.

Mizuno D, Agata K, Furue H, Kimura S, Narita Y, Watanabe N, Ishii Y, Ueda M, Tojo A, Kagami S. Limited but heterogeneous osteogenic response of human bone marrow mesenchymal stem cells to bone morphogenetic protein-2 and serum. Journal Growth Factors Volume 28, 2010 - Issue 1

Mizuno, H., Tobita, M. and Uysal, A. C. (2012), Concise Review: Adipose-Derived Stem Cells as a Novel Tool for Future Regenerative Medicine. STEM CELLS, 30: 804–810. doi:10.1002/stem.1076

Mohseni R, Hamidieh AA, Verdi J, Hassani AS (2014) Safe Transplantation of Pluripotent Stem Cell by Preventing Teratoma Formation. J Stem Cell Res Ther 4:212. doi:10.4172/2157-7633.1000212

Najar M, Raicevic G, Fayyad-Kazan H, Bron D, Toungouz M, Lagneaux L. Mesenchymal stromal cells and immunomodulation: A gathering of regulatory immune cells. Cytotherapy Volume 18, Issue 2, February 2016, Pages 160–171

Nakagawa, T., Lee, S. Y., & Reddi, A. H. (2009). Induction of chondrogenesis from human embryonic stem cells without embryoid body formation by bone morphogenetic protein 7 and transforming growth factor β1. Arthritis & Rheumatism, 60(12), 3686-3692.

Nakagawa, M., Karagiannis, P. and Yamanaka, S. (2016), When Myc's asleep, embryonic stem cells are dormant. EMBO J, 35: 801–802. doi:10.15252/embj.201694095

Nakamura, S., Yamada, Y., Katagiri, W., Sugito, T., Ito, K., & Ueda, M. Stem cell proliferation pathways comparison between human exfoliated deciduous teeth and dental pulp stem cells by gene expression profile from promising dental pulp. Journal of endodontics. v.35, n.11, p.1536-42, 2009. Elsevier Ltd. doi:10.1016/j.joen.2009.07.024

Nassiri, F., Cusimano, M. D., Scheithauer, B. W., Rotondo, F., Fazio, A., Yousef, G. M., ... & Lloyd, R. V. (2011). Endoglin (CD105): a review of its role in angiogenesis and tumor diagnosis, progression and therapy. Anticancer research, 31(6), 2283-2290.

Nauta AJ, Fibbe WE. Immunomodulatory properties of mesenchymal stromal cells. Blood 2007 110:3499-3506; doi:10.1182/blood-2007-02-069716

Ohmine, S., Squillace, K. A., Hartjes, K. A., Deeds, M. C., Armstrong, A. S., Thatava, T., ... & Ikeda, Y. (2012). Reprogrammed keratinocytes from elderly type 2 diabetes patients suppress senescence genes to acquire induced pluripotency. Aging (Albany NY), 4(1), 60-73.

Okita K, Ichisaka T, Yamanaka S. Generation of germline-competent induced pluripotent stem cells. Nature. 2007 Jul 19;448(7151):313-7. Epub 2007 Jun 6.

Okita, K., Nakagawa, M., Hyenjong, H., Ichisaka, T., & Yamanaka, S. (2008). Generation of mouse induced pluripotent stem cells without viral vectors. Science, 322(5903), 949-953.

Okita, K., Matsumura, Y., Sato, Y., Okada, A., Morizane, A., Okamoto, S., ... & Shibata, T. (2011). A more efficient method to generate integration-free human iPS cells. Nature methods, 8(5), 409-412.

Park, I. H., Arora, N., Huo, H., Maherali, N., Ahfeldt, T., Shimamura, A., ...& Daley, G. Q. (2008). Disease-specific induced pluripotent stem cells. cell, 134(5), 877-886.

Phelps, P. D., Lloyd, G. A., & Poswillo, D. E. (1983). The ear deformities in craniofacial microsomia and oculo-auriculo-vertebral dysplasia.The Journal of Laryngology & Otology, 97(11), 995-1005.

Phinney, D. G. and Prockop, D. J. (2007), Concise Review: Mesenchymal Stem/Multipotent Stromal Cells: The State of Transdifferentiation and Modes of Tissue Repair—Current Views. STEM CELLS, 25: 2896–2902. doi:10.1634/stemcells.2007-0637

Pittenger MF, Mackay AM, Beck SC, Jaiswal RK, Douglas R, Mosca JD, et al. Multilineage potential of adult human mesenchymal stem cells. Science. 1999;284:143–7. doi: 10.1126/science.284.5411.143.

Plomp, R. G., van Lieshout, M. J., Joosten, K. F., Wolvius, E. B., van der Schroeff, M. P., Versnel, S. L., ... & Mathijssen, I. M. (2016). Treacher collins syndrome: A systematic review of evidence-based treatment and recommendations. Plastic and reconstructive surgery, 137(1), 191-204.

Puri, M. C., & Nagy, A. (2012). Concise review: embryonic stem cells versus induced pluripotent stem cells: the game is on. Stem Cells, 30(1), 10-14.

Rada T, Reis RL, Gomes ME. Distinct stem cells subpopulations isolated from human adipose tissue exhibit different chondrogenic and osteogenic differentiation potential. Stem Cell Rev. 2011;7:64–76.

Robey, PG. Cell sources for bone regeneration: the good, the bad, and the ugly (but promising). Tissue engineering. Part B, Reviews. v.17, n.6, p. 423-30, 2011. http://www.pubmedcentral.nih.gov/articlerender.fcgi?artid=3223013&tool=pmcentrez&rendertype=abstract.

Robinton, D. A., & Daley, G. Q. (2012). The promise of induced pluripotent stem cells in research and therapy. Nature, 481(7381), 295-305.

Sánchez‐Danés, A., Richaud‐Patin, Y., Carballo‐Carbajal, I., Jiménez‐Delgado, S., Caig, C., Mora, S., ... & Canals, J. M. (2012). Disease‐specific phenotypes in dopamine neurons from human iPS‐based models of genetic and sporadic Parkinson's disease. EMBO molecular medicine, 4(5), 380-395.

Sakai, D., & Trainor, P. A. (2009). Treacher Collins syndrome: unmasking the role of Tcof1/treacle. The international journal of biochemistry & cell biology, 41(6), 1229-1232.

Sakai, D., Dixon, J., Achilleos, A., Dixon, M., & Trainor, P. A. (2016). Prevention of Treacher Collins syndrome craniofacial anomalies in mouse models via maternal antioxidant supplementation. Nature communications, 7.

Sarugaser, R., Lickorish, D., Baksh, D., Hosseini, M. M. and Davies, J. E. (2005), Human Umbilical Cord Perivascular (HUCPV) Cells: A Source of Mesenchymal Progenitors. STEM CELLS, 23: 220–229. doi:10.1634/stemcells.2004-0166

Sanz-Rodriguez, F., Guerrero-Esteo, M., Botella, L. M., Banville, D., Vary, C. P., & Bernabéu, C. (2004). Endoglin regulates cytoskeletal organization through binding to ZRP-1, a member of the Lim family of proteins. Journal of Biological Chemistry, 279(31), 32858-32868.

Seong, J. M., Kim, B.-C., Park, J.-H., Kwon, I. K., Mantalaris, A., & Hwang, Y.-S. Stem cells in bone tissue engineering. Biomedical materials (Bristol, England). v.5, n.6, 2010. 062001. doi:10.1088/1748-6041/5/6/062001

Sheridan, S. D., Theriault, K. M., Reis, S. A., Zhou, F., Madison, J. M., Daheron, L., ... & Haggarty, S. J. (2011). Epigenetic characterization of the FMR1 gene and aberrant neurodevelopment in human induced pluripotent stem cell models of fragile X syndrome. PloS one, 6(10), e26203.

Shi, Y., Kirwan, P., & Livesey, F. J. (2012). Directed differentiation of human pluripotent stem cells to cerebral cortex neurons and neural networks. Nature protocols, 7(10), 1836-1846.

Song, B., Sun, G., Herszfeld, D., Sylvain, A., Campanale, N. V., Hirst, C. E., ... & Short, M. (2012). Neural differentiation of patient specific iPS cells as a novel approach to study the pathophysiology of multiple sclerosis. Stem cell research, 8(2), 259-273.

Stadtfeld, M., Nagaya, M., Utikal, J., Weir, G., & Hochedlinger, K. (2008). Induced pluripotent stem cells generated without viral integration. Science, 322(5903), 945-949.

Stadtfeld, M., & Hochedlinger, K. (2010). Induced pluripotency: history, mechanisms, and applications. Genes & development, 24(20), 2239-2263.

Splendore, A., Silva, E. O., Alonso, L. G., Richieri‐Costa, A., Alonso, N., Rosa, A., ... & Passos‐Bueno, M. R. (2000). High mutation detection rate in TCOF1 among Treacher Collins syndrome patients reveals clustering of mutations and 16 novel pathogenic changes. Human mutation, 16(4), 315-322.

Tabar, V., & Studer, L. (2014). Pluripotent stem cells in regenerative medicine: challenges and recent progress. Nature Reviews Genetics, 15(2), 82-92.

Takahashi, Kazutoshi et al. Induction of Pluripotent Stem Cells from Mouse Embryonic and Adult Fibroblast Cultures by Defined Factors. Cell , 2006 Volume 126 , Issue 4 , 663 - 676

Takahashi K, Tanabe K, Ohnuki M, Narita M, Ichisaka T, Tomoda K, et al. Induction of pluripotent stem cells from adult human fibroblasts by defined factors. Cell. 2007 Nov 30;131(5):861-72.

Tiscornia, G., Vivas, E. L., & Belmonte, J. C. I. (2011). Diseases in a dish: modeling human genetic disorders using induced pluripotent cells. Nature medicine, 17(12), 1570-1576.

Trainor, P. A., Dixon, J., & Dixon, M. J. (2009). Treacher Collins syndrome: etiology, pathogenesis and prevention. European Journal of human genetics, 17(3), 275-283.

Trainor, P. A., & Merrill, A. E. (2014). Ribosome biogenesis in skeletal development and the pathogenesis of skeletal disorders. Biochimica et Biophysica Acta (BBA)-Molecular Basis of Disease, 1842(6), 769-778.

Trounson, A., Shepard, K. A., & DeWitt, N. D. (2012). Human disease modeling with induced pluripotent stem cells. Current opinion in genetics & development, 22(5), 509-516.

Twigg, S. R., & Wilkie, A. O. (2015). A genetic-pathophysiological framework for craniosynostosis. The American Journal of Human Genetics, 97(3), 359-377.

Villa‐Diaz, L. G., Brown, S. E., Liu, Y., Ross, A. M., Lahann, J., Parent, J. M., & Krebsbach, P. H. (2012). Derivation of mesenchymal stem cells from human induced pluripotent stem cells cultured on synthetic substrates. Stem Cells, 30(6), 1174-1181.

Zvaifler NJ, Marinova-Mutafchieva L, Adams G, et al. Mesenchymal precursor cells in the blood of normal individuals. Arthritis Research. 2000;2(6):477-488.

Zuk, P. A., M. Zhu, H. Mizuno, J. Huang, J. W. Futrell, A. J. Katz, P. Benhaim, H. P. Lorenz e M. H. Hedrick. Multilineage cells from human adipose tissue: implications for cell-based therapies. Tissue Engineering, v.7, n.2, Apr, p.211-28. 2001.

Zuk, P. A., M. Zhu, P. Ashjian, D. A. De Ugarte, J. I. Huang, H. Mizuno, Z. C. Alfonso, J. K. Fraser, P. Benhaim e M. H. Hedrick. Human adipose tissue is a source of multipotent stem cells. Molecular Biology of the Cell, v.13, n.12, Dec, p.4279-95. 2002.

WARRINGTON, K., HILLARBY, M. C., LI, C., LETARTE, M., & KUMAR, S. (2005). Functional role of CD105 in TGF-β1 signalling in murine and human endothelial cells. Anticancer research, 25(3B), 1851-1864.

Weiner, A. M., Scampoli, N. L., & Calcaterra, N. B. (2012). Fishing the molecular bases of Treacher Collins syndrome. PloS one, 7(1), e29574.

Whitman, M., & Raftery, L. (2005). TGFβ signaling at the summit. Development, 132(19), 4205-4210.

Witkowska-Zimny, M., & Walenko, K. Stem cells from adipose tissue. Cellular & molecular biology letters. v.16, n.2, p.236-57, 2011. doi:10.2478/s11658-011-0005-0

Woltjen, K., Michael, I. P., Mohseni, P., Desai, R., Mileikovsky, M., Hämäläinen, R., ... & Kaji, K. (2009). piggyBac transposition reprograms fibroblasts to induced pluripotent stem cells. Nature, 458(7239), 766-770.

Yamanaka, S. (2009). A fresh look at iPS cells. cell, 137(1), 13-17.

Yamanaka, S. (2012). Induced pluripotent stem cells: past, present, and future. Cell stem cell, 10(6), 678-684.

Yoshimura, Kotaro, et al. "Cell-assisted lipotransfer for cosmetic breast augmentation: supportive use of adipose-derived stem/stromal cells." Aesthetic plastic surgery 32.1 (2008): 48-55.

Yagi, T., Ito, D., Okada, Y., Akamatsu, W., Nihei, Y., Yoshizaki, T., ... & Suzuki, N. (2011). Modeling familial Alzheimer's disease with induced pluripotent stem cells. Human molecular genetics, 20(23), 4530-4539.

Yan, X., Qin, H., Qu, C., Tuan, R. S., Shi, S., & Huang, G. T. J. (2010). iPS cells reprogrammed from human mesenchymal-like stem/progenitor cells of dental tissue origin. Stem cells and development, 19(4), 469-480.

Yoshida, Y., & Yamanaka, S. (2010). Recent stem cell advances: induced pluripotent stem cells for disease modeling and stem cell–based regeneration. Circulation, 122(1), 80-87.

Yu, J., Vodyanik, M. A., Smuga-Otto, K., Antosiewicz-Bourget, J., Frane, J. L., Tian, S., ... & Slukvin, I. I. (2007). Induced pluripotent stem cell lines derived from human somatic cells. Science, 318(5858), 1917-1920.

Yusa, K., Rad, R., Takeda, J., & Bradley, A. (2009). Generation of transgene-free induced pluripotent mouse stem cells by the piggyBac transposon. Nature methods, 6(5), 363-369.

Zhang, J., Lian, Q., Zhu, G., Zhou, F., Sui, L., Tan, C., ... & Stewart, C. L. (2011). A human iPSC model of Hutchinson Gilford Progeria reveals vascular smooth muscle and mesenchymal stem cell defects. Cell stem cell, 8(1), 31-45.

Zapata-Linares, N., Rodriguez, S., Mazo, M., Abizanda, G., Andreu, E. J., Barajas, M., ... & Rodriguez-Madoz, J. R. (2016). Generation and characterization of human iPSC line generated from mesenchymal stem cells derived from adipose tissue. Stem Cell Research, 16(1), 20-23.